NTNU

Norwegian University of
Science and Technology

Long-term hydrothermal Scheduling with aggregate and individual Reservoirs

Jørgen Aarstad

Master of Energy and Environmental Engineering
Submission date: January 2016
Supervisor: Magnus Korpås, ELKRAFT

Norwegian University of Science and Technology
Department of Electric Power Engineering

Abstract

This thesis is a comparative analysis of two commensurable models used in long-term hydrothermal scheduling. The first model is the EMPS model, which is the most prevalent tool for long-term planning in the Norwegian power industry. The second model is known as the SOVN model, which is currently under development at SINTEF Energy Research. A tighter market coupling to the continental European power system with an increasing penetration of intermittent and non-storable renewable energy, requires models that better represent the flexibility of the Nordic hydropower system, since the reservoir aggregation of the EMPS model has proven inadequate to fully handle this. SOVN aims to circumvent this through a detailed simulation of the hydropower system, where the production at each individual power plant is optimized through a complex SLP algorithm using Benders decomposition. Moreover, the SOVN model does not require the same substantial user input as EMPS, which can help minimizing some of the uncertainty of the results.

The first part of this thesis covers the Nordic hydropower system, power system economics and the general framework for long-term hydrothermal scheduling. In the two subsequent chapters the EMPS and SOVN models are thoroughly introduced, both conceptually and mathematically. The analytical part of this thesis is initiated with a review of the case scenarios and power system data: The analysis addresses a confined power system in Northern Norway, where adjacent markets are represented as exogenous price files. The first part of the analysis examines the influence on the performance of SOVN by changing the settings in the `SOVN.ctrl` file. The remaining analysis investigates the power system in extreme surplus situations, by introducing increased wind power development in the region, given as discrete scenarios between 265 and 4,835 MW installed capacity.

In the most moderate of these cases, the share of unregulated production, i.e. production with zero opportunity cost, in EMPS and SOVN is 28.71% and 7.81%, respectively. With 4,835 MW installed wind energy these shares are increased to 44.06% and 9.28%. That is, not only does SOVN minimize its forced production, it also reduces the impact of surplus situations on its operational liberty. Consequently, spillage in SOVN is also significantly reduced: The total percentage of spillage to optional production in the three southernmost subareas, is more than 6% in EMPS and approximately 1% in SOVN. Power surplus results in lower wholesale prices for both models, and bottlenecks in the grid evoke price gaps between adjacent market. In the most extreme case, SOVN reduces the mean price gap with 3.04 €/MWh

relative to EMPS and maintains a more uniform price structure across all markets. The occurrence of extremely low prices is reduced significantly. There is still room for improvement regarding the socioeconomic performance of SOVN, whose results were slightly weaker than those in EMPS. Moreover, the pumping pattern of the SOVN model seems somewhat arbitrary and contradicts basic market logic, partly due to the significant drop in prices in time steps where the pumps are being used, relative to cases with no pumps.

Overall, the results from SOVN show consistently improved ability to allocate production such as to maintain a high level of operational flexibility. The heuristic drawdown allocation of the EMPS model seems less capable of providing the individual plants with the correct market signals, which results in higher levels of spillage and forced production. Comparing the output of individual plants in the two models generally shows that the less regulated plants, i.e. plants with only a few months storage capacity, increase their output in SOVN. These plants are generally the most prone to spillage and forced production, and it seems that these properties are incorporated in their respective water values. Likewise, plants with greater storage capacity and capability show higher tendency to withhold their water, which follows from increased water values. The more uniform price structure across all coupled markets is also an indication of the SOVN model's ability to utilize the transfer capacity more efficiently. The results show a higher utilization of the transfer capacity away from surplus areas, which indicates an improved market handling.

Sammendrag

Denne masteroppgaven er en komparativ analyse av to modeller brukt i langsiktig hydrotermisk kraftplanlegging. Den første modellen er Samkjøringsmodellen, som er den mest utbredte modellen for langsiktig planlegging i den norske kraftbransjen. Den andre modellen er kjent som SOVN-modellen, og er for tiden under utvikling ved SINTEF Energi AS. En tettere sammenknytning med det kontinental-europeiske kraftsystemet med en økende grad av uforutsigbar fornybar energi uten lagringsevne, krever modeller som er bedre egnet til å representere fleksibiliteten i det nordiske vannkraftsystemet, ettersom magasinaggregeringen i Samkjøringsmodellen har vist seg å være utilstrekkelig for å fullt ut omfatte dette. SOVN forsøker å omgå dette gjennom en detaljert simulering av vannkraftsystemet, der produksjonen ved hvert enkelt kraftverk er optimert ved hjelp av en kompleks SLP-algoritme som benytter Benders dekomposisjon. SOVN-modellen utmerker seg dessuten ved å ikke kreve samme omfattende brukerinnput som Samkjøringsmodellen, noe som kan bidra til å minimere usikkerheten til resultatene.

Den første delen av oppgaven tar for seg det nordiske vannkraftsystemet, kraftmarkeder og økonomi, samt de overordnede prinsippene for langsiktig kraftplanlegging. I de følgende to kapitler blir Samkjøringsmodellen og SOVN introdusert, både konseptuelt og matematisk. Den analytiske delen av oppgaven innledes med en gjennomgang av scenarier og kraftsystemdataen: Analysen tar for seg et begrenset kraftsystem i Nord-Norge, hvor tilstøtende markeder er representert som eksogene prisfiler. Den første delen av analysene tar for seg innvirkningen på ytelsen til SOVN ved å endre innstillinger i `SOVN.ctrl`-filen. De øvrige analysene ser på kraftsystemet ved ekstreme overskuddssituasjoner, ved å introdusere økende mengder vindkraftutbygging i regionen, gitt som individuelle utbyggingsscenarier fra 265 til 4 835 MW installert effekt.

I det mest moderate tilfellet er andelen uregulert produksjon – dvs. produksjon med null alternativkostnad – for Samkjøringsmodellen og SOVN lik henholdsvis 28,71% og 7,81%. Med 4 835 MW installert vindkraft øker disse andelene til 44,06% og 9,28%. Det innebærer at SOVN ikke bare minimerer andelen tvungen produksjon, men at den også sterkt reduserer innvirkningen av overskuddssituasjoner på sin driftsmessige frihet. Følgelig blir også flomtap i SOVN kraftig redusert: Ved å sammenligne flomtap mot frivillig produksjon i de tre sydligste delområdene, ser man at prosentandelen flom utgjør mer enn 6% i Samkjøringsmodellen og ca. 1% i SOVN. Kraftoverskuddet fører også til reduserte spotpriser for begge modellene,

og flaskehalser i nettet skaper prisforskjeller mellom tilstøtende markeder. SOVN minsker gjennomsnittlig prisforskjell med 3,04 €/MWh i det mest ekstreme scenariet, og opprettholder en mer uniform prisstruktur for alle markedene. Forekomsten av ekstremt lave priser er også redusert. Det er fremdeles mulighet til å forbedre den samfunnsøkonomiske ytelsen i SOVN, hvis resultater er noe svakere enn i Samkjøringsmodellen. Dessuten virker pumpemønsteret i SOVN noe vilkårlig og motstrider grunnleggende markedslogikk, dels som følge av det betydelige fallet i priser i tidssteg hvor pumpene benyttes, sammenliknet med scenariene uten pumper.

Resultatene antyder generelt at SOVN har en gjennomgående bedre evne til å fordele kraftproduksjonen slik at den høye driftsmessige fleksibiliteten er ivaretatt. Den heuristiske tappefordelingen i Samkjøringsmodellen virker mindre i stand til å levere korrekte markedssignaler til de individuelle kraftverkene, hvilket resulterer i høyere flomtap og mer tvungen produksjon. Ved å sammenligne produksjonsmengden for hvert enkelt kraftverk i de to modellene, viser det seg generelt at de mindre regulerte kraftverkene – dvs. kraftverk med mindre lagringsevne – øker sin produksjon i SOVN. Disse kraftverkene er generelt mest utsatt for flomtap og tvungen produksjon, og disse egenskapene viser seg å bli tatt hensyn til i de respektive vannverdiene. Tilsvarende viser kraftverk med større lagringsevne større tendens til å holde på vannet, hvilket er et resultat av høyere vannverdier. Den mer uniforme prisstrukturen blant alle sammenkoblede markeder er også en indikasjon på SOVN-modellens evne til å utnytte overføringskapasitet på en mer effektiv måte. Resultatene viser en større utnyttelse av overføringskapasitet bort fra overskuddsområder, hvilket tyder på en bedre markedstilnærming.

Preface

This thesis is the resulting work for the course TET4900 - Electric Power Engineering and Smart Grids - Master's thesis at the Department of Electrical Power Engineering at NTNU. The thesis was written during the fall semester of 2015 and submitted at January 28, 2016. The course has 30 credit points. The thesis can be seen as a continuation of my project thesis, *Simulations of the impact of interconnectors on prices and water values in the Nordic power market*, although the analyses and results only coincide to a minor extent. Both theses are written in collaboration with the Market analysis division at Statnett SF.

This thesis aims to make a qualitative assessment of the SOVN model, and to determine general characteristics of the model performance and its ability to model the flexibility of the Nordic hydropower system. Even at this stage, the SOVN model is still a prototype under development at SINTEF Energy Research. This was something I got to experience firsthand when I was first introduced to the model. Much time has been spent on repeated simulations and result interpretation, only then to discover logical errors, bugs, etc. It would be a lie to deny the frustration I felt sometimes during this process. Fortunately, the quality of the model, and hence the results, did eventually improve remarkably, and so did my spirits. Now, looking back at the whole process of writing this thesis, I must conclude that it was a nice few months, after all!

While working on this master's thesis, I have received excellent guidance and help from several people. I especially wish to thank Professor Magnus Korpås at the Department of Electrical Power Engineering and Ivar Døskeland at Statnett SF for their contributions and time over the last twelve months (which includes the project thesis). Our conversations have been extremely rewarding and helped make the work very interesting. I also wish to thank Geir Warland at SINTEF Energy Research for helping me understand the SOVN model, and the Market analysis division at Statnett, for accommodating me while I was working on my thesis in Oslo. Lastly, I wish to thank my parents for their encouragement and support.

Contents

List of Figures

List of Tables

Chapter 1
Background and introduction

1.1 General overview of Norwegian hydropower

A mountainous landscape combined with a rather humid climate, has for more than a century made Norwegian hydropower a profitable infrastructure investment. Hydropower represents the vast majority of the generation portfolio in Norway, e.g. in 2012 close to 97% of all power generation in Norway came from such sources[2]. With approximately 30 GW installed capacity, this makes Norway one of the leading nations in the world in terms of hydropower production.

Hydropower holds many advantageous characteristics which will be shortly presented here, and some elaborated more thoroughly later in the thesis: Firstly, hydropower is a renewable source of energy with a low carbon footprint. Depending on the type and size of the hydropower installation, emissions are roughly between 2 and 9 gCO_2 eq./kWh, most of which arise during production and construction of the plant[3]. Secondly, the Norwegian power system with its large share of hydropower enables production of electricity at great efficiency and flexibility. A state of the art turbine could convert the mechanical energy of the water flow into electrical energy at up to 95% efficiency. Also, Norwegian hydropower has favorable characteristics to provide balancing power[4]. Lastly, apart from substantial investment costs, Norwegian hydropower has very low operational costs. Given the extremely long operational lifetime of hydropower units, it follows that the Levelized cost of energy (LCOE)[1] of Norwegian hydropower is very low compared to most other sources.

Hydropower is a good that is characterized by its non-excludable nature, i.e. it is difficult, or even impossible, to prevent end users from gaining benefit from it. Moreover, hydropower is a rivalrous good. Assuming a one-to-one relationship between the stored water in hydropower reservoir and its equivalent energy output, it goes without saying that consumption of one unit of energy results in depletion

[1] Defined as the sum of the total costs over the project's lifetime, divided by the net energy output during the same period[5]

of one unit of water. Hydropower is thus a finite resource. Goods meeting such criteria are often denoted *common-pool resources*[6]. Moreover, reliable access to electrical power is precondition for virtually all parts of the society. Although the Nordic power market is largely liberalized and encourages competition between the producers, it is generally acknowledged that a free market alone is insufficient to provide goods of such nature[7]. The management of the Norwegian hydropower and the power system as a whole is therefore subject to a great social responsibility, and therein lies the requirement of socioeconomic optimal management. In an ever more continental and shifting power market, this task is becoming increasingly complex.

1.2 Hydropower flexibility

1.2.1 European perspectives

Norway is located geographically at the periphery of Europe, however its potential role in the future European power system could become central. The continental European power system is currently undergoing a paradigm shift, where conventional fossil based fuels are replaced by renewable energy sources, such as wind and solar power. This is crucial in order to fulfill the legislation proposed by the EU to reduce GHG emissions and increase deployment of RES[2], colloquially known as *EU202020*[3][8]. Still, such massive transitions underlines the need for radical changes both in technology, policy and market structures. The latter is particularly important for the established market players who long thrived under the fossil reign, but who is now in major financial distress[9].

The most prominent changes expected in the future pan-European power system is summarized below:

- New market structures and designs
- Increased deployment of RES
- Decommissioning of thermal units
- Increased demand for balancing units and total grid inertia
- Stronger interconnection between different regions and tighter market coupling

1.2.2 Power system flexibility as a commodity

Faced with a momentary imbalance between supply and demand, a hierarchical market structure is designed to recover the balance in a cost efficient and rapid manner[10]. The Nordic hydro dominated power system is unique in the way that there is a lot of rotating reserves which quickly absorbs fluctuations in frequency

[2]Short for renewable energy sources

[3]EU policy aimed to reduce GHG emission by 20% relative to 1990, and increase deployment of renewable energy generation by 20% within 2020.

resulting from discrepancies between load and demand. This is known as the primary reservers. Moreover, the large amount of regulated hydropower enables producers to rapidly ramp up or down production based on signals from the TSO. This is known as the secondary reserves, and is facilitated as a way to both release the primary reserves and recover the network frequency. Lastly, the tertiary reserves are used both to replace the secondary reserves and also to handle regional bottlenecks.

These ancillary services provided by the hydropower at a very low cost results in very low short-term price volatility across much of the Nordic region. In e.g. Germany on the other hand, flexible balancing power is a scarcity. Also, the increased intermittent generation from wind and solar power across the German and continental European power system results in an increased demand for such ancillary services; solar power does not involve rotating masses whatsoever, and modern wind turbines are often electrically decoupled from the grid, which results in a shortage of total system inertia[11]. A tighter market coupling between the Nordic region and the continental European power systems will export some of the price volatility to the Nordic markets, as was found in [12]. This is an indication that power system flexibility is a scarce commodity even in the Nordic region. To estimate the real value of the hydropower flexibility, one would need models that incorporate and represent the hydropower system in a realistic and detailed manner. This thesis aims to evaluate two commensurable models and, by observing their results, determine how well they represent the power market, and how they utilize the inherent flexibility of the Nordic hydropower system.

Chapter 2
Optimal scheduling in hydrothermal systems

2.1 Long-term production planning

The purpose of long-term hydrothermal scheduling is to find an overall hydro release policy which is coordinated with other production sources such as to meet the forecasted future demand at the minimum cost[13]. Such planning is an important prerequisite for a range of other analyses in the power system and power market, such as:

- Price forecasting
- Power balancing
- Investment analyses in generation and transmission

As a side note, the long-term scheduling in the Norwegian context is also subject to a rather peculiar duality: The players in the power system, i.e. the TSO or major producers and consumers, use long-term scheduling tools to determine their long-term strategies, and behave accordingly. On the other hand, when analyzing the power market, the user wants the results of their simulations to reflect the players in the power market in a realistic manner. This reveals a certain positive feedback loop, which calls for the somewhat philosophical question: Does the scheduling tool reflect the power system, or is it in fact the other way around?

2.2 Properties of hydrothermal scheduling

In a purely thermal power system the optimal scheduling problem can in principle be solved by inspection: Assuming that each unit in the system has a known marginal cost, the optimal scheduling can easily be obtained by allocating production at units with increasingly higher marginal costs, until demand is met. Of course, in reality this problem includes the effects of transmission losses and restrictions, start-up costs, ramping rates, etc., which severely complicates the problem. The same basic

logic does not apply for hydrothermal systems. Such systems have several important characteristics which separates them from the thermal systems:

- **Dynamic coupling**
  There are interdependencies between all time stages in the simulation period. Obviously, this interdependency is greatest for adjacent time stages, and weakens over time, i.e. decisions taken at stage t will strongly influence decisions taken at stage $t+1$, however, its effect on the decision taken at stage $t+n$ – where n is any sufficiently large number – is negligible. This property is known as *dynamic coupling*, and it adds considerably to the complexity of the scheduling problem[14].

- **Spatial coupling and complex watercourse topologies**
  Most hydropower plants in the Nordic system are physically connected to other plants in their watercourse. Discharge and spillage from upstream reservoirs flow into downstream reservoirs, thus causing an impact on the production opportunities for subjacent units. Consequently, the production allocation can not be viewed as a set of isolated problems, but must be resolved by considering the totality of the hydropower system, both in space and time.

- **Lack of distinct operational costs**
  The operating costs of a thermal unit is reflecting the fuel costs. The fuels are traded in an open market and the plant operators know the cost characteristics of the plant. Moreover, the operating costs of any single thermal unit is largely independent of the output and availability of other units in the system. For hydropower on the other hand, there is no direct operational cost associated with the power output. Unlike fossil fuels, water is obviously not traded in an open market in which prices are established based on the market clearance. Water is, however, provided as a free, yet limited resource from nature, whose marginal costs are reflecting the *opportunity costs* of production, i.e. the benefit of producing the next power unit from any other source in the system.

Chapter 3
Power system economics

This chapter gives a brief overview of the economic operation of the power system. For proofs and more thorough elaborations, please refer to e.g. [7], [15] or any similar works.

3.1 Elements of economic surplus

Below a set of cost elements are presented, and the total economic surplus in EMPS and SOVN is given as the sum of these elements.

3.1.1 Producer and consumer surplus

Applying common economic principles on the power system, the producer and consumer surplus indicate who gains or loses from changes in the power system. In the EMPS model, the total surplus is given as the sum of weekly surpluses over the year. The consumer surplus is the net deviation between the marginal willingness to pay (MWP) and the actual price the consumer pays, whereas the producer surplus is the net deviation between the price and the marginal cost. They are described mathematically below:

$$CS = \int_0^{X^*} (D(x) - p^*)\ \mathrm{d}x \tag{3.1}$$

and

$$PS = \int_0^{X^*} (p^* - S(x))\ \mathrm{d}x \tag{3.2}$$

where X^* is the net output in GWh, D and S are the demand and supply curves, respectively and x is the production variable.

3.1.2 Congestion rent

With sufficient transfer capacity between adjacent market the prices will be equal. With insufficient capacity, however, the grid company will receive a profit equal to the difference in prices times the transfer capacity in MW. This rent is seen as negative or positive depending on the perspective.

$$CR = (p_A - p_B)\xi \tag{3.3}$$

where A and B denotes two coupled markets, and ξ is the transfer capacity between A and B in MW.

3.1.3 Reservoir changes

Changed reservoir levels represent a total change in value proportional to the water value:

$$RV = \Delta R \cdot WV \tag{3.4}$$

where ΔR represents the net change in reservoir level and WV the water value for the given week.

3.2 Market coupling

This section aims to give a brief introduction to market coupling, and how transfer capacity changes the total societal welfare of a power system. In the remaining chapter, a simple two-bus system is used as an example. The example merely shows a static situation, but the principles are applicable even for dynamic systems.

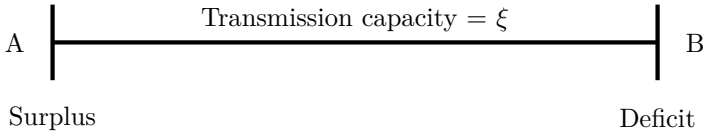

Figure 3.1: Simplified two bus system

Figure 3.1 shows the simplified power system as two busbars - area A with power surplus and area B with a power deficit. Between them is a transmission line with transmission capacity, ξ, in MW. In island mode, the market clearance for these two systems are given by the intersection of the supply and demand curves, which are given as solid lines in figure 3.2. As can be seen, surplus area A have substantially lower price than the deficit area B. However, when there is a transmission capacity between them equal to ξ, A can increase production and export to B which in turn decreases their production. This causes prices in A and B to increase and decrease, respectively, as will be shown:

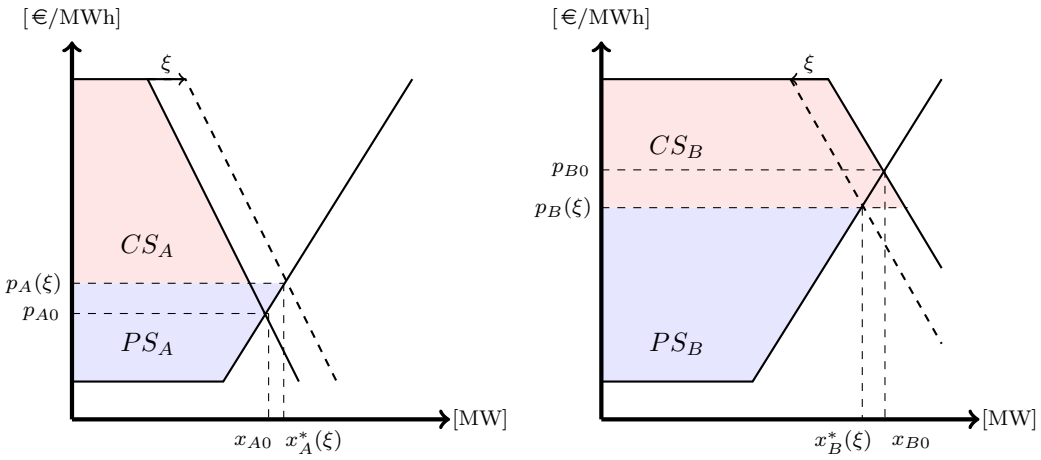

Figure 3.2: Market clearance for separate and connected two bus system

In island mode, the demand functions of the two subareas are given as follows:

$$D_{A0}(x_A) = \begin{cases} R, & 0 \leq x_A \leq \rho_A \\ L_A - \alpha_A x_A, & x_A > \rho_A \end{cases} \tag{3.5}$$

and

$$D_{B0}(x_B) = \begin{cases} R, & 0 \leq x_B \leq \rho_B \\ L_B - \alpha_B x_B, & x_B > \rho_B \end{cases} \tag{3.6}$$

R refers to the cost of rationing and is considered equal for all systems. ρ_A and ρ_B in this case represents the inelastic demand for both areas. The second line of the function refers to the elastic demand, where α is the slope of the segment and L is value at which the slope would intersect with the y axis. When the two subsystems are interconnected their demand functions are somewhat altered to take the opportunity of export into consideration:

$$D_A(x_A, \xi) = \begin{cases} R, & 0 \leq x_A \leq \rho_A + \xi \\ \tilde{L}_A - \alpha_A x_A, & x_A > \rho_A \end{cases} \tag{3.7}$$

and

$$D_B(x_B, \xi) = \begin{cases} R, & 0 \leq x_B \leq \rho_B - \xi \\ \tilde{L}_B - \alpha_B x_B, & x_B > \rho_B \end{cases} \tag{3.8}$$

The altered demand curves are in principle obtained by increasing and decreasing the inelastic demand, which causes a parallel shift of the demand curves. The supply

curves are for simplicity considered invariant to changes in transmission capacities:

$$S_A(x_A) = \begin{cases} 0, & 0 \leq x_A \leq \sigma_A \\ M_A + \beta_A x_A, & x_A > \sigma_A \end{cases} \tag{3.9}$$

and

$$S_B(x_B) = \begin{cases} 0, & 0 \leq x_B \leq \sigma_B \\ M_B + \beta_B x_B, & x_B > \sigma_B \end{cases} \tag{3.10}$$

Thus, equations (3.7) throughout (3.10) describe the economic market as function of the outputs and exchange capacity ξ.

3.2.1 Effect of transfer capacity on quantities and prices

In the following, it is assumed that the market clears at a price less than rationing price, i.e. the supply curve intersects with the elastic demand segment. Without transfer capacity the produced quantities in A and B are given as:

$$x_{A0} = \frac{L_A - M_A}{\alpha_A + \beta_A} \tag{3.11a}$$

$$x_{B0} = \frac{L_B - M_B}{\alpha_B + \beta_B} \tag{3.11b}$$

and the corresponding prices are given as

$$p_{A0} = L_A - \frac{L_A - M_A}{\alpha_A + \beta_A}\alpha_A \tag{3.12a}$$

$$p_{B0} = L_B - \frac{L_B - M_B}{\alpha_B + \beta_B}\alpha_B \tag{3.12b}$$

Now, a transfer capacity of ξ MW is connected between A and B. This causes the production in both areas to shift:

$$x_A^* = \frac{\tilde{L}_A - M_A}{\alpha_A + \beta_A} \tag{3.13a}$$

$$x_B^* = \frac{\tilde{L}_B - M_B}{\alpha_B + \beta_B} \tag{3.13b}$$

It can be shown that $\tilde{L}_A$ and $\tilde{L}_B$ are function of ξ, and given as

$$\tilde{L}_A = L_A + \alpha_A \xi \quad , \quad \tilde{L}_B = L_B - \alpha_B \xi \tag{3.14}$$

Hence, the new quantities of areas A and B are now:

$$x_A^* = \frac{L_A - M_A + \alpha_A \xi}{\alpha_A + \beta_A} \tag{3.15a}$$

$$x_B^* = \frac{L_B - M_B - \alpha_B \xi}{\alpha_B + \beta_B} \tag{3.15b}$$

From this, one can obtain the new prices:

$$(p_A \circ x_A^*)(\xi) = L_A - \frac{L_A - M_A}{\alpha_A + \beta_A}\alpha_A + \frac{\alpha_A \beta_A}{\alpha_A + \beta_A}\xi \tag{3.16a}$$

$$(p_B \circ x_B^*)(\xi) = L_B - \frac{L_B - M_B}{\alpha_B + \beta_B}\alpha_B - \frac{\alpha_B \beta_B}{\alpha_B + \beta_B}\xi \tag{3.16b}$$

Now comparing the prices and quantities of both areas, it can be shown mathematically that the transfer capacity ξ results in a net *increase* in prices for area A and similarly a net *decrease* in B. The net change in production is given as

$$\Delta x_A(\xi) = \frac{\alpha_A}{\alpha_A + \beta_A}\xi \tag{3.17a}$$

$$\Delta x_B(\xi) = -\frac{\alpha_B}{\alpha_B + \beta_B}\xi \tag{3.17b}$$

and likewise, the change in prices is given as

$$\Delta p_A(\xi) = \frac{\alpha_A \beta_A}{\alpha_A + \beta_A}\xi = \beta_A \Delta x_A(\xi) \tag{3.18a}$$

$$\Delta p_B(\xi) = -\frac{\alpha_A \beta_A}{\alpha_A + \beta_A}\xi = \beta_B \Delta x_B(\xi) \tag{3.18b}$$

3.2.2 Socioeconomic surplus as function of transmission capacity

The total socioeconomic surplus is given as the sum of the local surpluses in addition to congestion rent[1]:

$$ES_{TOT} = ES_A + ES_B + CR \tag{3.19}$$

We now want to know what transmission capacity that maximizes economic surplus. The problem can be formulated as follows:

$$\frac{\mathrm{d}}{\mathrm{d}\xi} ES_{TOT} = \frac{\mathrm{d}}{\mathrm{d}\xi}((CS_A + PS_A) + (CS_B + PS_B) + CR) = 0 \tag{3.20}$$

The resulting expression can be written as:

$$\begin{aligned} \frac{d}{d\xi} ES_{TOT} = {} & \frac{\mathrm{d}}{\mathrm{d}\xi} \int_0^{\hat{x}_A(\xi)} (D_{A0}(\xi) - p_A(\xi))\ \mathrm{d}x_A + \frac{\mathrm{d}}{\mathrm{d}\xi} \int_0^{x_A^*(\xi)} (p_A(\xi) - S_A)\ \mathrm{d}x_A \\ & + \frac{\mathrm{d}}{\mathrm{d}\xi} \int_0^{\hat{x}_B(\xi)} (D_{B0}(\xi) - p_B(\xi))\ \mathrm{d}x_B + \frac{\mathrm{d}}{\mathrm{d}\xi} \int_0^{x_B^*(\xi)} (p_B(\xi) - S_B)\ \mathrm{d}x_B \\ & + p_B(\xi) - p_A(\xi) \end{aligned} \tag{3.21}$$

where $\hat{x}_A$ and $\hat{x}_B$ are the quantities at which the demand curves intersect the price lines. By setting equation (3.21) to zero, and calculating for ξ, the optimal transfer

[1] The value of the residual reservoir is omitted

capacity can be found. A different approach, requiring less arithmetical operations, is to consider the increase in net social welfare as function of transfer capacity. For this, net surplus and net deficit functions need to be defined:

$$N_A = S_A - D_{A0} = M_A - L_A + (\alpha_A + \beta_A)\xi \tag{3.22a}$$
$$N_B = D_{B0} - S_B = L_B - M_B - (\alpha_B + \beta_B)\xi \tag{3.22b}$$

When plotted together, these functions form a triangle:

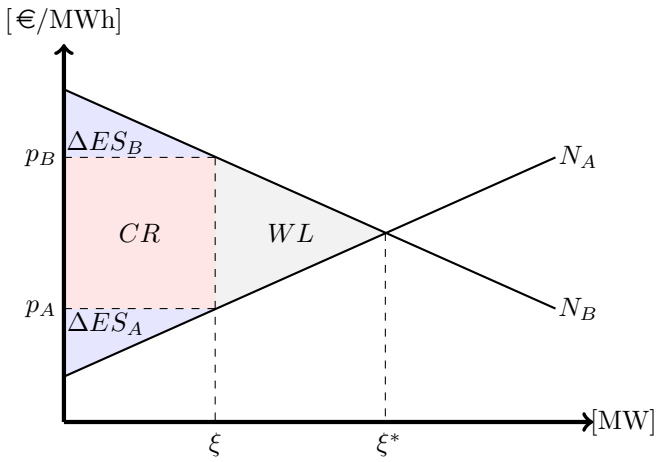

Figure 3.3: Effects of increased transfer capacity on social welfare

As seen in figure 3.3 increased transfer capacity up to ξ^* results in eliminated welfare loss and increased social welfare for both areas. It is obvious from the figure that economic surplus is maximized when

$$\frac{\mathrm{d}}{\mathrm{d}\xi}\int_0^{\xi}(N_B - N_A)\ \mathrm{d}y = 0 \tag{3.23}$$

i.e. when $\xi = \xi^*$. At this transfer capacity, the prices in A and B will be equal and the loss of welfare will be zero. At this socioeconomic optimal transfer capacity level, the congestion rent will be zero. Clearly, this is not in the interest of the grid companies. Assuming that the grid company is an unregulated monopolist, they would seek to maximize their own income. It can be seen that the optimal transfer capacity in the grid owners view, $\tilde{\xi}$, is less than the societal optimal transfer capacity. This is directly in accordance with economic theories on unregulated monopolies, claiming that profit maximization leads to underinvestment and withholding of capacity, and hence sub-optimal socioeconomic welfare.

It follows from the discussion above that price differences between adjacent markets are caused by limited transfer capacity. In areas with great surplus of unregulated production, the bottlenecks will limit export opportunities. With little to no opportunity to withhold excess production, it follows that prices will drop. This effect will be shown in the case study in subsection 7.5 where great amounts of wind is introduced in areas with limited infrastructure.

Chapter 4
The EMPS model

4.1 Overview

EMPS[1] is an abbreviation for **E**FI's[2] **M**ulti-area **P**ower market **S**imulator. The model is widely used by Nordic TSOs and utilities both as a power market simulator and investment tool. The governing principle of the model is to maximize socio-economic surplus of power generation[16]. This is achieved through minimization of the expected value of operational costs. In this context, it can in fact be shown that cost minimization is analogous to surplus maximization. This chapter is largely based on the theoretical introduction to the EMPS model as given in Statnett's manual for the Samlast model, *Håndbok for Samlast*[17], compendium used in postgraduate course ET6003, *Produksjonsplanlegging i vannkraftbaserte systemer – del 2* by G. Doorman et al.[18] and compendium used in graduate specialization course ELK15, *Course ELK15 – Hydro Power Scheduling* by G. Doorman[19].

The model itself consist of two parts – a large data set and the simulation software. The data set consist of a broad range of data for generation, power intensive industry, inelastic demand, etc. Knowing that the Nordic power system is highly sensitive to variations in inflow and precipitation, detailed historical data for inflow makes the basis for the stochastic nature of the power generation. Lately historical wind data has also been implemented to better model the increasing share of renewables in generation mix. The network topology of the power system is highly simplified. The network is merely given as a set of aggregate exchange capacities between adjacent regions. It follows that under such conditions there will be no power flow calculations, but rather a simplified allocation of production to meet demand. Extensions to the EMPS model such as Samlast or Samnett utilize more complex power flow calculations based on Newton-Raphson's method and the fast decoupled method, respectively.

[1] Known in Norwegian as *Samkjøringsmodellen*.
[2] Energiforsyningens Forskningsinstitutt. The predecessor to SINTEF Energy Research

4.2 Modeling of hydro power

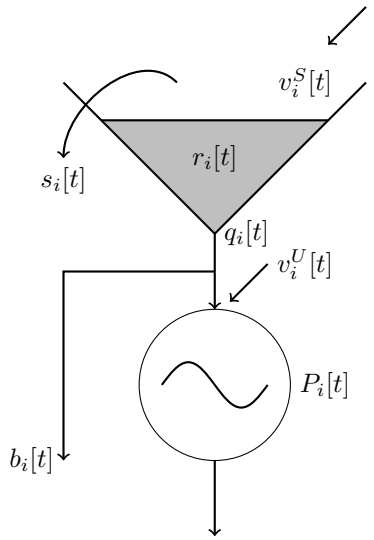

Figure 4.1: General representation of a power station module

The hydro power system in the EMPS model is comprised by standard modules as shown in figure 4.1[18]. A hydro power module consists of a reservoir with a downstream power station and three separate flows[5]. Inflow is given as regulated and unregulated inflow. The former refers to storable inflow to the reservoir, whereas the latter refers to non-storable inflow to the power station. The following quantities work as variables in the short-term optimization. The square brackets merely indicate that these are discrete variables, i.e. they are given with a weekly time resolution.

Variable/parameter	Explanation
$v_i^S[t]$	Regulated inflow to reservoir i in time step t, $[m^3/s]$
$v_i^U[t]$	Unregulated inflow to station i in time step t, $[m^3/s]$
$r_i[t]$	Reservoir level i at end of time step t, $[Mm^3]$
$s_i[t]$	Spillage from reservoir i in time step t, $[m^3/s]$
$b_i[t]$	Bypass from reservoir i in time step t, $[m^3/s]$
$q_i[t]$	Discharge from reservoir i in time step t, $[m^3/s]$

Table 4.1: List of variables and parameters for the hydro power module

4.2.1 Reservoir

The reservoir is characterized by its *degree of regulation*, R. This is a dimensionless quantity which is defined as follows:

$$R = \frac{\text{Reservoir size } [Mm^3]}{\text{Mean annual inflow } [Mm^3]} \tag{4.1}$$

Obviously, for small values of R the inflow is comparatively larger than the reservoir capacity, which yields a low degree of regulation. For such reservoirs the plant manager has low degree of production liberty, due to the risk of spillage. For reservoirs with large R values, on the other hand, there is opportunity to store the water for longer periods. It naturally follows that such reservoirs has lower risk of spillage which increases the set of production opportunities, i.e. the complexity of the optimal scheduling increases with increased degree of regulation. Furthermore, in the EMPS model the reservoir can be described by its reservoir curve, i.e. the relationship between the reservoir volume and the head. This non-linear relationship can be piecewise linearized and used as corrections to computations related to e.g. conventional production, pumping, etc.

4.2.2 Power station

The hydro power production at a single plant i is given as a function of the discharge flow q_i as shown below:

$$P_i(q_i) = \frac{1}{10^6} q_i \gamma g H_i(q_i) \eta_i(q_i) \tag{4.2}$$

As seen in equation 4.2 the output is proportional to both the plant head H_i as well as the plant's efficiency coefficient η. Noting that both of these are functions of the discharge flow q_i, it follows that $P_i(q_i)$ is a non-linear function of the discharge flow. Optimization of such non-linear functions is computationally demanding. The relationship between P_i and q_i is thus approximated as a piecewise linear function.

The power station modules, as described above, can be coupled hydrologically to form a watercourse. In the EMPS model this is achieved by specifying the respective downstream modules to which the plant's discharge, bypass and spillage flow. Such a network of hydro power modules results in a greater flexibility in production than single, isolated modules. However, as pointed out in section 2.2, this increases the complexity of the simulation models.

4.3 Water value method

This section largely refers to the chapter on water values as given in [16]. In the previous section it was discussed that optimal hydro power scheduling has complex

dependencies both in time and space, that strongly influence the nature of the optimization problem. The most common approach is the water value method. The objective of this method is to set an appropriate value of the water, such as to obtain a production policy that maximizes the expected profit. A formal approach to the optimal scheduling problem was proposed some 50 years ago[20], long before the power markets were implemented, but the governing principles of the method are still valid and relevant today.

4.3.1 Basic philosophy of the method

The term *optimality* is somewhat ambiguous, but for optimal hydro power scheduling it is defined as the production policy at which the total expected operational costs are minimized. Cost minimization was the objective in the era prior to the market liberalization, however it can be shown that this yields the same results as profit maximization, which is the current objective.

The variable costs of hydro power are very small, and may conveniently be neglected. Nevertheless, as a result of the properties presented in the previous sections, hydro power is characterized by a corresponding opportunity costs, that represents the operational costs C_O in this case:

$$C_O = C_{Th} + C_{Imp} + C_{LS} - R_{Inel} - R_{Exp}, \tag{4.3}$$

where C_{Th} is the cost of covering the inelastic demand[3] using thermal units, C_{Imp} is the cost of imported power, C_{LS} is the cost of load shedding, whereas R_{Inel} and R_{Exp} are revenues for inelastic demand and exports, respectively. The water value calculations are based on SDP[4]. Even for modest systems the computational load for this algorithm is enormous. It is thus necessary to reduce the overall model into an aggregate model with a single equivalent reservoir and power station for each area, as shown schematically in figure 4.2. The local power network could now be viewed as one busbar. It goes without saying that such a simplification fails to incorporate the inherent flexibility of the individual power stations, which has largely motivated the development and testing of other optimization algorithms, such as the SOVN model which will be presented later on.

[3]In the EMPS model, inelastic demand is modeled as binding contracts. They refer to the portion of the demand that should be covered at all costs, i.e. the consumption for ordinary customers such as households, etc., whose price elasticity of demand is close to zero. Elastic demand, on the other hand, refers to specific categories of consumption that are more sensitive to changes in the price, such as power intensive industry.

[4]Stochastic Dynamic Programming. Such optimization deals with problems of multiple time stages, where the *state* at the next *stage* is not completely determined by the policy decision of the current stage, but rather a stochastic distribution for what the next stage will be[21]. Contrary to deterministic optimization, stochastic optimization yields the optimal *expected value* of the objective function.

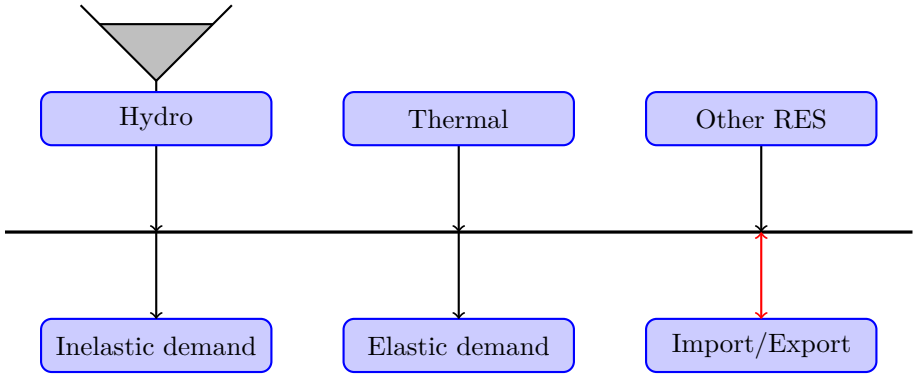

Figure 4.2: Single reservoir equivalent in EMPS

4.3.2 The market for hydro power

Again referring to figure 4.2, this can be viewed as a model for the local power market. The demand side is given as inelastic and elastic demand as well as exports, while the supply side is given as hydro power, thermal power, other RES and imports. The demand for hydro power is given as the *residual demand*, i.e. the demand for power when all other sources are subtracted. In the Norwegian power market the thermal capacity is not sufficient to cover the inelastic demand. In such a market without any hydro power, the market would clear at at the rationing price.

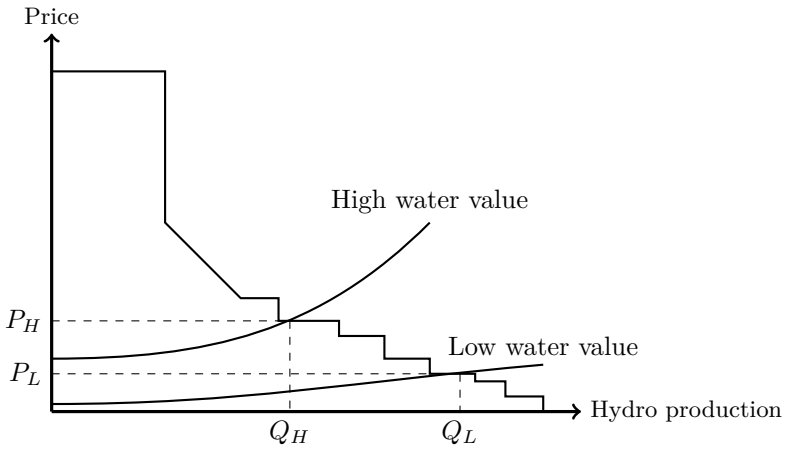

Figure 4.3: Local market balances given high and low water values

The demand for hydro power in such a system can be obtained through horizontal subtraction of the supply curve *without* hydro power and the demand curve. The

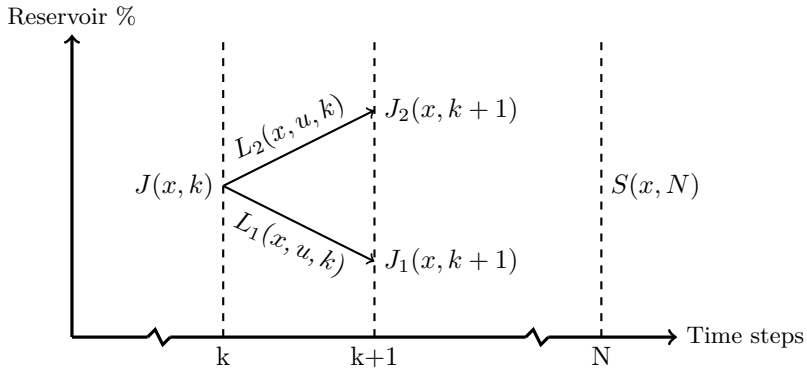

Figure 4.4: Partitioning of time segments in SDP algorithm

resulting *residual demand curve* is similar to the downward sloping demand curve in figure 4.3. The water values as function of hydro power production is plotted as the two upward sloping supply curves. The optimal hydro power production is given as the production level at which the residual demand curve intersects with the water value curve.

4.3.3 Mathematical formulations

In the EMPS model the time domain is partitioned into a set of weekly segments. The weekly time resolution is sufficient to achieve a satisfactory level of accuracy, within a reasonable computational load. In principle, the problem within every week is to determine the weekly production level such as to minimize the expected operational cost for the future time steps.

In figure 4.4 the planning period is divided into N separate time segments throughout the x-axis. The aggregated reservoir level is given along the y-axis. The expected cost at the beginning of time stage k is given as $J(x,k)$. This is formulated as follows:

$$J(x,k) = S(x,N) + \sum_{i=k}^{N} L(x,u,i) = L(x,u,k) + J(x,k+1) \tag{4.4}$$

where

$S(x, N)$	:	Residual value of the reservoir at end of period as function of reservoir level x.
$L(x, u, k)$	:	Total operational cost as given in equation 4.3. Seen as transitional costs when going from period k to $k + 1$.
u	:	Weekly production policy.

At time segment k the total operational costs equal the sum of the remaining transitional costs $L(x, u, i)$, $k \leq i \leq N$ and the residual value $S(x, N)$. u represents the weekly production decision of the aggregated reservoir in GWh[5]. It follows that for different values of u the transitional costs would take different values. The weekly decision problem then reduces to find the production policy at which the expected operational costs are minimized, i.e.

$$\min_u J(x, k) = \min_u \{L(x, u, k) + J(x, k + 1)\} \tag{4.5}$$

or written more compactly as

$$\frac{\partial J(x, k)}{\partial u} = 0 \tag{4.6}$$

Performing the differentiation in equation 4.6 yields:

$$\frac{\partial J(x, k)}{\partial u} = \frac{\partial L(x, u, k)}{\partial u_k} + \frac{\partial J(x, k + 1)}{\partial x_{k+1}} \frac{\partial x_{k+1}}{\partial u_k} \tag{4.7}$$

$$= \frac{\partial L(x, u, k)}{\partial u_k} + (-1) \cdot \frac{\partial J(x, k + 1)}{\partial x_{k+1}} \tag{4.8}$$

The subscripts k and $k + 1$ are assigned to u and x, respectively, in order to clearly stress their respective time segments. Using the chain rule of differentiation and utilizing the inverse proportionality between this week's production and next week's reservoir level, while utilizing equation (4.6), it is thus clear that

$$\frac{\partial L(x, u, k)}{\partial u_k} = \frac{\partial J(x, k + 1)}{\partial x_{k+1}} \tag{4.9}$$

where

$\frac{\partial L(x, u, k)}{\partial u_k}$	:	Marginal operational costs.
$\frac{\partial J(x, k + 1)}{\partial x_{k+1}}$	:	Per definition the water value.

This implies that optimal production can be achieved by matching the marginal operational costs with the water value. This explains why the water values are

[5]One unit of water is expressed in terms of its equivalent energy yield in (G/W)Wh, rather than volume in Mm^3

referred to as the production strategy. The water values are determined through a reverse SDP algorithm. That is, the water value at the end of the simulation period is assumed known and set to any arbitrary value. The water values for the preceding weeks are then determined through backward recursion. Thus, in the long run, given sufficiently many time stages in between, the assumed water value at the end of the simulation period are then decoupled from the water value in week k.

The stochastic nature of the water value method is a result of the weekly stochastic inflows. For simplicity, the weekly stochastic inflows are merely treated as outcomes of a discrete probability distribution, such that

$$\sum_{i \in \mathcal{N}} p_i = 1 \tag{4.10}$$

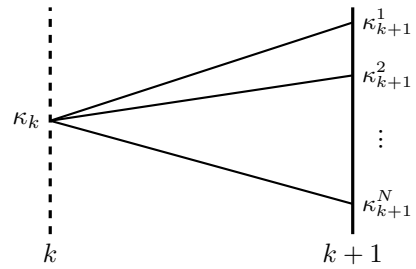

Figure 4.5: Water value calculation based on stochastic inflows

where $\mathcal{N}$ is the sample space and p_i is the given probability of a discrete realization of the inflow. The water value, κ_{k+1}^i, where the subscript $k+1$ denotes the time stage and the superscript i the discrete realization, is computed as shown in this subsection, $\forall i \in \mathcal{N}$, and stored for each time stage. Due to serial correlation, a weighted probabilistic average of the set of water values is computed to determine the water value in the preceding week. This is shown schematically in figure 4.5.

4.4 Weekly decision making process

4.4.1 Strategy part

The solution in the EMPS model is generated through a two-stage iterative procedure; first the strategy part, and then the simulation part. In the strategy part the water values are first iteratively and independently calculated for each de-coupled area in the model using the procedure as describes in subsection 4.3.3. The resulting *water value matrix* contains fifty water values per week, i.e. one for every second per cent

of the aggregated reservoir level. When acting in the market, the water values can be seen as guidelines for optimal production scheduling. The individual water values does not incorporate market couplings, so once the water values for all subareas are obtained, the impact of imports and exports is calculated to modify the water values.

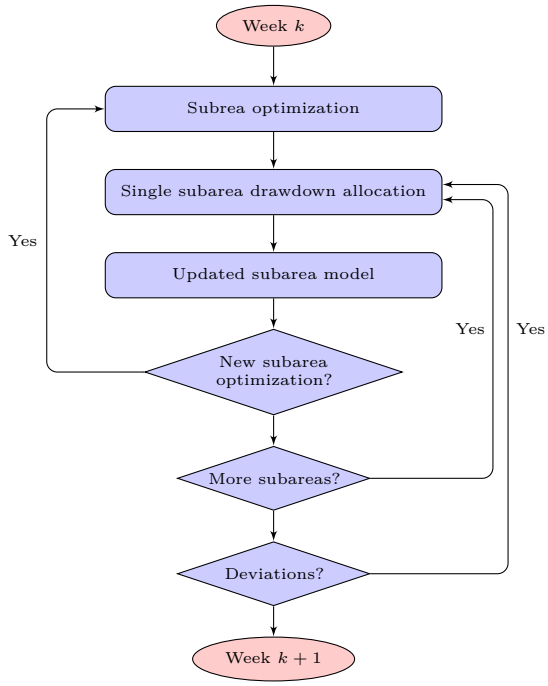

Figure 4.6: Weekly simulation process in the EMPS model

4.4.2 Simulation part

The simulation part gives results for the total system operation. The optimization process utilizes the water value and other market details to determine the optimal hydro release policy for each subarea and for each inflow alternative. Because all inflows are known, the problem can be solved deterministically[6]. The optimization problem is formulated as a minimization problem with restrictions related to power balance, reservoir balance, etc. This simulations can be performed in two ways; serial or parallel simulations. In the former, all years are interrelated, i.e. the reservoir level for the last week of year n is equal to the reservoir level for the first week of year $n+1$. In the latter, all inflow years start with the same reservoir level.

[6]In a deterministic model, the input parameters are *not* subject to stochastic variations.

The *drawdown allocation* is based on the subarea optimization. This complex disaggregation algorithm is based on a set of heuristics and meta-heuristics to allocate the total production of the aggregated reservoir to each individual plant within the subarea. Such a rule based approach, rather than a formal optimization, is implemented in order to reduce the computational effort and represent a realistic market. Some reservoirs could e.g. be subject to certain constraints in reservoir levels, etc. that must be fulfilled, and which are met in the heuristic approach.

The drawdown allocation is performed individually for each subarea. The actual allocation procedure is aborted if the resulting system violates any predetermined restrictions, e.g. if unregulated production deviates from unregulated inflow, etc. A new simulation is then run and the drawdown allocation procedure is repeated individually for all subareas. The system is likely adjusted several times during the simulation procedure. The whole procedure is repeated until all deviations are eliminated, or until the upper limit for iterations are reached. A summary of the simulation procedure in the EMPS model is given in figure 4.6.

4.5 Modular programs

The simulation software is designed as a set of modular programs with separate functionality, performed in sequence. The modular programs can be divided into four categories, i.e. preprocessing, facilitating of data, simulation and result processing. Apart from the simulation part, all the modular programs are also used in the SOVN model. Note that this is a very general presentation, where any specific details are omitted. For a more thorough elaboration, please refer to SINTEF's user manual for the EMPS model[22].

4.5.1 Preprocessing

Enmdat and Vansimtap are used in the preprocessing phase to adjust simulation settings. They adjust the input parameters to the model. The programs write data to the single area equivalent files, <SUBAREA.ENMD>. These files are then read by the modular program Saminn, which in turn rewrites the files to formats that can be read and interpreted by the simulation programs.

4.5.2 Facilitating of data

Stfil is used to determine calibration and control data, such as the first and last weeks of simulation, subareas to be simulated with a high level of detail and whether to use parallel or serial simulation.

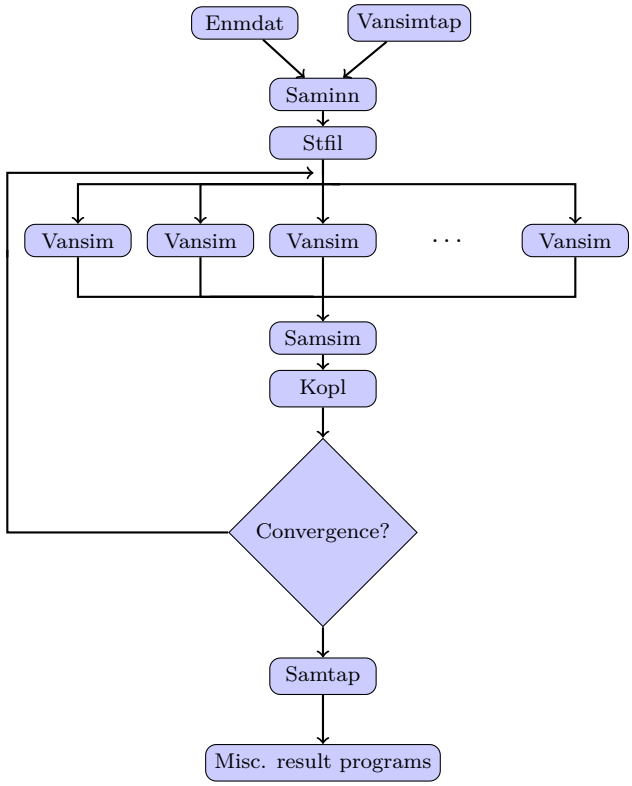

Figure 4.7: Flow of modular programs in EMPS

4.5.3 Simulation

The simulation part, in this context, is the large bulk of operations related to water value calculations and simulations in the EMPS model. After Stfil is run, the simulation proceeds with individual water value calculations for each subarea using Vansimtap. Samsim performs the subarea optimization, where each subarea is simulated individually. Kopl is used to couple the individual subareas together, and deals with model calibration, as will be presented in section 4.6. The model checks for convergence, and returns to the water value calculations if the results are not within the converge tolerance. This iterative process is described more thoroughly in section 4.4. Once the optimal and correct water values are calculated, the process continues to Samtap, which runs the detailed simulation and drawdown allocation.

4.5.4 Result processing

There is a number of modular programs designed to retrieve and present data. Which program to use depends on the desired data to be collected. Some of the most

important programs include:

- Kurvetegn - Graphical presentation
- Samoverskudd - Socio-economic surplus
- Utslipp - GHG emissions
- Avregn - Energy balance at subarea level
- Samutskriv - Results at subarea level

In this thesis Kurvetegn and Samoverskudd will be used. The programs generates output files in a number of formats, and writes the data to these files. In this thesis the data is mostly written to .csv files which are imported to Matlab for graphic processing.

4.6 Calibration

The calibration is a complex process to adjust the water values. The calibration process connects the subareas together by adjusting factors that influence the demand curve. These factors are:

- **Feed-back factor** - Determines the extent to which the subareas are connected
- **Shape factor** - Determines the load distribution throughout the year
- **Elasticity factor** - Determines the price elasticity of demand

The calibration procedure could either be done automatically or manually by the user. Either way, the user must decide on the quality of the results, and interpret the results accordingly. Obviously, this is a source of great uncertainty, and thus an inherent weakness with the EMPS model.

The calibration aims to adapt to the restrictions set by the user, which could be to maximize socio-economic surplus, to mimic the historical reservoir curves, etc. The calibration policy at Statkraft, and consequently Statnett, is to use historical reservoir curves as guidelines for their calibration.

Chapter 5
The SOVN model

5.1 Purpose and characteristics

The SOVN model is an improved method to solve long-term hydrothermal scheduling problems. This model is based on LSP[1], and it aims to circumvent some of the drawbacks of the water value method, as presented below:

- **Reservoir aggregation**
  The dimensionality problem of the SDP algorithm is the most fundamental downside of the water value method. In a system with N reservoirs and M time steps, the number of discretized states in the state space is given as M^{kN}, where k is the number of unique variables for every reservoir. Obviously for conventional SDP, the computational effort increases exponentially with the number of state variables, and solutions even for modest systems are thus practically infeasible[23]. In optimization literature this problem is know as the *curse of dimensionality*.

- **No need for model calibration**
  The strategy of the EMPS model needs substantial user-input to modify the coupled markets and the reservoir curves. The model calibration is one of the greatest uncertainties of the EMPS model, and even experienced users may find it difficult to separate the effects of the calibration with the strategy of the model. SOVN follows a formal optimization, which does not depend on the same form of user based model calibration.

- **Discretization of state space**
  An additional consequence of the dimensionality problem is the need to discretize the sample space. The state variables in the water value matrix is defined for every second percent of the total reservoir level.

[1] Linear stochastic programming

- **Fails to fully value flexibility**
  Nordic hydropower is generally able to cost efficiently reallocate the production to peak hours, thus mitigating short-term price volatility and causing a rather uniform price structure and lower differences between water values. However, with the expected growth in RES deployment, decommissioning of thermal plants and more exchange capacity to continental Europe, there will be a scarcity for flexibility, causing greater differences in water values between different reservoirs[24].

5.2 Other modeling approaches

Despite its shortcomings, the SDP algorithm has been used to solve complex hydrothermal scheduling problems for a long time, while attempts have been made to improve the scheduling approach: ReOpt is model developed by SINTEF Energy Research, that solves the detailed production allocation as a LP problem based on the weekly aggregate reservoir levels and corresponding water values obtained from the EMPS model[25]. The MAD project is another newly initiated model which seeks to improve and generalize the reservoir aggregation and disaggregation in EMPS.

The SDDP[2] algorithm for hydrothermal scheduling purposes was first introduced by M. Pereira, and it is well presented in a number of scientific papers, e.g. in [26][27][28][29]. Similarly to SLP, the solution method is based on approximation of the expected-cost-to-go function, which are obtained from the dual solution of the primary scheduling problem at each time step. This approach circumvent the issues related to dimensionality and discretization of state space.

Other methods are based on further developments of the SDP algorithm: In [30] it is found that complex discretization of the state space might mitigate dimensionality issues. [31] models the expected cost-to-go functions of the SDP problem by using the Convex Hull algorithm, allowing the dynamic subproblems to be solved with LP solvers rather than more complex algorithms.

For further reading, Yakowitz[32] provides a comprehensive survey on a number of DP models for hydro power scheduling.

5.3 The SFS algorithm

In this section, a thorough outline of the so-called *SFS algorithm*[3] implemented in the SOVN model is presented. Such a detailed review of the algorithm is needed to fully appreciate the differences between the SOVN model and the EMPS model. The

[2]Stochastic dual dynamic programming
[3]Scenario fan simulator

theory presented in this section is largely based upon the technical report *Stochastic optimization model with individual water values and power flow constraints*[33] by SINTEF Energy Research and related papers by Helseth et al.[13] and Pereira et al.[23]. Any additional sources are presented consecutively.

5.3.1 Weekly decision problem

The nomenclature of the optimization problem is listed below:

Sets:

$\mathcal{N}_A$	Set of areas
$\mathcal{N}_P$	Set of load periods
$\mathcal{N}_G(i)$	Set of thermal generators in area i
$\mathcal{N}_C(i)$	Set of curtailment steps in area i
$\mathcal{N}_D(i)$	Set of elastic demand steps in area i
$\mathcal{N}_R(i)$	Set of reservoirs in area i
$\mathcal{R}(r)$	Set of reservoirs hydrologically coupled to $r \in \mathcal{N}_R(i)$
ω_i	Set of areas connected to i

Main indices:

i	Area
j	Objective function variables
p	Load period
r	Reservoir
t	Time stage

Variables within subarea i:

y^g_{ipj}	Thermal power production, generator j, load period p
y^c_{ipj}	Curtailed power at curtailment step j, load period p
y^d_{ipj}	Coverage of elastic demand at elastic demand step j, load period p
$x_{ir,t}$	Reservoir storage in reservoir $r \in \mathcal{N}_R(i)$ at beginning of time step t
$v^S_{ir,t}$	Storable inflow to reservoir $r \in \mathcal{N}_R(i)$ in time step t
$q_{ir,t}, s_{ir,t}, b_{ir,t}$	Discharge, spillage and bypass from reservoir $r \in \mathcal{N}_R(i)$ in time step t
h_{ipr}	Hydropower generation from unit $r \in \mathcal{N}_R(i)$, load period p
$f_{ik,p}$	Transported power between areas i and k, load period p

Parameters:

C^g_{ij}	Cost of thermal generation for generator j
C^c_{ij}	Cost of curtailment at curtailment step j
C^d_{ij}	Value of elastic demand at elastic demand step j
D_{ip}	Inelastic demand in area i and load period p

β_{ik} Transportation loss coefficient between areas i and k

The weekly cost minimization problem Z can be formulated as a linear optimization problem as given in equation (5.1). It can be seen that the objective function aims to minimize variable costs related to thermal production, load curtailment and unserved elastic demand. This approach is completely analogous to the water value method.

$$\min Z = \sum_{i\in\mathcal{N}_A}\sum_{p\in\mathcal{N}_P}\left[\sum_{j\in\mathcal{N}_G(i)} C^g_{ij}y^g_{ipj} + \sum_{j\in\mathcal{N}_C(i)} C^c_{ij}y^c_{ipj} + \sum_{j\in\mathcal{N}_D(i)} C^d_{ij}y^d_{ipj}\right] \tag{5.1}$$

Subscript t in equation (5.1) and (5.3) is omitted for convenience. The objective function is subject to non-trivial constraints related to reservoir and market balances.

$$\begin{aligned} x_{ir,t} + v^S_{ir,t} - q_{ir,t} + \sum_{\rho\in\mathcal{R}(r)} q_{i\rho,t} \\ -s_{ir,t} + \sum_{\rho\in\mathcal{R}(r)} s_{i\rho,t} - b_{ir,t} + \sum_{\rho\in\mathcal{R}(r)} b_{i\rho,t} = x_{ir,t+1} \end{aligned} \tag{5.2}$$

Equation (5.2) is defined for the following sets and subsets: $\forall i \in \mathcal{N}_A, \forall r \in \mathcal{N}_R(i), \mathcal{R}(r) \subseteq \mathcal{N}_A(i)$. It corresponds to the state transition equation in the SDP algorithm, and incorporate the complexity of the water course topology as described in subsection 4.2.1.

$$\begin{aligned} \sum_{r\in\mathcal{N}_R(i)} h_{ir,t} + \sum_{j\in\mathcal{N}_G(i)} y^g_{ipj} + \sum_{j\in\mathcal{N}_C(i)} y^c_{ipj} - \\ \sum_{j\in\mathcal{N}_D(i)} y^d_{ipj} + \sum_{k\in\omega_i}\left[(1-\beta_{ik})f_{ki,p} - f_{ik,p}\right] = D_{ip}, \quad \forall i \in \mathcal{N}_A, \forall p \in \mathcal{N}_P \end{aligned} \tag{5.3}$$

Equation (5.3) refers to the market balance, and it simply states that production must equal load demand with opportunities for exchange between adjacent areas. In addition to the constraints mentioned, there are also a great number of constraints related to ramping rates of thermal units, exchange capacities, etc.

The hydropower generation is modeled as a piecewise linear function of the discharge flow, given by equation (5.4). The efficiency of the power station is considered to be constant. As can be seen in figure 4.1, unless the maximum discharge Q^{max}_{ir} is reached, the production is proportional to the sum of the weekly discharge $q_{ir,t}$ and non-storable inflow $v^U_{ir,t}$.

$$h_{ir} = \begin{cases} \eta_r(q_{ir,t} + v^U_{ir,t}) & \text{if } q_{ir,t} + v^U_{ir,t} \le Q^{max}_{ir} \\ \eta_r Q^{max}_{ir} & \text{if } q_{ir,t} + v^U_{ir,t} \ge Q^{max}_{ir} \end{cases} \tag{5.4}$$

5.3.2 SFS simulation logic

The SFS algorithm is based on two-stage stochastic linear programming, i.e. the weekly problem formulated in equations (5.1) to (5.3) is formulated in one deterministic part and one future stochastic part, as shown in equation (5.5). This new objective function is subject to the same constraints as the weekly decision problem formulated above, in addition to a set of transitional constraints incorporating the dynamic nature of the optimization problem.

$$\min \text{SLP} = Z_{t,m}(u_{t,m}) + \sum_{n \in \mathcal{N}_K} p_n \left[\sum_{\tau=t+1}^{T+t} Z_{\tau,n}(u_{\tau,n}) + \alpha_{T+t}(x_{T+t,n}) \right] \tag{5.5}$$

$Z_{t,m}$ refers to the first stage problem of week t subject to first-week inflow scenario m. Correspondingly $Z_{\tau,n}$ refers to weekly decision problem for week τ subject to a realization n of the set of weekly inflow scenarios $\mathcal{N}_K$. $u_{t,m}$ and $u_{\tau,n}$ simply represents a vector of all decision variables at the given time step and inflow scenario. Decision variables in this case may be reservoir discharge, bypass, etc. $\alpha_{T+t,n}$ is the future cost function at the end of the planning horizon, and it incorporates the water value strategies from the EMPS model. Thus, this entity works as the connection between the SOVN and EMPS models. If the planning horizon is sufficiently long, this residual value is of less importance. Hence, it can be said that the level of autonomy of the SOVN model is proportional to the planning horizon.

The solution of 5.5 provides a starting point for $t+1$, as summarized below:

1: **for** all scenarios $n \in \mathcal{N}_K$ **do**
2: **for** all time steps $[t+1, T+t]$ **do**
3: Build and solve the SLP in equation 5.5
4: Store results from first week decision $sol(n,t)$
5: Pass on $sol(n,t)$ to equation (5.5) for $t+1$

The logic of the scenario fan simulator is presented in figure 5.1 below. The structure and size of the problem is kept constant by skewing the time horizon.

5.3.3 Benders decomposition

The dynamic linking of equation (5.5) makes it difficult to obtain a direct solution to the problem. *Benders decomposition principle*[4] is a technique that divides the whole problem into one master problem and $|\mathcal{N}_K|$[5] subproblems, which are solved iteratively. This method has proven well suited to deal with complex stochastic problems such as hydrothermal scheduling.

[4]Invented by Jacques F. Benders in 1962
[5]Note that $|\mathcal{N}_K|$ is the cardinality, i.e. the number of elements in the set $\mathcal{N}_K$.

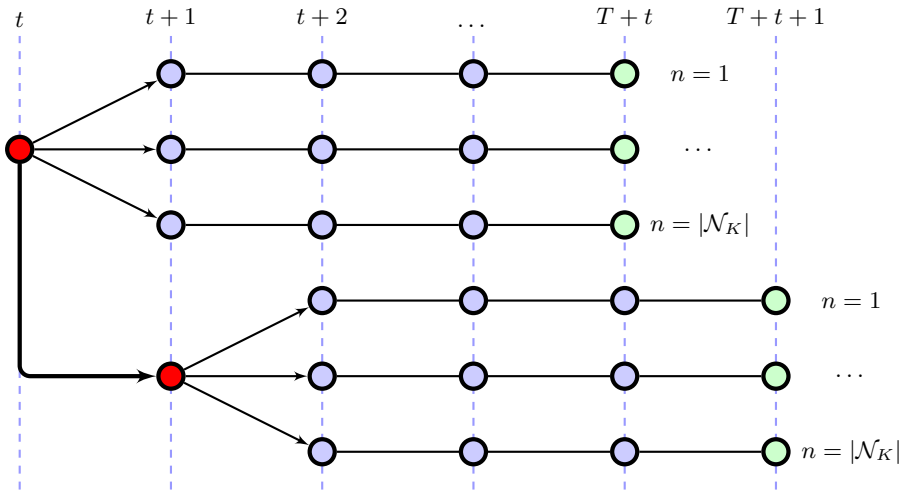

Figure 5.1: Illustration of simulation logic

Both the master and the subproblems given below are subject to the same constraints as presented earlier. $\tilde{\theta}$ represents an approximation of the second-stage costs, contrary to the *real* second-stage cost $\theta(u_{t,m})$. $\tilde{\theta}$ can be interpreted as a variable that changes for each iteration. Superscripts M and S denote master and subproblems, respectively.

$$\min Z^M = Z_{t,m}(u_{t,m}) + \tilde{\theta} \tag{5.6}$$

$$\min Z^S = \sum_{\tau=t+1}^{T+t} Z_{\tau,n}(u_{\tau,n}) + \alpha_{T+t}(x_{T+t,n}), \quad \forall n \in \mathcal{N}_K \tag{5.7}$$

First, the master problem is solved with an initial approximation of $\tilde{\theta}$. The resulting variables from the solution of the master problem is denoted $u^l_{t,m}$, where l is an iteration counter, and m is the given inflow scenario for the first-stage problem. Once the solution of the master problem is obtained, the resulting state variables $u^l_{t,m}$ are passed on to the subproblem as right hand side parameters in the transtitional constraints. There are $|\mathcal{N}_K|$ second-stage subproblems, i.e. one for each inflow scenario. Each of these problems are decomposed into a new master and subproblem as given in equations (5.6) and (5.7), thus resulting in the nested approach, as illustrated in figure 5.1.

Now, let π^l_{rn} denote a vector containing the shadow prices for all $n \in \mathcal{N}_A$ scenarios for reservoir $r \in \mathcal{N}_R$, and iteration l. These are obtained from the constraints in equation (5.2). Likewise, π_{an} are shadow prices for *all* subproblem constraints. When

all subproblems are solved, the expected value of the reservoir multipliers can be found:

$$\pi_r^l = \sum_{n \in \mathcal{N}_K} p_n \pi_{rn}^l \tag{5.8}$$

New optimality cuts are generated from the dual solutions of the second-stage problems[6] and added to the master problem in equation (5.6):

$$\tilde{\theta}^l \geq \sum_{n \in \mathcal{N}_K} p_n \pi_{an}^l H_n - u_{t,m}^l \sum_{n \in \mathcal{N}_K} p_n \pi_{rn}^l \tag{5.9}$$

Where $\sum_{n \in \mathcal{N}_K} p_n \pi_{an} H_n$ corresponds to the total expected value of the second stage costs and $u_{t,m}^l \sum_{n \in \mathcal{N}_K} p_n \pi_{rn}$ represents the effect of changing the first-stage decision variables. It should be noted that π_{an} and h_n are related to the entire set of constraints, whereas π_{rn} and $u_{t,m}^l$ are merely related to the reservoir balances.

In subsequent iterations, i.e. for any $l > 1$, $\tilde{\theta}^l$ is included as a variable. From this it can be found that

$$\underline{Z}^l = Z^{M,l} + \tilde{\theta}^l \tag{5.10}$$

i.e. the lower bound of the two-stage problem. For every iteration, new cuts are added that diminished the convex hull, with the effect that $\tilde{\theta}^{l-1} \leq \tilde{\theta}^l$. Moreover, note that π_r^l and $u_{t,m}^l$ refer to water value for reservoir r in €/GWh and reservoir policy in GWh, respectively, which corresponds to a purely economical entity. This is shown in section A.3.

When the master and subproblems are solved, an upper bound to the two-stage problem can be calculated as follows:

$$\bar{Z}^l = \min(\bar{Z}^{l-1}, Z^M(u_{t,m}^l) + \sum_{n \in \mathcal{N}_K} p_n Z_n^S(u_{\tau,n}^l)) \tag{5.11}$$

The upper boundary might not be strictly decreasing, hence the need for comparison. Convergence is obtained by a predetermined criterium, e.g. by setting a given tolerance level ε to the deviation between upper and lower boundary:

$$\bar{Z}^l - \underline{Z}^l \leq \varepsilon \tag{5.12}$$

It might also be necessary to establish a secondary convergence criterium related to a maximum number of iterations.

The SFS methodology proves highly suitable for *warm-starting* of the subproblems. This technique utilizes information from the solution of previous subproblems, such as to obtain better initial approximations of future cost function $\tilde{\theta}$[34]. Improved initial estimations could potentially reduce the computational effort.

[6]For every primal problem, there is a corresponding dual problem formulated with the exact same data

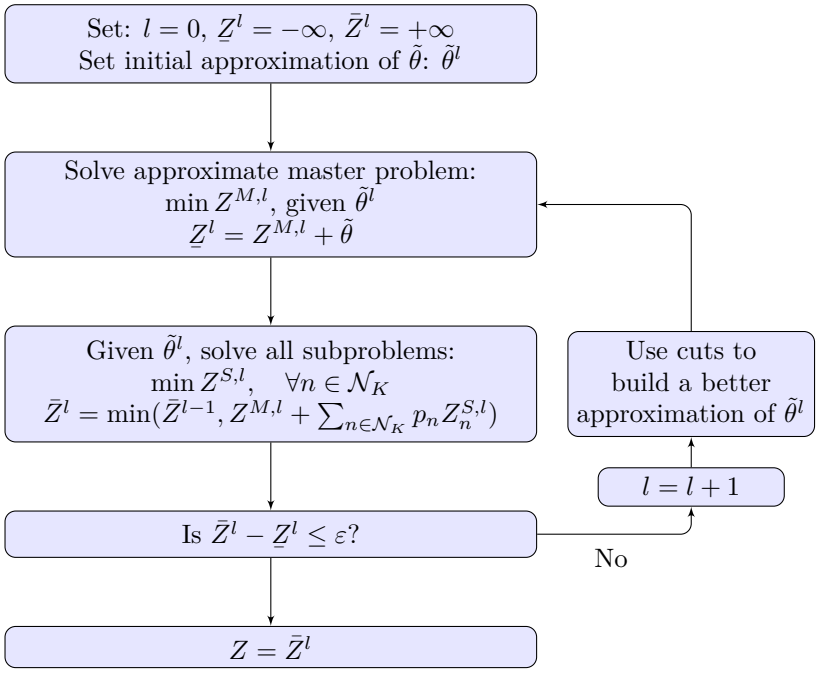

Figure 5.2: Simplified scheme of Benders decomposition algorithm

A highly simplified structure of the algorithm is presented in figure 5.2. This flow chart is not a general representation of the algorithm, and it omits any conditional constructs related to e.g. infeasibilities, etc. For a more thorough elaboration and proves of Benders decomposition, please refer to e.g. [35], or proof in section A.2.

5.3.4 Correction of uncorrelated inflows

In reality, inflows are subjects to correlations both in space and time[36], and these aspects should be included in the operation planning. In the SFS procedure as described above, the master problem is subject to one inflow scenario, and the subsequent subproblems are subject to $|\mathcal{N}_K|$ different inflow scenarios. If the scenarios in the subproblems are implemented directly with a discrete uniform distribution, there might be abrupt changes in inflows, from one time stage to the next, i.e. there is a need to smooth the transition of the stochastic inflow variables between the time stages. In [13] a correction approach was presented, which was later implemented in the SOVN model:

$$\hat{v}_{j,n} = v_{j,n}\left[1 + \frac{v_{t,m} - v_{t,n}}{\bar{v}_j}\frac{\sigma_j}{\sigma_t}a^{j-t}\right], \quad \forall n \in \mathcal{N}_K \tag{5.13}$$

where:

$\hat{v}_{j,n}$ Corrected inflow in week j subject to scenario n

$v_{j,n}$ Real inflow in week j subject to scenario n

$v_{t,m}$ Inflow in first-week t and first-week scenario m

$\bar{v}_j$ Average inflow in week t

a^{j-t} Correlation coefficient to the power of $j-t$

σ_j Inflow standard deviation for week j

The correlation coefficient a is typically set to $0.6-0.8$. As can be seen, the difference $v_{t,m} - v_{t,n}$ can be both negative and positive, and this governs whether the original inflow should be regulated up or down. Also, as the exponent $j-t$ increases the level of correction goes to zero. This is intuitive, as future correlation weakens over time.

5.4 SOVN.ctrl file

The simulation procedure in SOVN is less complex than that in the EMPS model, in the sense that the entire set of modular programs is replaced by one program performing the SFS algorithm. Every simulation in SOVN is subject to a control file which can be modified by the user[37]. This file contains double, integer and boolean parameters, and is used as exogenous input to the model. An example of such a file is given below:

```
MAXITER          ,             200 ,
NWEEKSCEN        ,              13 ,
NSCEN            ,               7 ,
MINDIFF          ,       0.100D-04 ,
V_REFCOST        ,          10.000 ,
NCUT             ,               0 ,
LSEKV            ,               0 ,
LASTWEEKSEQ      ,               1 ,
LASTWEEKACC      ,              13 ,
MAGMINGRENSE     ,           0.200 ,
NSES             ,               1 ,
SESWEEK          ,           1,  52 ,
CSPILLSCEN       ,           0.000 ,
CSPILL           ,           0.020 ,
CBYPASSSCEN      ,           0.000 ,
CBYPASS          ,           0.010 ,
CPENUPPERRES     ,           7.000 ,
CPENRES          ,         300.000 ,
CPENQMIN         ,         200.000 ,
CPENQFOMIN       ,         200.000 ,
FYEARSIM         ,               1 ,
NYEARSIM         ,               7 ,
RGREIDDATA       ,               0 ,
```

A brief explanation of the most important parameters are given below. These parameters are the most central to understand how the SFS is implemented, thus certain generic parameters are omitted. In section 7.2 the sensitivity of the SOVN model to changes in some of these settings is tested.

- **MAXITER**
  The maximum number of iterations in Benders decomposition.
- **NWEEKSCEN**
  As mentioned, the last week of the scenario fan is coupled to the water value matrix from the EMPS model, it can thus be said that the length of the scenario fan determines the level of autonomy of the SOVN model. With a sufficiently long time horizon, the reservoir levels at the end of the second-stage problem will be "decoupled" from that in the first-stage problem.
- **NSCEN**
  Number of inflow scenarios in the scenario fan. Setting NSCEN=0 results in a problem formulation without any second-stage problems. The weekly problem will then be reduced to the master problem. Setting NSCEN=1 results in a deterministic problem with only one inflow scenario for the second-stage problems. Setting NSCEN equal to the number of inflow years results in a full scenario fan. Any numbers between this and 1 results in a reduced scenario fan, where the algorithm picks a set of appropriate inflow scenarios for each week.
- **MINDIFF**
  The predetermined convergence criterium referred to as ε in subsection 5.3.3.
- **SEQ**
  SEQ=0 means accumulated simulation, and SEQ=1 means sequential simulation. The former is the most widely used approach, and it entails aggregation of the weekly load periods. With e.g. five weekly load periods, it will thus be five weekly simulations. Sequential simulation, on the other hand, could best be understood by an example: Starting at Monday, the 6 hours in load period NIGHT is simulated, followed by 2 hours in MO-EV, which in turn is followed by 5 hours in PEAK, and so on. The same procedure is done in order for the remaining days of the week. Obviously, this will lead to far more weekly simulations than for the accumulated simulation approach, resulting in longer simulation time. On the upside, sequential simulation can incorporate physical aspects, such as start-up costs, where the actual order of the load periods is significant.
- **LASTWEEKSEQ** and **LASTWEEKACC**
  LASTWEEKSEQ and LASTWEEKACC refer to the week when the scenario fan enters a new type of time resolution.
- **NYEARSIM**
  Number of historic inflow years.

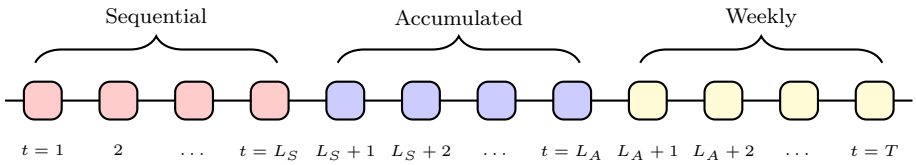

Figure 5.3: Distribution of simulation modes in the time domain

5.5 Stochasticity with limited computational capacity

When initiating a simulation the user must determine the number of cores to be used. A good practice is to run simulations with $N + 1$ cores, where N is the number of inflow years. This is a consequence of the problem structure, where the cores can solve the master problem and the N subproblems in parallel. This parallelization contributes to faster simulation, but it also reveals the compuational scale of the problem.

In stochastic optimization the *expected value of perfect information*, or EVPI, is the difference between the wait-and-see and here-and-now approaches, and given as

$$EVPI = WS - RP \tag{5.14}$$

Given a finite set of stochastic scenarios, the wait-and-see approach involves solving the optimization problem for every stochastic scenario, and – given the probability distribution of the set – compute the expected value of these optimal solutions. This value corresponds to WS. RP is the value of the recursion problem, which is the two-stage problem described earlier in this chapter[38]. Generally, the EVPI decreases with the number of inflow years in the stochastic set, i.e. in order to obtain the least uncertain results one should include as many inflow years as possible. However, in most cases the number of historic inflow years would surpass the number of cores. Thus, there is a trade-off between fast computational time and low EVPI. This trade-off is likely depending on the type and purpose of the simulation.

Chapter 6
Power system data and scenarios

This chapter aims to provide a brief overview of the power system data, and also to elaborate on the choice of case scenarios. In section 6.1 the construction of the new data set is covered, section 6.2 gives an overview of the power system and section 6.3 presents the set of case scenarios.

6.1 New data set

6.1.1 Overview and topology

The SOVN and EMPS models are based on the same underlying data, with different simulation approaches. For this thesis a new set of data was constructed, aiming to minimize computational time while still maintaining the complexity of a diverse power system. The four northernmost subareas in Norway where chosen for the simulations, and the schematic representation is given below in figure 6.1.

The subareas given in blue, i.e. FINNMARK, TROMS, SVARTISEN and HELGELAND[1] represent the simulable subareas. These subareas are described with a very high level of detailed information regarding production, demand, etc. The adjacent subareas in red, i.e. SE1, SE2 and NO3, denote the exogenous surroundings to the simulable set of subareas.

6.1.2 Construction of the data

The new data set was constructed based on Statnett's basic data set *2020 Basis (sbds027)*. This basic data set contains 32 subareas with a particular emphasis on the Nordic region, whose power system is described in great detail. Great Britain, The Netherlands, Germany, Poland and Russia are exogenous inputs to the model and

[1] Please note that, throughout this thesis, the subareas in the model are referred to in capital letters. This is done in order to distinguish them from their corresponding geographical counties and regions, which are referred to in lowercase letters. Also note that the subareas do not fully coincide with the real geographical borders.

the Baltic countries are described with some degree of detail. All the subareas given in figure 6.1 correspond to subareas in the basic data set. The simulable subareas are simply retrieved from the basic data set, whereas the exogenous subareas, i.e. SE1, SE2 and NO3, are based on SVER-SNO1, SVER-SNO2 and TRONDELAG, respectively. Their names have been changed in order to emphasize the fact that they are merely dummy nodes in the system. In the remainder of this subsection, a brief overview of the modifications is presented.

6.1.2.1 Price files

The basic data set was first simulated with grid losses. Price files for the exogenous subareas were generated using the program *GENPRIS*. This program simply take the simulated prices as input and generate price files which can be read and interpreted by the EMPS model. The generated price file for NO3 works as the main price sequence in the new data set.

6.1.2.2 .ENMD and .DETD files

The .ENMD and .DETD files are unique to each subarea. The former contains a general overview of firm contracts, load profiles, etc., whereas the latter contains a detailed description of the hydropower system in the subarea. The .ENMD and .DETD files for the simulable areas were copied from the basic data set into the new folder. The .ENMD files for the exogenous subareas on the other hand, were made based on the .ENMD file for Germany in the basic data set.

6.1.2.3 MASKENETT.DATA

The file MASKENETT.DATA contains aggregated transfer capacities between subareas, to be used as transfer constraints in the models. For the new data set, this file was modified, in order to only cover exchange capacities related to the simulable subareas[2]. This can be seen in figure 6.1 where SE1 and SE2 are connected to TROMS and HELGELAND, respectively, but not to each other. A summary of the transfer capacities is found in table 6.1.

6.1.2.4 Miscellaneous files

Subareas specific files related to wind power, regulated and unregulated inflows, etc. were copied to the new data set, in addition to general files related to price sections, and files containing commands related to the running and operation of the simulations.

[2]In the basic data set, FINNMARK is also interconnected with FIN-NORD. However, due to the low transmission capacity and the wish to minimize computational effort, FIN-NORD was neglected for convenience.

6.2 The power system of Northern Norway

The power system of Northern Norway is subject to certain general characteristics as well as local and regional issues. On a large scale, Northern Norway is characterized by its potential for growth in both generation, especially from land based wind power. Nevertheless, there are local bottlenecks that isolates parts of the northern grid. This can lead to challenges in order to meet the projected developments. The case study presented in this thesis aims to enlighten some of the effects caused by increased deployment of wind energy to make a qualitative assessment of the EMPS and SOVN models.

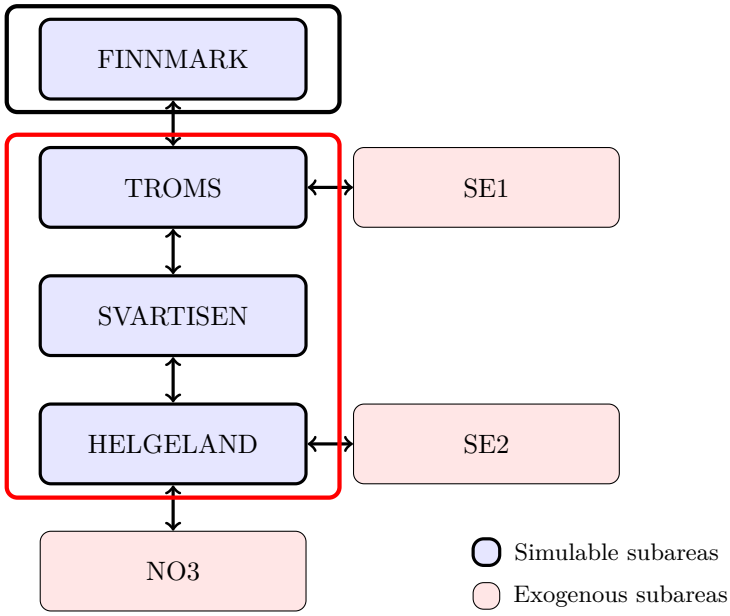

Figure 6.1: Topology of simulable and exogenous subareas

The black and red rectangles as seen in figure 6.1 represent different price areas, i.e. areas with limited transmission capacity to adjacent regions. The red rectangle encapsulate three subareas into an *ad hoc* aggregate region named NORD. As seen in table 6.1 these three subareas are joined by virtually unlimited transfer capacities. Under such conditions the price structures will remain uniform, and any price difference is simply due to a transfer fee of 0.1 €/MWh implemented in the models. The capacity constraints limit the potential for future wind energy development in the region, since there are problems transporting the surplus energy to areas with demand sufficient demand. On a grand scale, there are several ways to stem this problem:

- **Improved hydropower scheduling**
  Improvements in the planning part of the power system operation may provide a better allocation of the water, in order to achieve a more efficient utilization within the limits of the power system.

- **Stimulate growth in the industry**
  There is already a well established industry in the region, and due to the energy surplus, there is potential for further development in the industrial sector. Greater industry could increase the demand for power, and thus contribute to reducing the capacity problems.

- **Increase transmission capacities**
  Increased transmission capacity could increase the flexibility of the area and alleviate problems related to transportation of surplus power and energy.

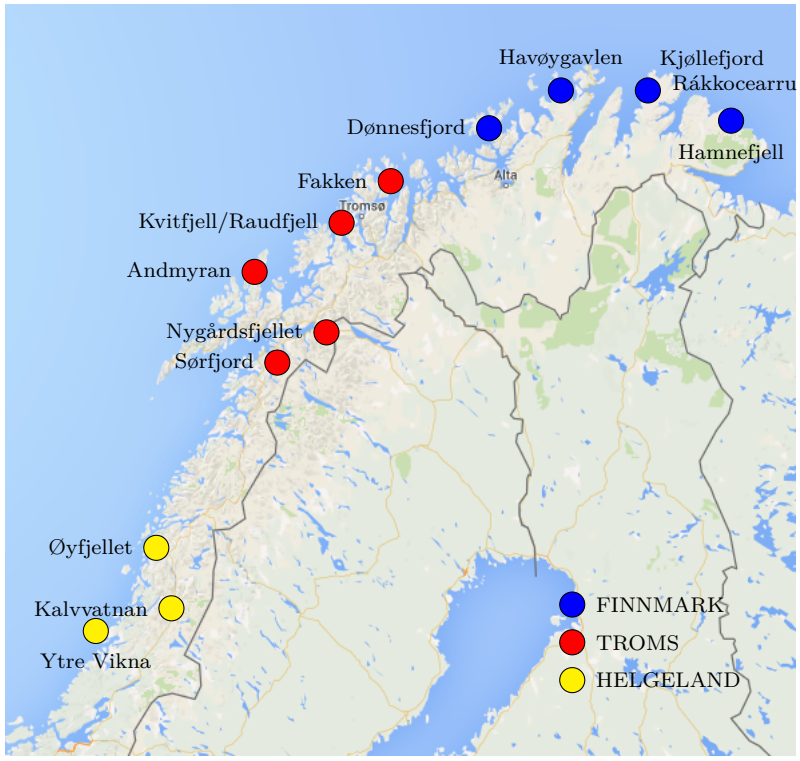

Figure 6.2: Locations of wind farms[1] and industry sites

Figure 6.2 shows the location for all wind parks in the model.

6.2.1 Wind farms

The set of wind farms consists of existing projects as well as major projects with licenses granted from NVE. As shown in the map, there is a huge potential for wind power development along the coast of Northern Norway. These wind farms are usually located in areas with poorly developed infrastructure, but this issues goes beyond the scope of this thesis. The wind in the model is represented by wind series, i.e. recorded wind speeds for certain areas which form the basis for the wind power generation. The wind farms in the model are all affiliated with a wind series and a conversion factor. This conversion factor is equivalent to installed capacity in MW, which in turn results in an annual production in GWh.

6.3 Analysis approach

The case study aims to investigate the effect of increased wind power development. For this, four separate cases are to be analyzed, as shown in figure 6.3.

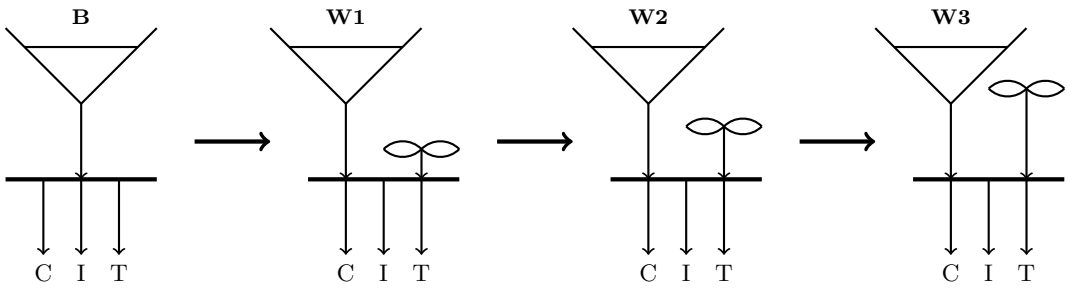

Figure 6.3: Case scenarios

The figure shows simplified schemes of the power market in the region. The supply side is represented by hydro and wind power, and the demand side is broadly divided into three categories, i.e. inelastic consumption (C), price elastic industrial consumption (I) and trade to/from adjacent regions (T). The height of the wind turbine merely indicates the relative magnitude of wind power development in the different cases, relative to the base case.

6.3.1 Exchange capacities

The transmission capacities between the subareas are given in table 6.1 below. Note that certain cuts have different restrictions for maximum power transfer depending on the direction of the flow.

Cuts			To	From
FINNMARK	⇔	TROMS	400	500
TROMS	⇔	SVARTISEN	9.000	9.000
TROMS	⇔	SE1	600	600
SVARTISEN	⇔	HELGELAND	9.000	9.000
HELGELAND	⇔	SE2	350	350
HELGELAND	⇔	NO3	1.300	1.300

Table 6.1: Exchange capacities in MW between subareas

6.3.2 Wind energy development

Wind farm	Subarea	B	W1	W2	W3
Donnesfjørd	FINNMARK	0	10	10	10
Havøygavlen	FINNMARK	40	40	40	40
Kjøllefjord	FINNMARK	40	40	40	40
Rákkocearru	FINNMARK	45	200	200	200
Hamnefjell	FINNMARK	0	120	120	120
Additional	FINNMARK	0	0	500	1.000
Andmyran	TROMS	0	160	160	160
Nygårdsfjellet	TROMS	40	40	40	40
Kvitfjell/Raudfjell	TROMS	0	300	300	300
Fakken	TROMS	60	60	60	60
Sørfjord	HELGELAND	0	90	90	90
Additional	TROMS	0	0	500	1.000
Ytre Vikna	HELGELAND	40	250	250	250
Kalvvatnan	HELGELAND	0	225	225	225
Øyfjellet	HELGELAND	0	330	300	300
Additional	HELGEAND	0	0	500	1.000
	Total:	265	1.865	3.365	4.865

Table 6.2: List of wind farms and their corresponding capacity in MW

The wind energy in the scenarios are based on existing wind farms and projects with license from NVE. Case B represents the default power system given in Statnett's 2020 basic data set. For case W1 the wind power development corresponds to

the total amounts of concessions granted at the present time, i.e. that all current concessions are realized. Cases W2 and W3 have an additional 1.500 MW and 3.000 MW of wind energy, respectively, distributed equally on FINNMARK, TROMS and HELGELAND.

6.4 Pumped storage hydropower

Pumping is the reverse process of power generation, where water is relocated from a downstream to an upstream reservoir. As shown in [12] EMPS only covers seasonal pumping, which fails to fully utilize the short-term flexibility of the hydropower system. The main reason for this is the fact that short-term pumping or day-to-day pumping involves utilization of the difference in water values between two hydrologically coupled reservoirs. In SOVN on the other hand, the water values are implicitly obtained from the cuts in the Benders decomposition, as shown in subsection 5.3.3. In their report on pumped storage production[39], NVE points out Northern Norway as an ideal region for developing pumped storage hydropower. This is seen in context with the grid bottlenecks, and the high potential for wind power development.

The pumping scenarios in the case study are based on the wind power scenarios as given in subsection 6.3.2. In addition to the original scenarios, a set of similar secondary scenarios are introduced. These cases also cover increased wind power penetration, but the price files of the exogenous subareas are replaced with similar price files for Germany. The prices in Germany are generally more volatile than in the Nordic region, due to the combination of intermittent renewables and expensive balancing gas units. This will alter the price structure of Northern Norway, and help provoke greater volatility which should stimulate the utilization of pumping units.

In the remainder of this section the new pumping stations, along with any additional required changes, are presented. The original data set has no pumps, and in order to implement them certain assumptions regarding flows and elevations, etc. have been made.

	FINNMARK		TROMS	
	Lassajávre	Småvatna	Slunkajávre	Rekvatn
Reservoir cap. [GWh]:	109.21	74.20	88.80	40.81
Nom. discharge height [m]:	145	225	245	207
Contour heights [m]:	674-692	519-543	516-531	272-283

Table 6.3: Reservoir data for pumped storage production

For the analysis of pumping pattern, two pairs of subjacent reservoirs were chosen. Finding ideal sites for pumped storage production can be rather tricky as the pump should connect two reservoirs with a certain storage capacity and capability. One site in FINNMARK and one in TROMS have been chosen, to see the difference in pumping utilization for the two different price markets. Two large pumps of 700 MW were chosen in order to enable transport of large amounts of water in short time periods. This decision is based on the fact that the reservoirs can only store water for a few months at the time, thus making seasonal pumping counterproductive.

The reservoir data is given in table 6.3, and parts of the watercourses are shown in figures 6.4 and 6.5.

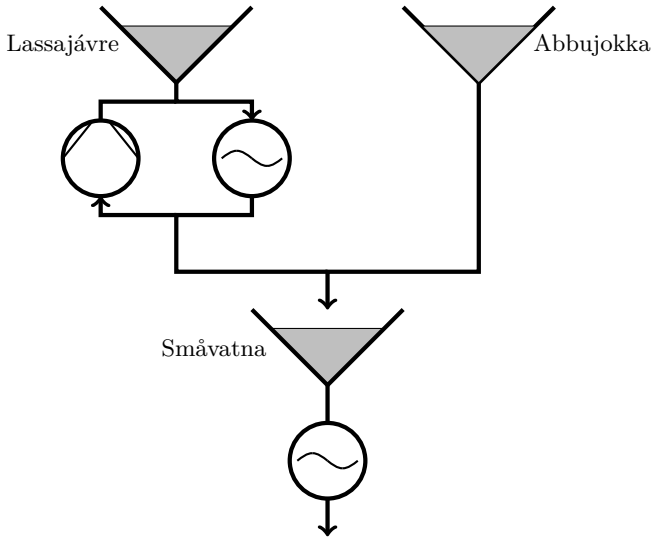

Figure 6.4: Part of Kvænangen watercourse

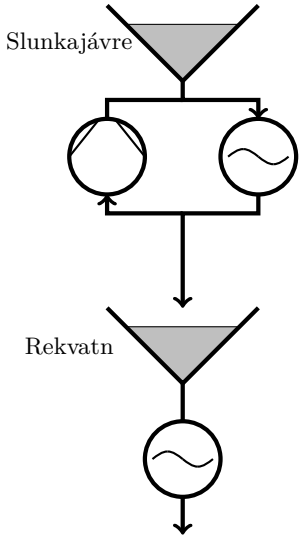

Figure 6.5: Small part of Sagfossen watercourse

Chapter 7
Results

This chapter contains a thorough presentation of the results obtained from the EMPS and SOVN simulations. The first section, 7.1, deals with issues related to model calibration in EMPS. In section 7.2, simulations are run for various settings of the `SOVN.ctrl` file to evaluate the sensitivity of the simulation results to changes in simulation settings. The subsequent sections deal with the case study presented in chapter 6. A brief overview of these sections and what they aim to cover are given below:

7.3: Impact on prices and price structures.
7.4: Changes in production pattern.
7.5: Utilization of transfer capacities.
7.6: Handling of spillage.
7.7: Ability of SOVN to handle pumped storage production.
7.8: Socioeconomic performance of the models.

For the analysis in this chapter, it is referred to a number of statistical entities that are defined in appendix D. In order to avoid confusion, the figures are properly labeled with axis units, etc., and for comparative figures, results from EMPS is consistently placed to the left and results from SOVN to the right. The simulation tool used will also be shown on the actual figure.

The scope of this chapter is only to present the data in a clear manner. The tables and figures are the most essential product of this chapter, but brief descriptions and explanations will be provided along the way. The results presented in this chapter are the foundation for the in-depth analysis given in chapter 8.

7.1 Model calibration

As mentioned, one of the greatest uncertainties with the EMPS model is the need for extensive user input. The model calibration is one of these forms of model-user interaction, where the user has to evaluate the results and possibly modify the simulations in order for them to better represent the realistic power market.

The need for model calibration arises when, among other things, the reservoir curves are deformed, i.e. if they have an unnaturally high or low profile, low seasonal differences, etc. Note that the calibration does not alter the reservoir curves, themselves, but rather inherent market mechanisms which ultimately affect the shape of the reservoir curves. The policy of Statnett is to calibrate the model based on historical reservoir curves. For this analysis it was decided to use the reservoir curves of Scenario B as a guideline for the calibration of the remaining scenarios.

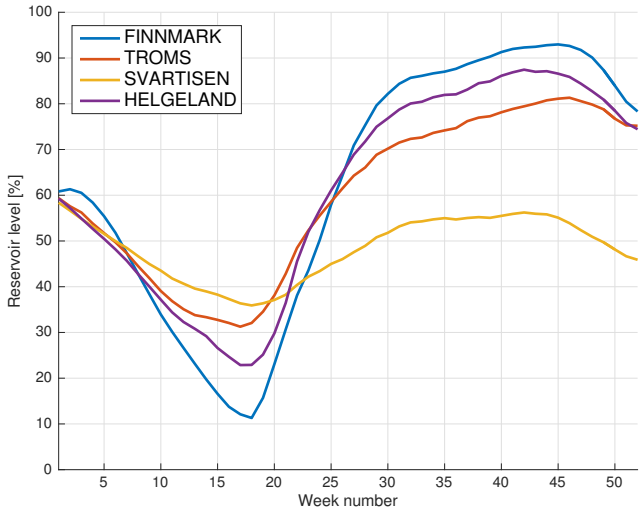

Figure 7.1: Mean reservoir curves when calibrated - Scenario B

The initial step was the automatic calibration functionality of the EMPS model. When initializing the automatic calibration, an input file will be generated prior to the iterative calibration procedure. In this input file, the end user could specify the *modus operandi* of the heuristic algorithm. By default, the algorithm will tune the three factors such as to maximize socioeconomic surplus. For this calibration it was chosen to adjust these to best mimic the reservoir curves of Scenario B. In order to achieve this, a set of reservoir levels was added to the input file for reference. Reservoir

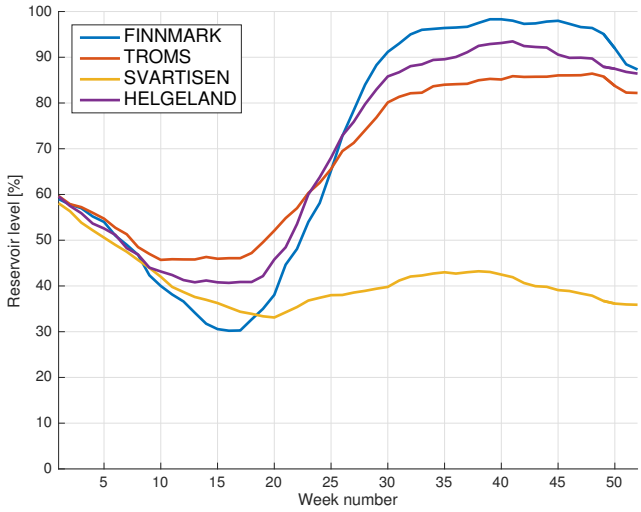

Figure 7.2: Mean reservoir curves when *not* calibrated - Scenario B

levels for weeks 1, 17 and 44 were chosen. The resulting mean reservoir profiles for all subareas are shown in figure 7.1 above[1]. Figure 7.2 depicts the mean reservoir curves for Scenario B *without* calibration. As seen, all subareas but SVARTISEN, has a higher profile than in figure 7.1, i.e. there is more water in the reservoirs throughout the entire year. Also there is a general tendency to withhold production in the spring when the reservoirs normally would be drained due to expected inflow from the melting snow. Note that the calibration of the EMPS model is indeed subject to great uncertainty. It was attempted to calibrate the model to the best effort, but to achieve a perfect calibration could be very demanding.

[1]Note that SVARTISEN consists of one watercourse with a very large reservoir, hence the significant difference in shape

7.2 Performance testing of the SOVN model

The SFS algorithm of SOVN can to some extent be modified by the user. In section 5.4 the `SOVN.ctrl` file was discussed. As stated, this file provides opportunity for the user to modify the simulation procedure itself in a number of ways. In addition to this, the user also has the opportunity to adjust more generic settings, related to e.g. set of inflow years to be used in the simulations, number of computational cores, etc. Such degree of user input is a feature which is more applicable in the SOVN model than the EMPS model. There are two main reasons for this: Firstly, SOVN is a computationally highly demanding model. Depending on the user needs, there may be good reasons to simplify certain aspects of the simulation in order to reduce simulation time – which can indeed be substantial; secondly, the simulation in SOVN is solely based on the SFS algorithm, which is highly flexible. The simulations in EMPS on the other hand, follows a flow of modular programs and are thus more rigid.

A number of simulations with different settings were performed on the Northern Norway data set to test for simulation time, reservoir allocation and socioeconomic surplus. The tests shown below are the last ones from a long sequence of test from different versions of SOVN. When these initial tests began in the autumn of 2015, the first results showed some major logical errors such as consistently higher prices in surplus areas, draining of reservoirs during the filling season, etc. These results were then reported back to SINTEF Energy Research, who performed the debugging, resulting in new versions of SOVN on which new tests were performed. This iterative procedure went back and forth between testing and debugging for several weeks, eventually resulting in a version of SOVN thought adequate and from which the results of this thesis are obtained.

The main purpose of these simulations is merely to investigate the impact of adjusting the settings in the SOVN model. It should be noted that the results themselves are not the most essential in this context, but rather the relative differences in results for the different settings.

7.2.1 Overview of settings

Referring to section 5.4, a selection of settings was chosen for investigation based on their fundamental effect on the simulation algorithm, and hence their expected impact on the overall simulation performance. Below is a list of these settings:

- NWEEKSCEN
- LASTWEEKSEQ
- LASTWEEKACC

Setting	NWEEKSCEN			LASTWEEKACC			LASTWEEKSEQ		
Simulation name	T13	T26	T52	L4	L26	L52	S1	S4	S13
nweekscen	**13**	26	**52**	26	26	**52**	26	26	26
NScen	7	7	7	7	7	7	7	7	7
SEQ	0	0	0	0	0	0	**1**	**1**	**1**
LastWeekSeq	1	1	1	1	1	1	1	**4**	**13**
LastWeekAcc	13	13	13	**4**	**26**	**52**	13	13	13
First year	1982	1982	1982	1982	1982	1982	1982	1982	1982
Number of years	7	7	7	7	7	7	7	7	7
Number of cores	8	8	8	8	8	8	8	8	8

Table 7.1: Various settings in SOVN.ctrl

The different test cases are classified by categories and presented above. All test were run for the same inflow years, i.e. 1982-1988, and with equal number of cores.

The settings can be subdivided into three categories: Adjusting the time horizon, i.e. length of the scenario fan; changing the number of weeks with *accumulated* time resolution; changing the number of weeks with *sequential* time resolution. T26 is the base case, and any changes relative to T26 is given in boldface figures. Testing of deterministic simulations, i.e. setting NScen equal to 1, were also performed, but these tests failed consistently.

7.2.2 Analyzing the impact of changed settings in `SOVN.ctrl`

The causal effects of changing selected settings in the control file is to be investigated in this subsection. Based on the assessments, this analysis will also work as reference for the further simulations in SOVN. The model performance will be viewed in terms of three parameters: Reservoir handling, price distribution and socioeconomic surplus. Obviously, these parameters are macroscopic entities, and fails to enlighten the performance of the model at a detailed level, but this bottom-down perspective is adequate to evaluate the overall impact of the different settings on the model. Throughout this assessment, TROMS is the object of analysis. This is done of the basis that TROMS is the largest subarea in the model in terms of the number of reservoirs.

7.2.2.1 Reservoir allocation

Figures 7.3 to 7.5 depict the mean aggregate reservoir development for TROMS, for each of the specific cases. The base case T26 is shown as a dashed line, and

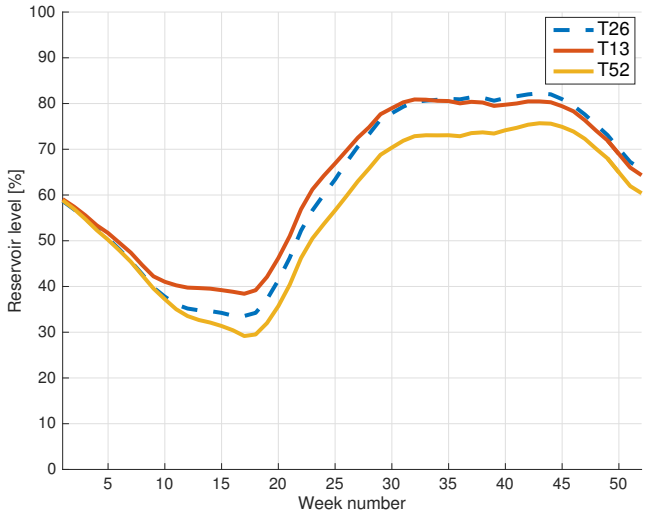

Figure 7.3: Aggregate reservoir level for varying time horizons - TROMS

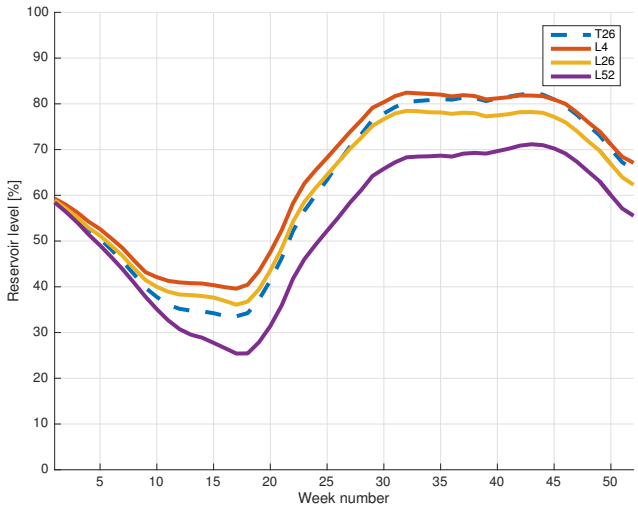

Figure 7.4: Aggregate reservoir level for varying accumulated load periods - TROMS

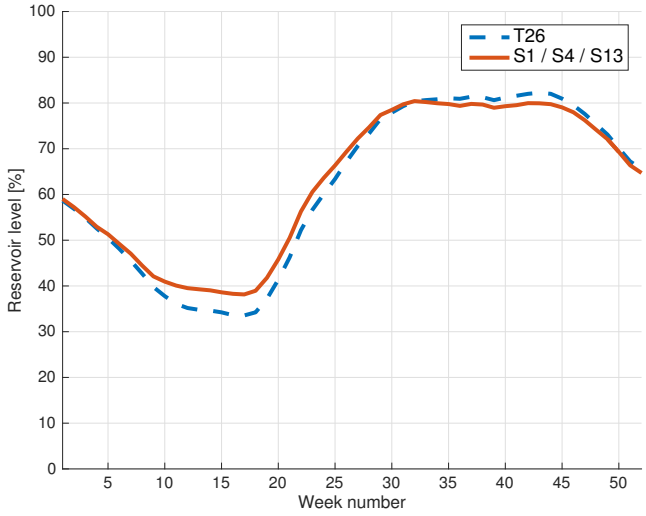

Figure 7.5: Aggregate reservoir level for varying sequential load periods - TROMS

represents the reference.

For all cases, the reservoirs starts at 60%. As can be seen, the reservoir curves all follow a fairly predictive pattern, i.e. drawdown season during the autumn/winter and filling season during the spring/summer. Comparing the reservoir curves, it seems that the central setting is related to the length of the scenario-fan. Shorter scenario fans gives higher water values, which results in less production and higher reservoir levels. As seen in figure 5.1 the end values of the scenario fan are linked to the water value matrix of the EMPS model. With a shorter time horizon, the impact of the EMPS strategy will be greater. SOVN has not implemented a functionality to obtain mean aggregated water values for the subareas, which makes it difficult to fully test the following hypothesis, but through propositional logic it could seem that, since higher water values result in higher reservoir levels and the simulated cases with highest reservoir levels are most influenced by the EMPS strategy, SOVN is generally calculating the water values lower than EMPS. Also, as shown in figure 7.5, all sequential simulations, i.e. S1, S4 and S13, have completely congruent reservoir curves. One explanation for this might be the fact that they all have the same time horizon in their scenario fans.

7.2.2.2 Price distribution

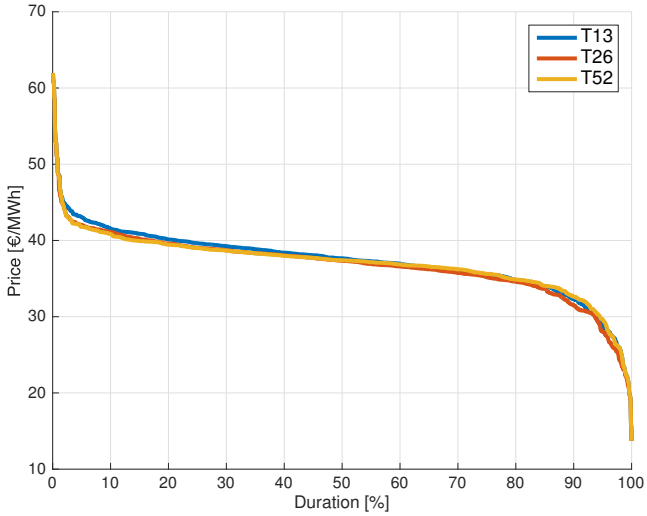

Figure 7.6: Price duration curves for varying time horizons - TROMS

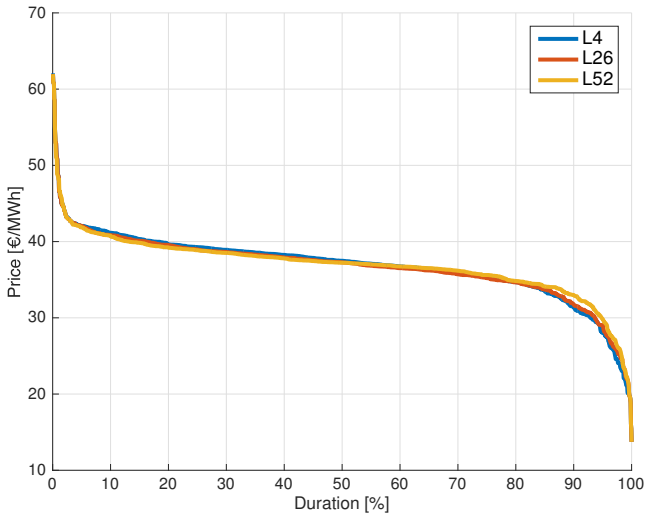

Figure 7.7: Price duration curves for varying accumulated load periods - TROMS

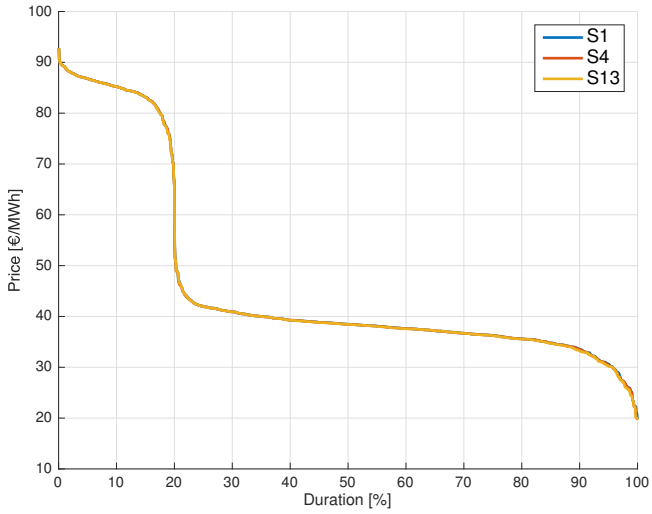

Figure 7.8: Price duration curves for varying sequential load periods - TROMS

Price duration curves for the different cases are presented in figures 7.6 to 7.8. They show, for most settings, very similar price distributions. Besides, the duration curves also imply a continued price distribution with fairly modest deviations. The exception is found in figure 7.8, where there seems to be a secondary and much higher price level for approximately 20% of the time. As a realistic representation of the prices, this is plain wrong, and must be attributed to an error in the implementation of the sequential time resolution.

As a side note, it should be mentioned that the impact of the exogenous price files are so dominant, that one should not expect great deviations in price structure based on the different settings alone.

7.2.2.3 Simulation time

A central assessment of the simulation settings concerns the simulation time. There is a trade-off between precise results and simulation time that the user must consider. In the table below are the simulation times for the different settings.

	T13	T26	T52	L4	L26	L52	S1	S4	S13
Time spent [hh:mm]:	00:56	01:19	02:40	00:26	04:35	21:56	01:44	11:33	81:21
Perctg. of T26 [%]:	71	100	203	33	348	1666	132	877	6178

Table 7.2: Simulation time for different settings

7.2.2.4 Socioeconomic surplus

The socioeconomic performance of the simulations are presented in table 7.3 below. Apart for the sequential simulations, the operational performance varies very little with the changed settings. Obviously, the simulation of sequential time resolutions should not be paid much attention anyway, as these are shown to be wrong.

	T13	T26	T52	L4	L26	L52	S1	S4	S13
Surplus [10^9 €/y]:	13.05	13.03	12.91	13.05	13.01	12.82	10.48	10.47	10.47
Perctg. of T26 [%]:	100.2	100	99.1	100.1	99.8	98.4	80.4	80.4	80.4

Table 7.3: Total socioeconomic surplus for different settings

The following sections contain results from the case scenarios introduced in section 6.3. For this, the scenarios B, W1, W2 and W3 are to be analyzed. Throughout the remainder of this thesis, it will be referred to the *ad hoc* region NORD, which is composed of the three subareas TROMS, SVARTISEN and HELGELAND. This aggregate region is shown in figure 6.1. The next sections will provide the figures and tables obtained from the simulations, and present them in an ordered fashion. The accompanying text aims to describe and explain the figures, but the in-depth analysis of the results is first conducted in chapter 8. The reason for this is the fact that the figures must be seen in conjunction with each others to form an overall picture. Based on the assessment in section 7.2, it was chosen to run the simulation with settings similar to T26. In order to achieve the best basis for comparison, the simulations in EMPS and SOVN are both run in parallel with 7 inflow years (1982-1988) as input.

7.3 Price structures

7.3.1 Mean prices and volatilities

This section will examine the effects of increased penetration of wind power production in Northern Norway on the wholesale prices. Additional results on prices can be seen in chapter D.2 in the appendix.

	Volatility				Mean prices			
	EMPS		SOVN		EMPS		SOVN	
	FINN	NORD	FINN	NORD	FINN	NORD	FINN	NORD
B	4.62	4.60	4.56	4.55	37.52	37.52	37.23	37.23
W1	5.07	4.48	4.90	4.59	36.20	36.62	35.51	35.78
W2	8.41	3.52	8.36	5.52	28.35	34.67	30.32	33.29
W3	10.82	4.36	11.31	7.68	11.34	26.39	16.88	28.91

Table 7.4: Mean prices and standard deviations

Figure 7.9 shows the trends in spot prices as function of increased wind power capacity. The solid lines represent mean spot prices taken from full sets of price data with all price segments and all inflow years. The dashed lines represent the standard deviation or *price volatility*. The line segments between the breakpoints are mere interpolations for illustrative purposes, as the prices and standard deviations are drawn from from the four scenarios given above. For simplicity, the price data for region NORD is simply drawn from subarea TROMS, as all the subareas in NORD have virtually identical prices. Numerical values are shown in table 7.4.

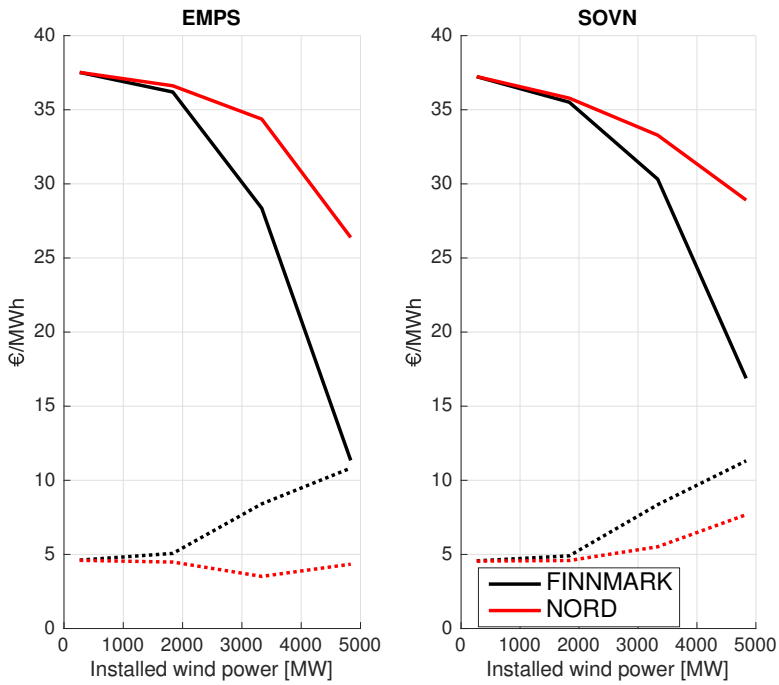

Figure 7.9: Mean prices and standard deviations

For case B it can be seen that the mean prices and volatilities for FINNMARK and NORD are very equal. Both results from EMPS and SOVN indicate largely similar price structures. This is further confirmed in the correlation matrix in table 7.5, where rank correlations between spot prices for all subareas are given. The high correlation between subareas within NORD remains for all wind power scenarios, due to the practically unlimited transfer capacity between them.

	EMPS				SOVN			
	F	T	S	H	F	T	S	H
F	1.0000	0.9929	0.9925	0.9920	1.000	0.9998	0.9994	0.9993
T	0.9929	1.000	0.9998	0.9995	0.9998	1.0000	0.9998	0.9997
S	0.9925	0.9998	1.000	0.9999	0.9994	0.9998	1.0000	0.9999
H	0.9920	0.9995	0.9999	1.000	0.9993	0.9997	0.9999	1.0000

Table 7.5: Correlation matrix between subareas - scenario B

The price structure remains largely unchanged for wind power deployment equal

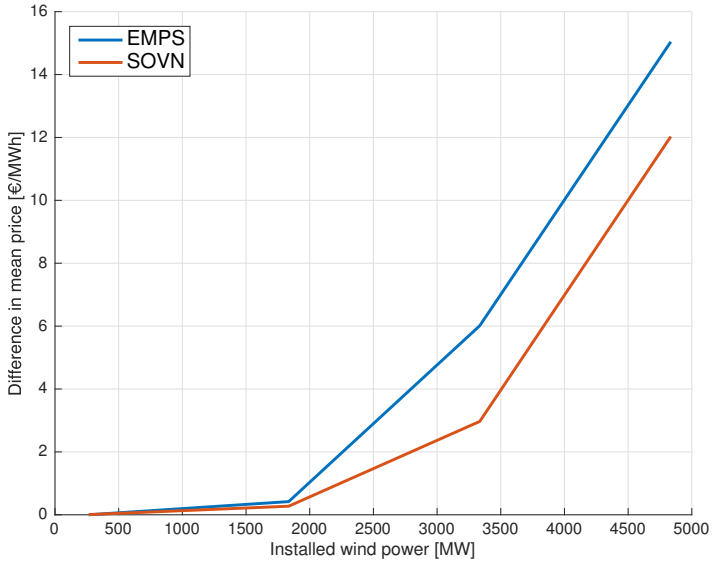

Figure 7.10: Mean price difference between FINNMARK and NORD

to that in scenario W1. This is directly in accordance with figures 7.24 and 7.25, where the transmission lines are largely uncongested. However, at some point roughly between 2,000 and 3,000 MW installed wind power the deviation in price structures becomes significant. As seen in figure 7.9, the mean prices decline as function of increased wind power production, and this decline is most noticeable in FINNMARK. Similarly, FINNMARK also has the greatest increase in price volatility. It seems that introducing vast amounts of wind energy in the region results in two new price areas.

Comparing EMPS and SOVN, it can be seen that the SFS algorithm not only reduces the absolute drop in prices seen in EMPS, it also reduces the relative price differences between FINNMARK and NORD. Referring to figure 7.10, the mean price difference between TROMS and NORD are plotted as function functions of wind power capacity. The curves actually represent the relative distance between FINNMARK and NORD in figure 7.9.

7.3.2 Occurrence of extremely low prices

As shown in subsection 7.3.1, the mean wholesale price of electricity plummeted with increased penetration of wind power. The price duration curves for all subareas and scenarios are given in appendix subsection D.2.1, where the occurrence of zero-prices, i.e. prices literally set to zero, is shown to appear rather frequently in FINNMARK.

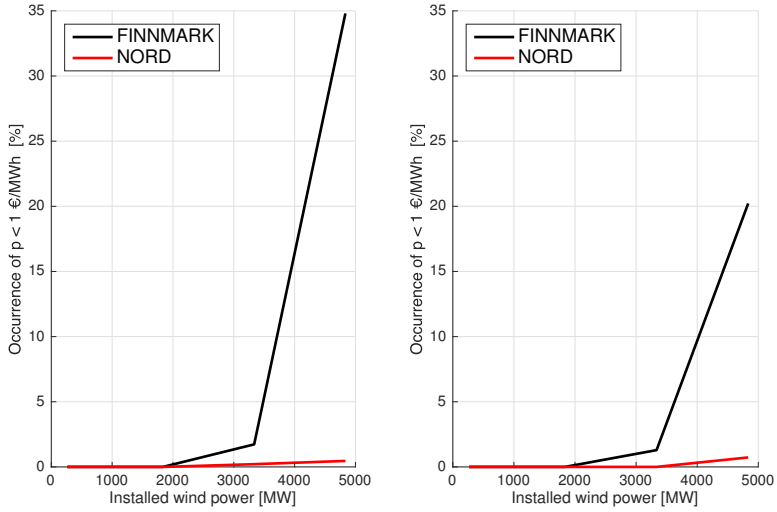

Figure 7.11: Occurrence of zero pricing in EMPS and SOVN

This is proved in figure 7.11, where the relative occurrence of such wholesale prices are shown. These numbers are adjusted to incorporate the non-uniform distribution of load segments, i.e. prices are broken down to an hourly level from which the share of extremely low prices are calculated. *Extremely low* in this case refers to prices less than 1 €/MWh.

Again, NORD is for simplicity represented by TROMS. Referring to figure 7.11, the market in NORD clears above zero nearly hundred percent of the time, even when the supply side has extreme amounts of wind power. FINNMARK, on the other hand, faces a radically different market where extremely low prices are frequent. In SOVN, hours with price less than 1 €/MWh is reduced with 42.1 % relative to EMPS. It should also be mentioned that EMPS and SOVN does not incorporate the possibility of negative prices. The possibility for this in a realistic market case is something that cannot be ruled out.

7.4 Production patterns

7.4.1 Individual changes in utilization

Figures 7.12 to 7.15 below show the percent change in full load hours between EMPS and SOVN for individual power stations as function of their respective degrees of regulation as introduced in subsection 4.2.1. The degree of regulation simply refers to the relationship between the reservoir capacity and mean annual inflow, and tells

something about the reservoir's ability to store water for long periods. The plots are generated by the formula below:

$$\Delta FLH_i = \frac{FLH_i^{SOVN} - FLH_i^{EMPS}}{FLH_i^{EMPS}} \cdot 100\% \tag{7.1}$$

where

$$FLH_i^{EMPS} = \frac{\frac{1}{7}\sum_{y=1}^{7}\sum_{n=1}^{5\cdot 52} W_{iny}^{EMPS}}{1000^{-1} \cdot P_i} \tag{7.2}$$

and

$$FLH_i^{SOVN} = \frac{\frac{1}{7}\sum_{y=1}^{7}\sum_{n=1}^{5\cdot 52} W_{iny}^{SOVN}}{1000^{-1} \cdot P_i} \tag{7.3}$$

These are the full load hours for a given power station i for EMPS and SOVN, respectively. The total annual production per year is obtained by summarizing the output in GWh over all 5 weekly price segments for 52 weeks of the year. Then, the entire simulated production is then simply calculated as the mean production over all inflow years. The resulting mean annual production is subsequently divided by the production capacity of the plant in MW to finally obtain the average number of full load hours for the power station. The Matlab script is given in appendix B.

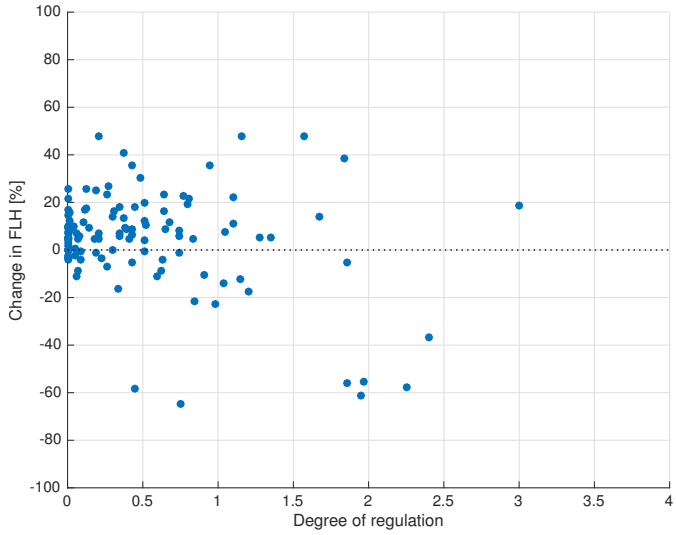

Figure 7.12: Change in utilization for individual power stations - scenario B

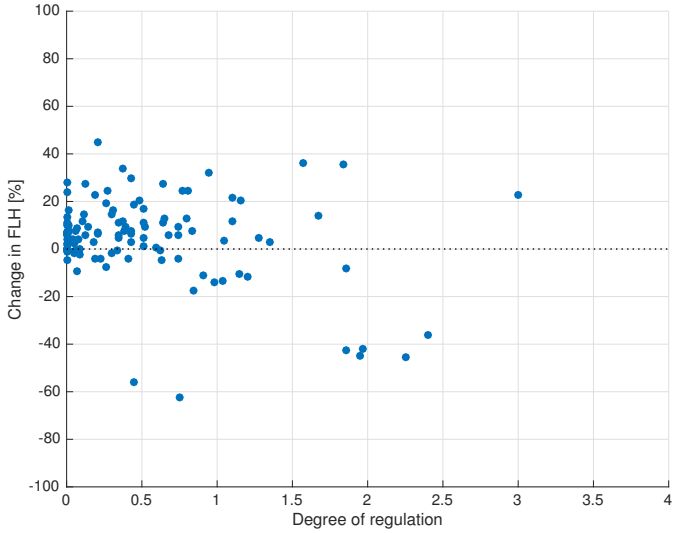

Figure 7.13: Change in utilization for individual power stations - scenario W1

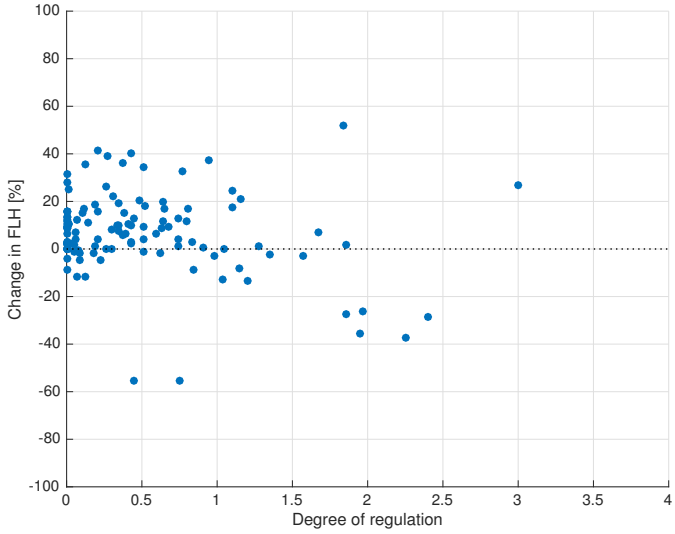

Figure 7.14: Change in utilization for individual power stations - scenario W2

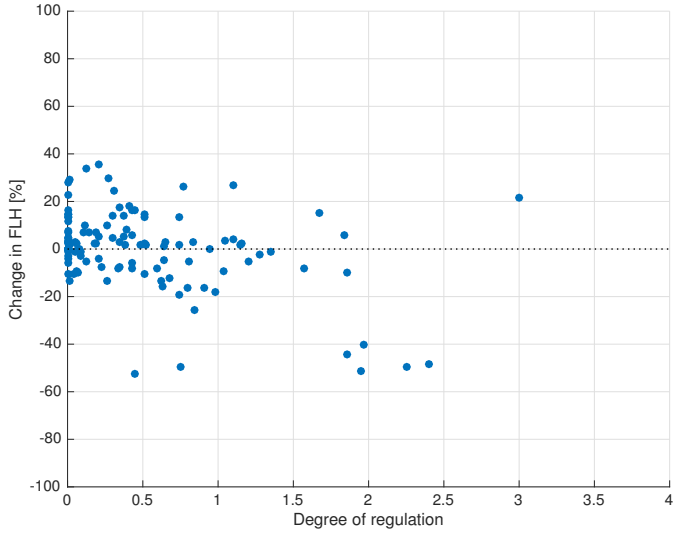

Figure 7.15: Change in utilization for individual power stations - scenario W3

As seen, the plants with low degree of regulation show propensity to increase FLH, thus increasing its output in SOVN relative to EMPS. Plants with a higher degree of regulation on the other hand, sees a decline in production, which is likely attributed to an increased tendency to save water. It should be said that the number of highly regulated reservoirs is too small to draw a full conclusion, but the indications are strong. This altered production pattern indicates the SFS algorithm's ability to minimize the occurrence of water values at zero by utilizing the flexibility of the entire hydropower system, i.e. the smaller, less regulated plants can produce more, thus reducing spillage, at the expense of the larger more regulated plants, which in turn store their water for longer periods instead of contributing to the continuous operation.

This effect is illustrated below,where the utilization of two greatly different power stations are shown. Figures 7.16 and 7.17 show the production at the power station Krokvatn in TROMS for scenarios B and W3. The left subplots show the production during a typical wet year – in this case 1982 – and the right subplots for a typical dry year – 1987. Inflow statistics are shown in appendix D.1.

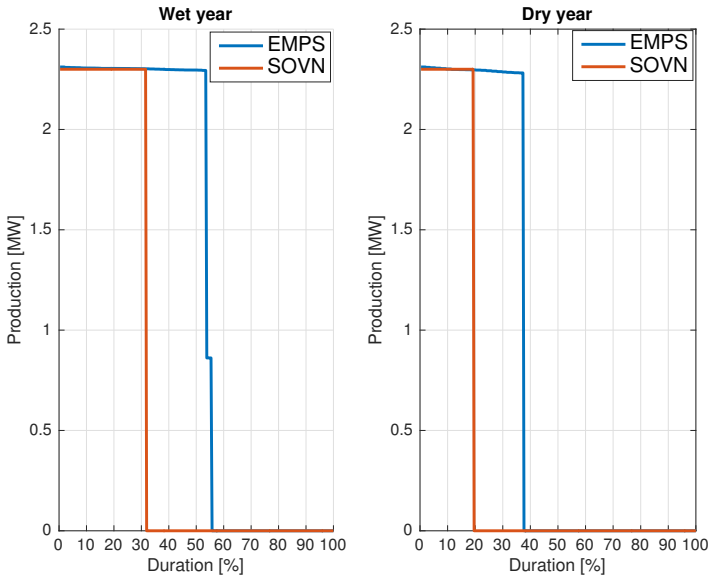

Figure 7.16: Utilization curve for Krokvatn during wet and dry year - scenario B

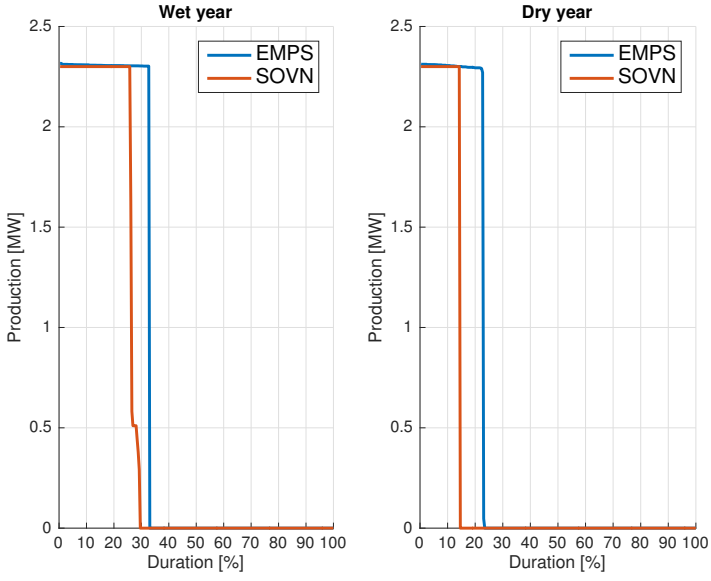

Figure 7.17: Utilization curve for Krokvatn during wet and dry year - scenario W3

Krokvatn is a small power station with a large storage capacity. The reservoir is sufficiently large to store nearly two years of inflow, given normal hydrological conditions. As seen in the figures, SOVN consistently shows lower utilization than EMPS. This gap in utilization is greatest for scenario B. This illustrates the fact that the optimization problem is relaxed with lower levels of wind power in the generation portfolio, while in scenario W3 the excess wind power causes stricter boundaries for the power producers, hence the greater coherence between SOVN and EMPS. Moreover, the output is strongly correlated with the regional inflow, with a higher production in wet years than dry years. The utilization is also severely reduces as more wind power is introduced.

Figures 7.18 and 7.19 similarly show the utilization of Sjønstå power station in TROMS. This is a large, unregulated run-of-river hydropower plant. Contrary to Krokvatn, this power station has an increased output in SOVN relative to EMPS. This may explain the reduced spillage levels in SOVN as seen in figure 7.26.

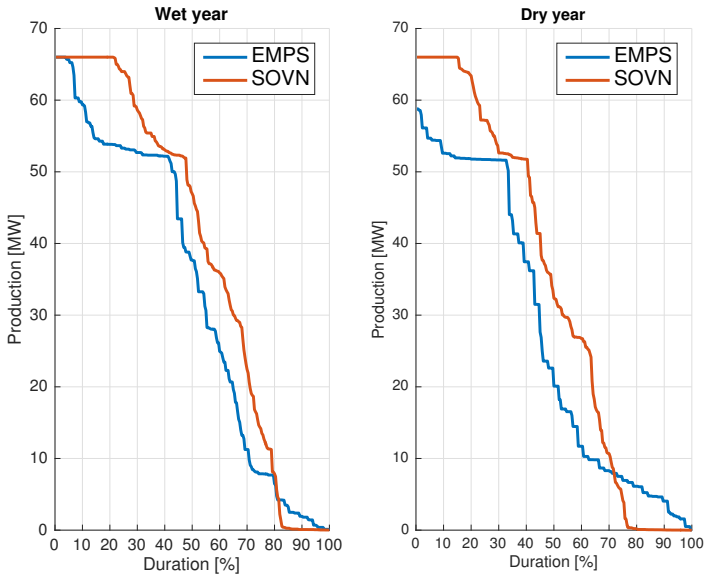

Figure 7.18: Utilization curve for Sjønstå during wet and dry year - scenario B

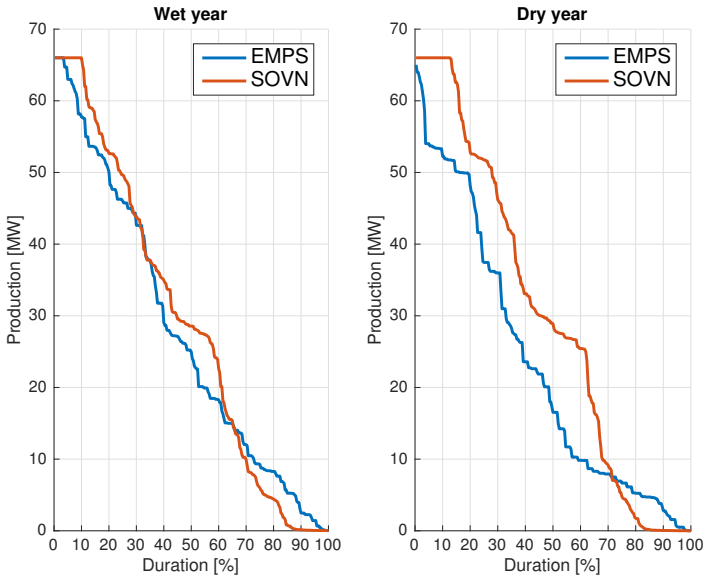

Figure 7.19: Utilization curve for Sjønstå during wet and dry year - scenario W3

7.4.2 Overall redistribution of production

The unregulated production in EMPS and SOVN is the part of the total production whose water is subject to zero opportunity value, and hence zero water value. This can arise in a number of situations, e.g. in run-of-river plants with zero degree of regulation, or in full reservoirs where the water is otherwise lost as spillage. The forced or unregulated production is comprised by the following production categories:

Unregulated production
= Production due to unregulated inflow
+ Production due to minimal flow constraints
+ Production to avoid spillage

The figures 7.20 to 7.23 show the aggregate distribution of *optional* and *forced* production for all subareas. Forced production in this case is equal to the unregulated production, and optional production is consequently the difference between total production and unregulated production.

In the figures below, optional production is shown to the left and forced production to the right. The weekly production is given as solid lines in descending order, and the related revenues are given as dashed lines in ascending order, in order to more

easily tell them apart. From the definition of unregulated or forced production, it follows that the optional production is indeed subject to an opportunity value, and this opportunity value is a manifestation of the flexibility of the hydropower system. Throughout all scenarios, SOVN shows a significant shift in production pattern from forced to optional, which is also shown in table 7.6.

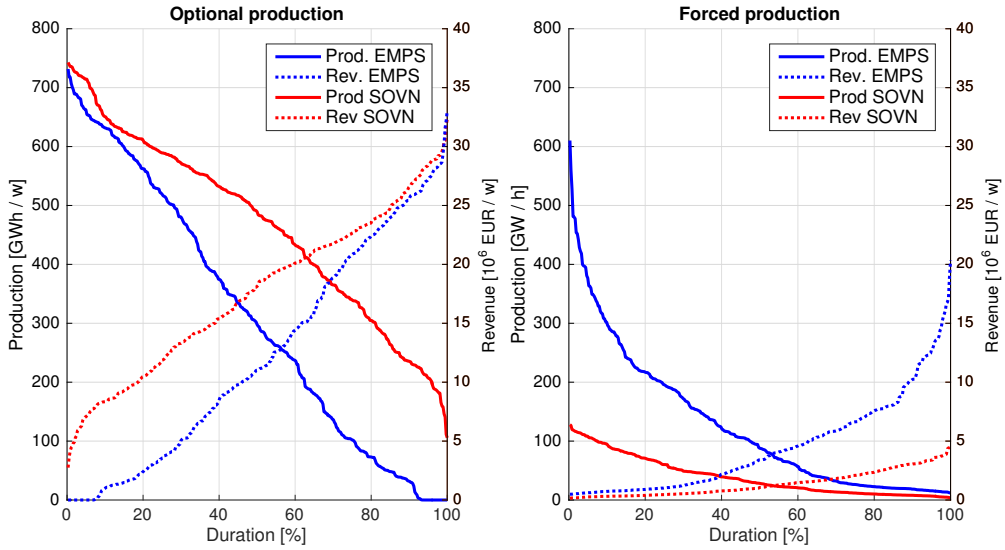

Figure 7.20: Duration of optional and forced production and their respective revenues, scenario B

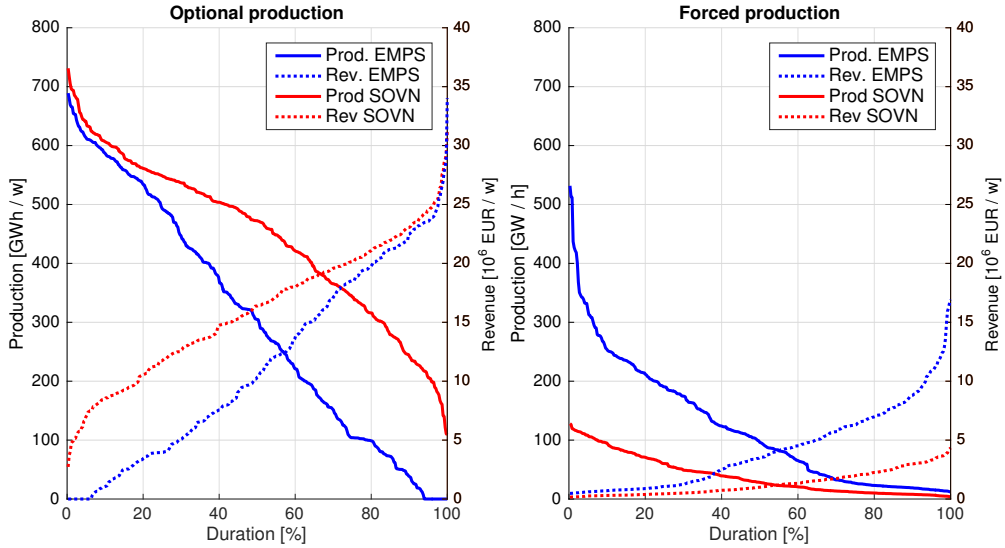

Figure 7.21: Duration of optional and forced production and their respective revenues, scenario W1

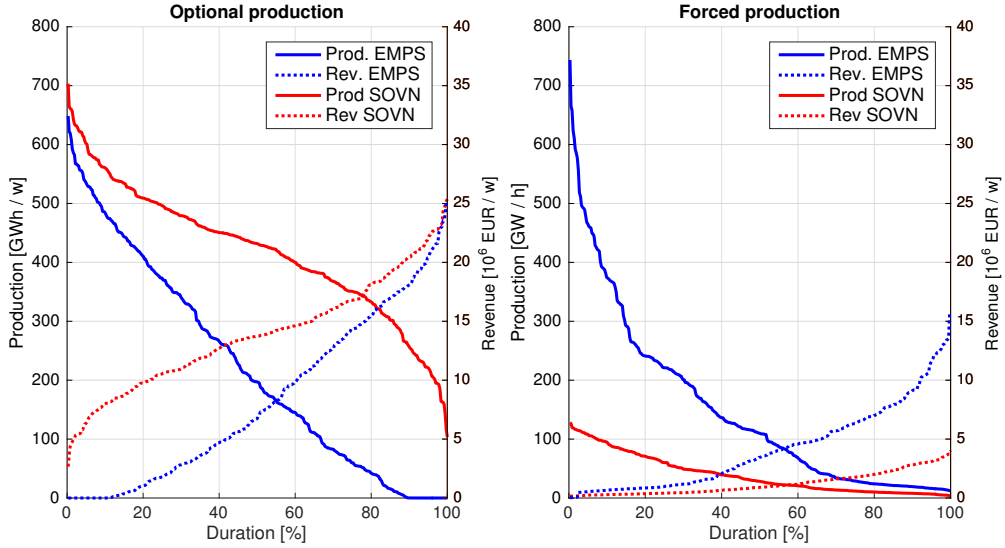

Figure 7.22: Duration of optional and forced production and their respective revenues, scenario W2

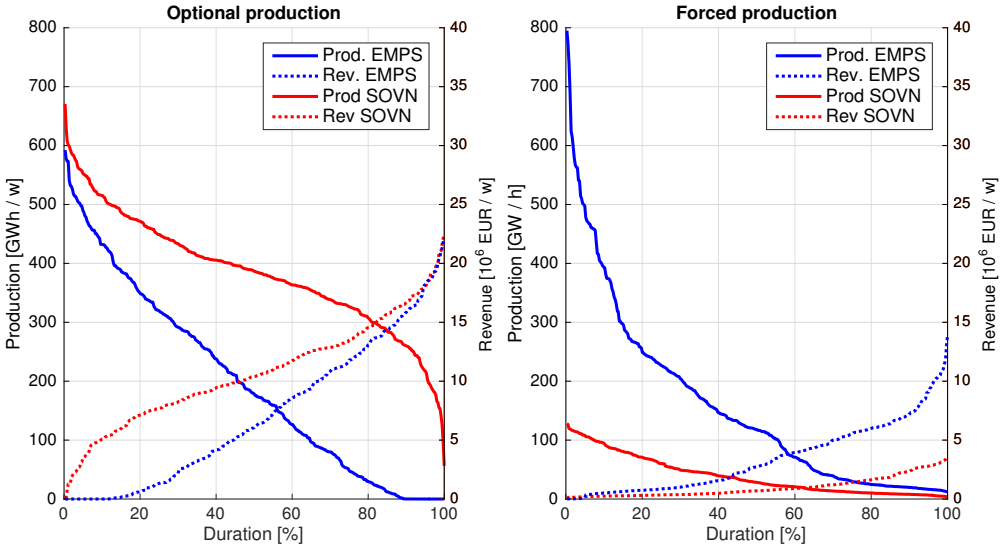

Figure 7.23: Duration of optional and forced production and their respective revenues, scenario W3

	Production				Revenue			
	B	W1	W2	W3	B	W1	W2	W3
EMPS	71.29%	71.58%	59.89%	55.94%	73.30%	73.04%	66.74%	67.48%
SOVN	92.19%	91.87%	91.42%	90.72%	92.68%	92.36%	91.95%	91.52%

Table 7.6: Share of optional production and resulting revenue in percent for EMPS and SOVN

SOVN shows a drastic increase in optional production relative to EMPS. As seen in table 7.6 this also applies for all scenarios, as the difference in optional production is almost negligible in scenario W3 compared with B. EMPS shows an increase in forced production as function of increased surplus. The distribution of revenues is also shown in the table, and there is a fairly uniform relationship between production and income for the SOVN model. For EMPS the total share of revenues from optional production is decreasing with increased surplus, though slightly less than the share of optional production itself.

7.5 Increased exchange

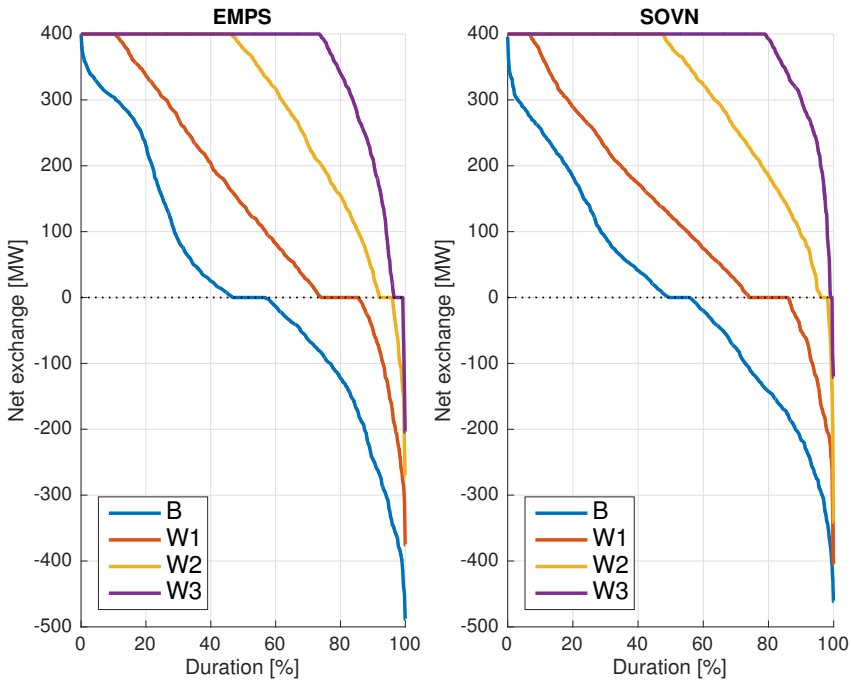

Figure 7.24: Duration curves for exchange over FINNMARK-TROMS section

Figures 7.24 and 7.25 show the utilization of the transfer capacity for FINNMARK and NORD. By convention, in figure 7.24 positive figures represent power flowing *out* of FINNMARK to TROMS, and likewise in figure 7.25 positive figures represent net power flow *out* of region NORD to the coupled markets. In table 7.7 the mean annual utilization is given as trade surplus, or percentages of full export. Full export in this case corresponds to a hypothetical situation where the transmission lines are constantly exporting to adjacent markets at full capacity. A trade surplus of zero percent means that there is perfect balance between imports and exports, and negative trade surplus consequently refers to net import. From this table it can be shown that Northern Norway indeed is a surplus market, even at low degrees of wind power development.

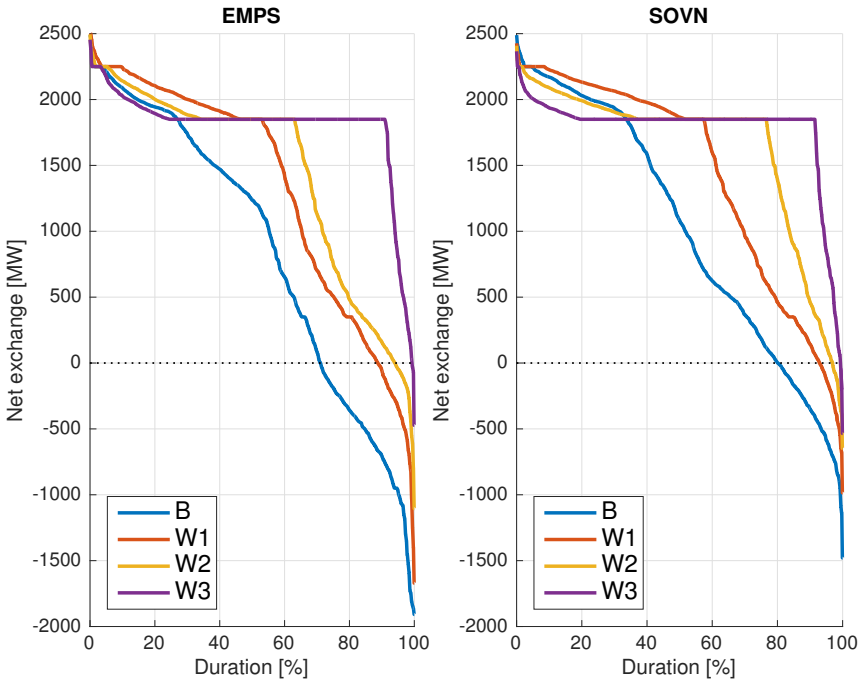

Figure 7.25: Duration curves for net exchange into/out of NORD

	EMPS		SOVN	
	FINNMARK	NORD	FINNMARK	NORD
B	4.74	34.25	2.63	40.67
W1	37.08	53.14	33.27	57.49
W2	71.89	57.53	75.32	65.25
W3	88.10	71.67	93.21	72.97

Table 7.7: Trade surplus [%]

From scenario B it can be seen that Northern Norway already has a total power surplus. This surplus is taken to the extreme with increasingly more wind power introduced in the mix. This surplus causes greater supply and greater incentives to export excess power to adjacent areas. Between FINNMARK and TROMS there is reasonable transmission capacity even for scenario W1. As seen in figure 7.24 there

is congestion between the areas approximately 10% of the time. In scenarios W2 and W3 on the other hand, the impact of the bottleneck is growing. In scenario W3 the transmission lines are fully utilized about 50% of the time. For region NORD the net exchange is depicted in figure 7.25. This represents the sum of all power flowing from from NORD to FINNMARK, SE1, SE2 and NO3. This region shows similar propensity as FINNMARK, with increasingly greater congestion. While the net capacity out of NORD equals 2,750 MW, there is a secondary threshold level at 1,850 MW, which is the result of the net import from FINNMARK.

7.6 Improved spillage handling

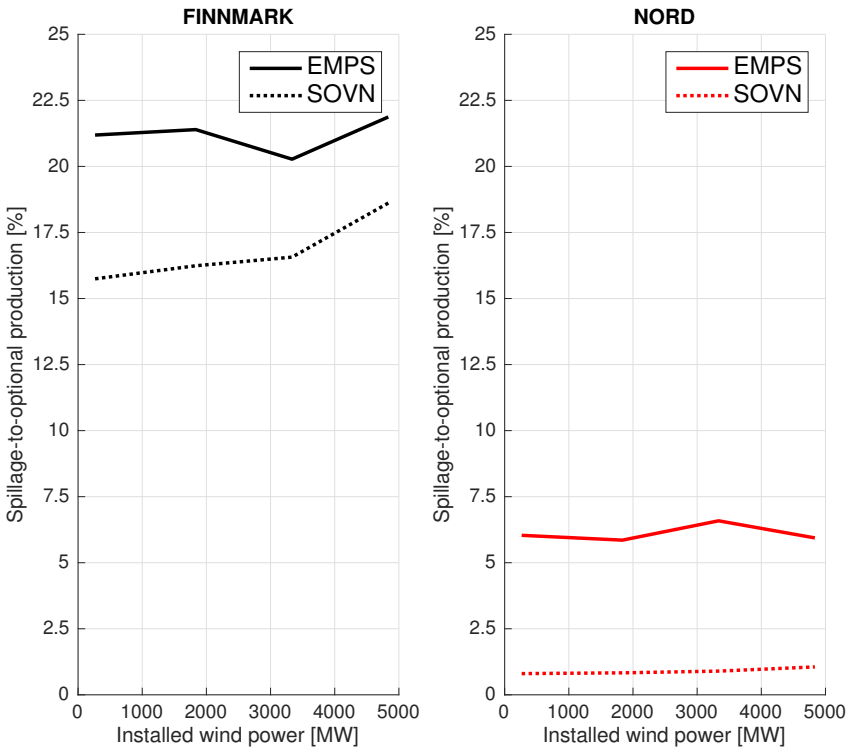

Figure 7.26: Share of total spillage to total optional production

Spillage arises as a result of challenging scheduling, i.e. situations where the hydropower producers are either forced to withhold their production, or where the net benefit of production is zero or negative. The system's overall ability to minimize

spillage is a manifestation of the adaptability of each individual reservoir. This is ultimately an indication of the ability of the optimization algorithm to deal with the flexibility of the hydropower system at a microscale. Figure 7.26 shows the ratio of total spillage over total optional production for FINNMARK and NORD. The spillage ratio r_{spill} is computed by the following formula:

$$r_{spill} = \frac{\sum_{y=1}^{7} \sum_{d=1}^{52} s_{yd}}{\sum_{y=1}^{7} \sum_{d=1}^{52} p_{yd}} \cdot 100\% \tag{7.4}$$

where s_{yd} is the recorded spillage at day d, year y, and p_{yd} is likewise the recorded *optional* production.

In figure 7.26 there is a substantial loss of water already for scenario B in EMPS. This loss of business opportunity is maintained as increased wind power capacity is added to the mix. SOVN shows immense improvement in spillage handling compared with EMPS. Overall, SOVN greatly reduces the flooding, virtually ruling it out completely in NORD. Reduced spillage consequently results in increased production

7.7 Pumped storage hydropower

Two pumped storage hydropower stations are included for all scenarios, as shown in section 6.4. For this analysis, only SOVN has been used, as EMPS is only able to handle seasonal pumping. In systems with large power surplus from intermittent sources, it is more natural to see pumping in a short-term perspective where excessive power from wind farms is either exported to adjacent markets or stored as water in upstream reservoirs. Also, as said in section 6.4, German price files are implemented for the exogenous subareas as a set of secondary scenarios to provoke greater short-term price volatility.

For the original scenarios, i.e. with local price files for the exogenous subareas, there is generally a very low usage of the pumps. The pumps operate only in extreme surplus scenarios, and with only modest input. By inspection, it was found that the pumps were only operating at prices very close to zero. For FINNMARK the maximum price was found to be 0.1 €/MWh, and in TROMS 3.29 €/MWh. Comparing the price for the exact same time step with and without pumps, the price was consistently lower in cases *with* pumps. This is contrary to normal market behavior, where use of the pumps would be included as demand, thus pushing the price up. For a full overview of the deviations in prices with and without pumps, please refer to figure D.10.

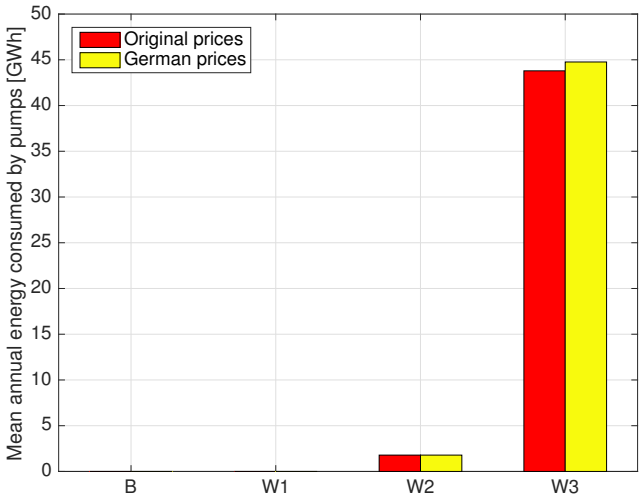

Figure 7.27: Energy consumed by pumps in FINNMARK

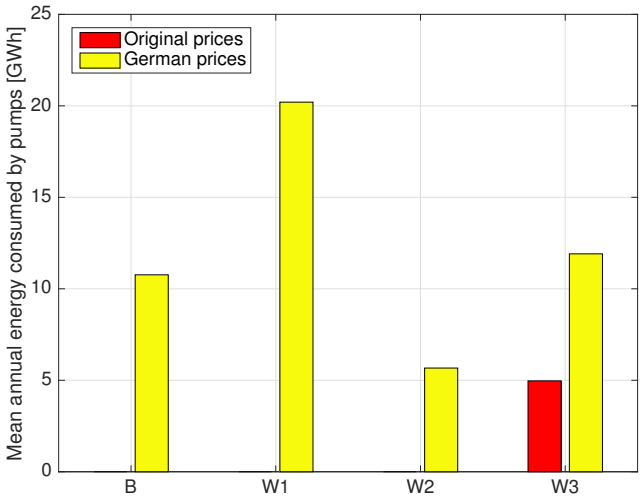

Figure 7.28: Energy consumed by pumps in TROMS

The increased price volatility induced by the German price files give rise to a greater utilization of the pumping units in TROMS. There is a only marginal difference in FINNMARK, relative to the original scenarios, which is somewhat less than expected. The utilization of pumps in TROMS is counterintuitive considering the increased surplus situation of the region. In a realistic situation the need for the pumps to alleviate the power surplus should increase as excessive wind power is introduced. The somewhat arbitrary use of the pump in TROMS is thus inconsistent, which may indicate errors in the implementation of pumping modules in the source code.

7.8 Socioeconomic surplus

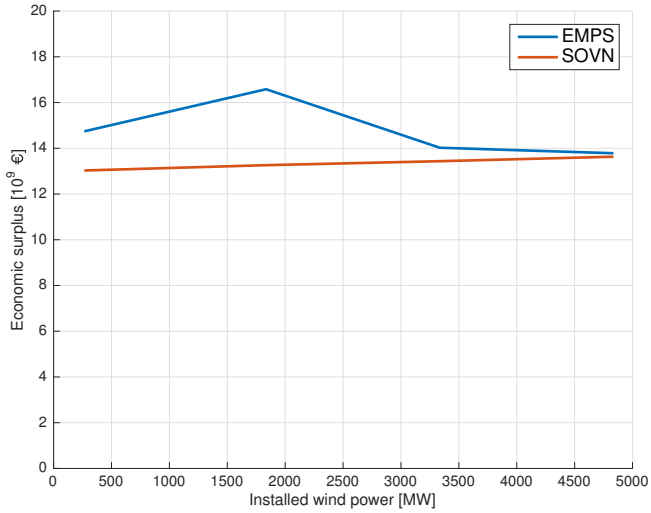

Figure 7.29: Mean total socioeconomic surplus per year for EMPS and SOVN

The total socioeconomic surplus is calculated as the sum of the elements shown in section 3.1. They are calculated for weekly clearances in the power market, and accumulated as total surplus for the entire inflow year. Figure 7.29 shows the total economic surplus for EMPS and SOVN as function of the installed wind power capacity. The figure clearly demonstrates the issues related to inconsistency of the EMPS model: By introducing additional wind power in the generation portfolio, the socioeconomic performance first increase greatly, and is then reduced for the more radical scenarios.

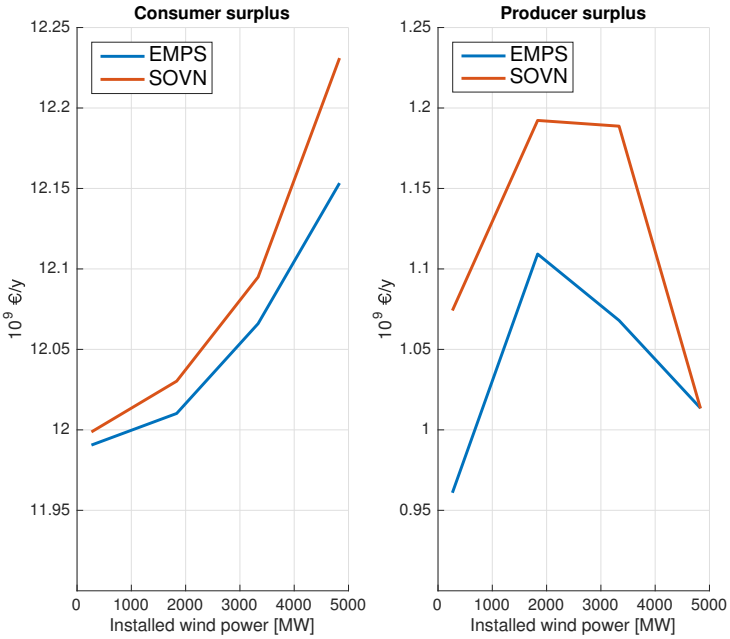

Figure 7.30: Consumer and producer surplus of EMPS and SOVN

In SOVN, however, there is a slight increase in socioeconomic performance as more wind power is introduced. The results generally show a higher level of consistency than those from the EMPS model. Overall, SOVN seems to better represent the realistic market response to such vast investment in generation.

The consumer and producer surpluses are plotted as functions of wind power development in figure 7.30. The two subplots are to scale, but note the shift of the y axis. The consumer surplus seems to be steadily increasing for both EMPS and SOVN, whereas the consumer surplus reaches a peak roughly between 2,000 and 3,000 MW installed wind power. By observing the producer and consumer surplus alone, SOVN seems to outperform EMPS. The fact that the total socioeconomic surplus is greater still in EMPS must be attributed to the value of the stored water in the residual reservoirs.

Chapter 8
Discussions

8.1 Impact of specific model properties on price structure

Throughout the project planning of SOVN there has been uncertainty as to how the price structures of SOVN would deviate from EMPS[1]. As shown, SOVN operates in a radically different manner than EMPS, and prior to any simulations, a set of possible effects on prices was proposed based on the model structure of SOVN. In the following two subsections two such effects are briefly explained, and seen in context with the results in chapter 7.

8.1.1 Individual reservoir representation

The first effect is seen in context of the individual reservoir representation in SOVN. The individual water values in SOVN are obtained independently as the shadow prices of the respective reservoir balances, and this allows great differences in water value calculations. EMPS has only one water value per area, from which the production allocation is based. The rule-based drawdown allocation of EMPS will *in principle* yield equivalent individual water values for each reservoir, but these cannot be interpreted directly. Moreover, as these theoretical water values are obtained implicitly based on one aggregate water value for the whole subarea, it is fair to assume that SOVN has greater variability for the marginal costs bid into the market than EMPS. The economic interpretation of this is illustrated in figure 8.1 below:

Figure 8.1 depicts a simplified representation of the market clearance in EMPS and SOVN. The demand curve D is the original demand curve, and D_{RES} is the residual demand for hydropower in a hydro dominated system with a large share of wind power. The demand curves are assumed identical for both EMPS and SOVN, whereas their respective supply curves are different. The supply curves are merely based on the marginal costs of the individual plants in increasing order, and the slope of the SOVN supply curve is drawn steeper than that of the EMPS model in order

[1]Referring to discussions with I. Døskeland and A. Kringstad at Statnett

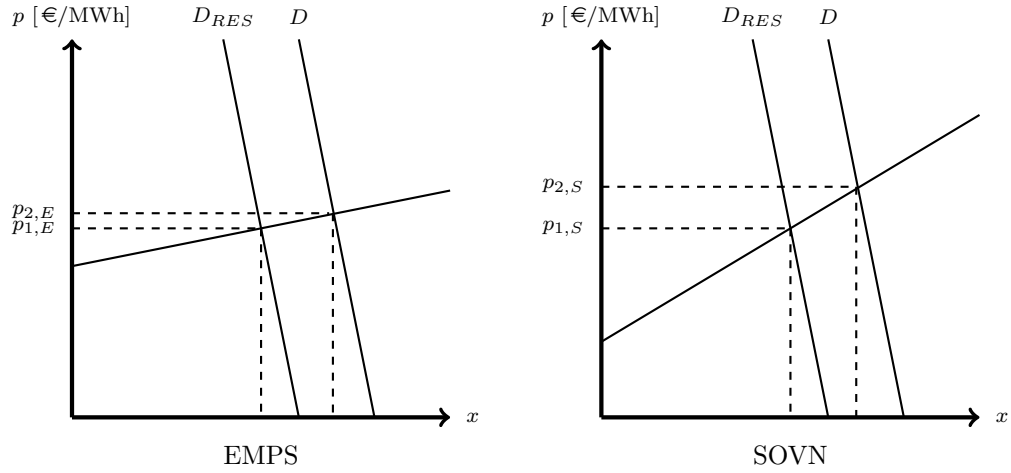

Figure 8.1: The effect on prices from different supply curves in EMPS and SOVN

to represent the expected greater dispersion in water values compared with EMPS. From this theoretical point of view it can postulated that SOVN will give greater short-term price volatility than EMPS when great levels of wind power is introduced in the power market. The intermittent nature of wind power causes random changes in supply, which can be seen as rapid horizontal shifts for the curve representing the residual demand for hydropower. Under such conditions the intermittency of the wind power will cause greater variability in prices for SOVN than EMPS.

Referring to figure 7.8 and table 7.4 it can be seen that the standard deviation in prices for FINNMARK increases proportionally to the installed wind power capacity. In both EMPS and SOVN the set of simulated prices has a standard deviation roughly between 4.50 €/MWh and 5.00 €/MWh for scenarios B and W1. Beyond this point, increased wind power development leads to far greater variability in spot prices. This effect is equal for both EMPS and SOVN. The region NORD shows more moderate developments in price variability. For EMPS there is actually a net decline in volatility for increased wind power penetration. This is somewhat counterintuitive, but might be attributed to calibration effects. SOVN shows a slight upward tendency in price volatility for great levels of wind power developments.

It is hard to determine whether the price volatility is directly in accordance with the proposed effect shown in figure 8.1. For extreme surplus situations, SOVN does show greater variability in spot prices than EMPS. Comparing e.g. FINNMARK in scenario W3, it can be seen that there is a 0.49 €/MWh increase by using SOVN, compared to EMPS. It can also be argued that the somewhat unexpected volatility

in NORD by using EMPS is an unrealistic representation of the true price structure that would in a real life scenario.

8.1.2 Formal optimization

The objective of the formal optimization in SOVN is to schedule the hydropower production such that the socio-economic surplus is maximized. As shown in section 3.2 market couplings influence the welfare in a positive manner. It was shown that, when neglecting investment costs, welfare is maximized when all coupled markets have equal prices. In such a system, there is a non-congested flow of power between adjacent areas.

In equation 5.3 in section 5.3 it was shown how the SOVN model utilizes trading between the different markets in its production handling. Exports and imports are merely treated as variables included in the market balance constraints. Thus, the utilization of transfer capacities between adjacent markets is part of the optimization problem.

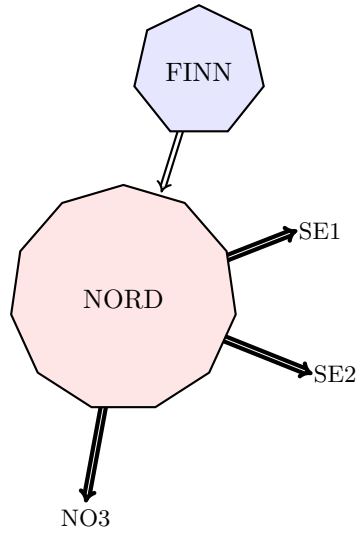

Figure 8.2: General power flow in Northern Norway with high output from wind power

As shown in section 3.2, up to a certain level, the prices gap between two markets will diminish as more power is traded between the two. The actual price gap as function of wind power capacity is shown in figure 7.10, where EMPS shows a higher relative price difference than SOVN. This is largely attributed to the SOVN model's ability to make use of the transmission lines. In table 7.7 it was shown how the

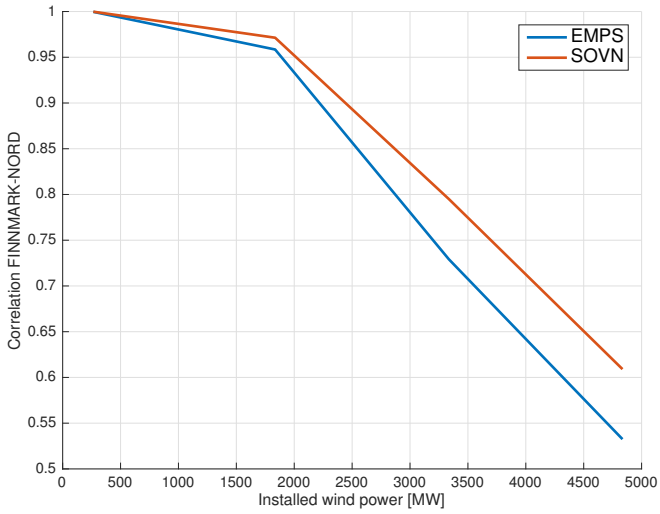

Figure 8.3: Price correlations between FINNMARK and NORD as function of wind power developments

trade surplus of FINNMARK and NORD is affected by increased wind power. The table shows that both markets are surplus markets even at moderate wind power development, and that the trade surplus grows to the extreme as more wind power is introduced. In figures 7.24 and 7.25 it is shown how the transmission lines turns from bidirectional power exchange to unidirectional flows in scenarios W2 and W3, transporting excess power away from its origin. This effect is shown in figure 8.2, which is a highly simplified illustration of the net power flow.

From this discussion, it may be assumed that the increased – and more efficient – utilization of the transfer capacities is partly influenced by the use of a direct optimization. A more efficient utilization of the transfer capacity in SOVN is also contributing to a significantly lower price gap between FINNMARK and NORD. The argument can also be reversed: The lower price gap between FINNMARK and NORD is attributed to a better usage of the transmission lines, which in turn points to the optimization algorithm of SOVN. Referring to figure 8.3 it could also be seen how SOVN consistently outperforms EMPS in terms of maintaining a uniform price structure in the region. The figure shows the rank correlation for all simulated prices in FINNMARK and NORD as function wind power penetration. These results are very coherent with the general image of two divergent markets, and the price correlation plummets with increased surplus, as expected.

The consistently lower price gap between these two markets is one of the most

important results from this analysis. Generally when assets, e.g. transmission lines, can be used more efficiently it would influence decisions on investments, possibly leading to significant cost savings. To follow up on this particular example, it is clear that the Northern Norwegian grid needs to be strengthened and upgraded if the large wind power potential in the region is to realized. In such an investment case, a more efficient usage of the transmission lines could potentially tip the cost-benefit analysis in favor of the investment.

8.2 Changed production pattern

8.2.1 Reallocation of production

The individual water values in SOVN give different incentives for the reservoirs and hydropower plants to determine their optimal production level. As discussed in subsection 8.1.1 above, it was argued how the individual reservoir representation leads to a greater variability in water values. Through observing trends in individual production one can argue roughly how the distribution in water values would look like.

Figures 7.12 to 7.15 show the relative change in production in SOVN for individual plants plotted against their respective degrees of regulation. As seen, there is a clear tendency for the plants with a low degree of regulation to increase its output. Similarly, the reservoirs with greater storage capacity seems to decrease their production, i.e. they show a higher propensity to store their water. This would indicate that the water values for the less regulated plants are adjusted down in SOVN compared to EMPS, and vice-versa for the highly regulated plants. In that case, this implies that the individual water values calculated in SOVN better incorporate the underlying production liberty for the respective plants than the aggregated water value and following drawdown allocation of EMPS.

8.2.2 Operational flexibility

8.2.2.1 Spillage handling

Figure 7.26 shows the share of spillage to regular production in EMPS and SOVN. The most notable feature to be interpreted from this figure is the improved spillage handling in SOVN compared to EMPS. In SOVN, both FINNMARK and NORD show substantial reduction in spillage, virtually eliminating it completely in NORD. This can be seen directly as a consequence of the individual reservoir optimization; when the water value of each individual reservoir is known, it gives much clearer incentives to either produce or withhold water. In principle, when a reservoir is at risk of becoming full, producers are faced with low optional value for their water, i.e. low water value. Under such conditions there are clear incentives for the plants to produce

to maximize profits, hence to avoid loss of water and lost business opportunity. This is a drawback for the drawdown allocation in the EMPS model; only one aggregate water value per area is insufficient to provide clear market signals for the individual plants, and the heuristics of the drawdown allocation proves to be less able to respond to potential spillage situations.

8.2.2.2 Less forced production

The definition of unregulated production in the EMPS and SOVN models are given in subsection 7.4.2 as the sum of various production categories from water with no optional value. From the figures 7.20 to 7.23 it was shown how the share of unregulated, or forced, production in EMPS increases proportionally with the wind power production. This can be seen in context with the high spillage levels in EMPS: Large amounts of wasted water signals an inability of the model to respond quickly to the reservoir situation. The resulting production pattern of EMPS indicates that the producers are faced with less options regarding their production, i.e. they are frequently in a position where they are actually forced to produce to avoid lost business opportunity.

Table 7.6 shows the distribution of forced and optional production in SOVN. The share of unregulated production seem to be rather invariant to the wind power scenarios, increasing only about 1.5% from scenario B to W3. This is indeed a remarkable result, as it was expected that the increased intermittent production from wind power would ultimately force a greater amount of water to be lost as spillage. Then, the share of unregulated production that still does arise, may possibly cover the share of unregulated production which cannot be eliminated, whatsoever. This arises e.g. in unregulated reservoirs where the net inflow exceeds the maximum allowed discharge, etc.

From an optimization point of view, lower spillage levels and greater shares of optional production is an intuitive result, given that the optimization model truly provides the producers with correct market information. The market information, in this case, is the set of water values for each individual plant. Now, imagining a hypothetical scenario, where a single producer is faced with a reservoir on the brink of spilling. In this case, the reservoir has a water value equal to zero. In such a case, the producer is faced with two options: Either produce now in order to avoid spillage, or withhold production resulting in loss of water. Obviously, in this very simple problem the producer would settle for the most optimal alternative, which is to produce. The fact that every single plant sees the short term gain of producing instead of wasting water can to some extent explain the reduced spillage levels in SOVN relative to EMPS. Since the decision to produce now rather than waste water is not influenced by any future market scenarios, it is an entirely static optimization

problem. However, in the situation described above, the resulting production would be forced, i.e. there is no opportunity for the producer to save the water for later. From the results, it was shown how SOVN manages to greatly reduce its forced production relative to EMPS, which would indicate that such situations seldom arise. Thus, the ability of the SOVN model to consistently maintain high operational flexibility indicates the inherent quality of the model to plan ahead and incorporate the dynamic and uncertain nature of the power market modeling.

8.3 Socioeconomic performance

8.3.1 Socioeconomic surplus

Figure 7.29 shows the mean economic surplus per year for every wind power scenario for both EMPS and SOVN. It was briefly stated in section 7.8 how the results from EMPS seem counterintuitive compared to the expected performance of a real life power market. Relative to the base case, there is a drastic improvement when a small portion of wind is introduced in scenario W1, but then a rapid decline as more wind power is pushed into the market in scenarios W2 and W3. Intuitively, introducing more wind power in the mix should not aggravate the welfare; on the contrary, more wind power would yield greater market flexibility which in turn would induce a positive effect on the overall socio-economic performance.

This is illustrated in figure 8.4, where the market clearance for a power system with W_0 MWh wind power is shown as the intersection between S_0 and the demand curve. When an additional amount ΔW is bid into the market, there is a horizontal shift of the supply curve. The new market clearance is then given at the intersection between S_w and the demand curve. This leads to an improvement in economic surplus which is equivalent to the darker shaded areas. Also note the shift in consumer and producer surplus. The area enclosed by S_w, the demand curve and the x axis represents the economic potential for increased wind power production. The mathematical proof is omitted, but it is clear from the figure that a marginal increase in wind power production results in a marginal reduction of the enclosed area, which corresponds to a marginal increase of the socio-economic surplus. However, for every additional unit of wind power bid into the market, the resulting reduction for this area is less than it was for the previous unit. This suffices as a proof to show how wind power is subject to the law of diminishing returns.

Again referring to figure 7.29, it seems that the performance in SOVN is much more according to this description than EMPS. Of course, the market model given above does not incorporate the dynamic nature of the hydrothermal scheduling, and there are also other aspects to take into account which makes the realistic market representation much more complicated. Nevertheless, the fact that the socio-economic

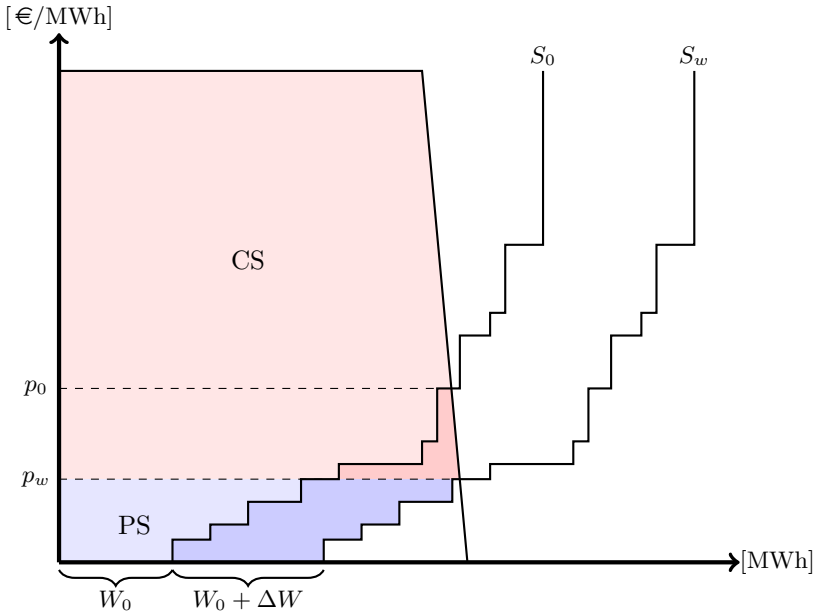

Figure 8.4: Impact of increased wind power penetration on economic surplus

surplus as function of wind power capacity is steadily increasing is a good indication that the SOVN model is operating according to basic economic logic. It is also fair to believe that this is a more realistic representation of the real life power market in the Nordic region.

8.3.2 Socioeconomic profitability of wind power

The smooth, nearly linear increase in socio-economic surplus from increased wind power production can be used to calculate the overall social benefit and profitability of wind power in the Northern Norwegian power system. Figure 8.5 shows the socio-economic results from SOVN as blue dots, and the orange line represents the linear regression from these results. This line was obtained using a simple least squares approach[40] to obtain an equation for a straight line given as

$$y = \alpha + \beta x \tag{8.1}$$

where y equals economic surplus in €, x refers to the wind power capacity in kW. α and β are represented by

$$\hat{\beta} = \frac{\sum_{i=1}^{4}(x_i - \bar{x})(y_i - \bar{y})}{\sum_{i=1}^{4}(x_i - \bar{x})^2} \tag{8.2}$$

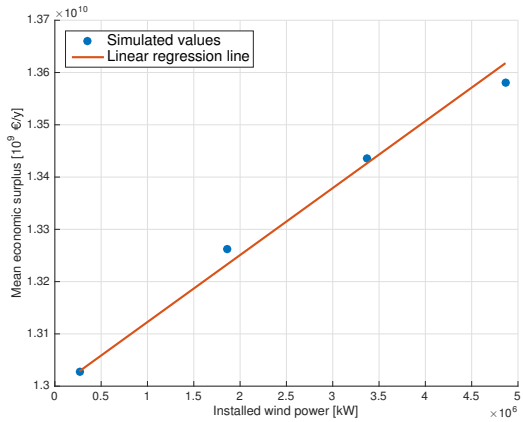

Figure 8.5: Linear regression of economic surplus in SOVN

and

$$\hat{\alpha} = \bar{y} - \hat{\beta}\bar{x} \tag{8.3}$$

which are the values that minimize the square errors. Inserting real observed values for $x_i \wedge y_i, \quad \forall i = 1, \ldots, 4$ gives:

$$y = 12,995 \cdot 10^9 + 128.1172x \tag{8.4}$$

It is now established a linear relationship between the wind power capacity and the total economic surplus, which makes it possible to investigate the marginal social utility of the wind power. This is simply calculated as $y'(x)$, and it can easily be seen that the marginal utility of wind power is equal to 128.1172 €/kWy.

In their most recent report on costs in the power industry[41], NVE has identified as set of cost elements for land based wind power such as turbine structures, project management, infrastructure, etc. Throughout their analysis, NVE has used a discount rate of 4% and an economic life time of 20 years. Based on these economic assumptions, they found that the theoretical total cost of wind energy per installed kW is equal to 10,250 NOK/kW, or roughly 1,280 €/kW[2]. The present value of the utility from wind power in SOVN is equal to

$$\begin{aligned} B &= 128.1172\,€/\text{kWy} \cdot \frac{1}{\varepsilon_{4,20}} \\ &= 128.1172\,€/\text{kWy} \cdot \frac{1-(1+0.04)^{-20}}{0.04} \\ &= 1,741.15\,€/\text{kW} \end{aligned}$$

[2]Assuming a historic conversion rate of 1 € = 8 NOK

Thus, the theoretical net present value of wind power is equal to the difference between the total utility per kW and the total costs per kW, i.e.

$$NPV = 1,741.14\,€/\text{kW} - 1,280\,€/\text{kW} \approx 460\,€/\text{kW}$$

This calculation shows that the net present value of the wind power development is positive, i.e. throughout the project's economic life time, the total socio-economic benefit is expected to surpass the costs. Again referring to [41], it was shown how the realized projects in 2011-2013 had a total cost of approximately 1,500 €/kW. As seen from the total benefit per kW, this raised cost would greatly reduce the margins, but the project decision would still come out as positive.

Obviously, this analysis is considerably simplified, and fails to enlighten several uncertainties regarding the investment decision. Also, it should be emphasized that although an investment project is profitable from a socio-economic point of view, there is a discrepancy between socio-economic and business economic investment assessments. As a side note, it should also be mentioned that this calculation is based on a linear relationship between socio-economic surplus and installed wind power capacity. This is a fallacy - as discussed in subsection 8.3.1 wind power is subject to diminishing returns, which is suggested when comparing the linear approximation in figure 8.5 with the realized socio-economic surpluses of the simulations.

8.4 The potential of the SOVN model

As argued in this thesis the need for calibration in EMPS is a major model weakness. The results obtained from the EMPS simulations are very sensitive to user input, and the fact that the calibration procedure is largely experience based makes the model operation and result interpretation of the EMPS model dependent on the experience of the user. Of course, when analyzing results obtained from simulation models one should always be aware of the inherent limitations of the model. With EMPS the results are also influenced by the quality of the user input and this effect can be hard to isolate from the purely model specific qualities. The fact that the quality of the results in EMPS is so coherent with the experience of the user is also a significant drawback for its value as a commercial product.

In SOVN the user interaction is merely limited to the simulation settings, and these are only affecting the manner in which the SFS algorithm is run. Moreover, the impact of these settings are easier to understand than the calibration factors of the EMPS model, and as shown in section 7.2, the results are very consistent and independent to e.g. changing the number of weeks in the scenario fan, etc. The SOVN model can be criticized for significantly longer simulation time than EMPS, and as seen in table 7.2 this can indeed be substantial. To reduce the computational load is currently one of the major targets in the further development of the SOVN

model. Nonetheless, the need for repeated adjustments of the model calibration with subsequent simulations in EMPS is indeed very time consuming as well, so the time invested to reach satisfactory results in EMPS is far more than the time it take to run the simulation.

Chapter 9
Conclusions

Large scale implementation of intermittent renewable energy and tighter coupling to markets with different price structures contribute to new challenges in the long-term hydrothermal scheduling. The established EMPS model, with its reservoir aggregation and disaggregation, is not fully adapted to the aspects that this introduces. The need for generalized simulation models that provide the individual production units with accurate market information is thus necessary, since the new power system paradigm requires improved utilization of the inherent flexibility of the hydropower system. This thesis is a comparative analysis of two different, but commensurable models for long-term hydrothermal scheduling – the EMPS and SOVN models. The latter obtains a direct production policy for the individual plants through a complex SLP algorithm using Benders decomposition, and aims to circumvent the drawbacks of the reservoir aggregation in the EMPS model.

The analysis is based on a confined power system in Northern Norway with different levels of wind power development, given as discrete scenarios between 265 and 4,835 MW. With only 265 MW wind power, EMPS and SOVN have a share of unregulated production, i.e. production with zero opportunity cost, at 28.71% and 7.81%, respectively, and for the most extreme case these shares are increased to 44.06% and 9.28%. Consequently, the spillage levels are also significantly reduced in SOVN. These results indicate an improved operational flexibility for the SOVN model compared to EMPS. The aggregated water value and the heuristic drawdown allocation of EMPS seem to be less capable of providing the correct market signals to the individual plants, which results in a high degree of forced production and lost business opportunity. For SOVN, however, the optimization of individual reservoirs shows the ability of the hydropower system to handle even extreme surplus situations, while maintaining a high level of flexibility. When investigating the individual plants, the results indicate a higher utilization of the less regulated ones, i.e. plants that can only store water for a few months at the time. These plants are generally prone to spillage and forced production, and it seems that SOVN has a high ability to incorporate this for their respective water values. Likewise, the plants with high

storage capacity and capability show a slight tendency to withhold their production, thus saving water. This results from a higher water value for such plants.

The high penetration of wind power in the most extreme cases results in significantly lower wholesale prices for both models. Bottlenecks in the grid also evoke general price differences between adjacent markets, as export of the surplus power is constrained. Still, SOVN manages to reduce the mean price gap in such cases, relative to EMPS – it was shown that SOVN reduced the mean price gap with 3.04 €/MWh for the most extreme case. Also, the model manages to maintain a more uniform price structure across the various markets. This indicates the model's improved utilization of the transfer capacity in a market efficient manner. Lastly, it still appears to be slight room for improvement related to the socioeconomic performance of SOVN. Moreover, the pumping pattern seems somewhat arbitrary and reveals certain market contradictory properties.

When comparing the usability of the two models, one can conclude that both models have good and bad qualities. The major drawback of the SOVN model is the simulation time and computational load. In this analysis, a power system containing only 217 hydropower modules was used, and even then the simulation time was substantial. For greater and more complex systems the simulation time will grow rapidly and it goes without saying that this will reduce the model's applicability. However, SOVN is not depending on the same level of user input as EMPS, whose results are very sensitive to the model calibration. It can be concluded that SOVN shows very promising signs in the way it handles the flexibility of the power system. Nevertheless, the two models will likely coexist for some time into the future, possibly finding their own niches.

Chapter 10
Further work

Although the SOVN model shows clear signs of maturity, the model is still only at the prototype phase. This means that the model itself will be developed further as new tests are performed. This work will continue for some time, and a full commercial release is set to happen in 2016. It is only when the use of model becomes widespread that one can fully determine the strengths and weaknesses of the model. Thus, for the coming months a great number of simulations in SOVN should be run under different conditions to test for differences in the model behavior. A number of suggested cases are presented below:

- This analysis has shown how SOVN handles power surplus, and similar scenarios should be established to test the ability of the model to handle power deficit.
- The model shows high ability to utilize the inflow and thus increase its hydropower production. Under these circumstances it would be interesting to compare the SOVN model to the EMPS model in a power system with a larger share of expensive thermal units, to test for substitute effects. This is a realistic scenario for a large data set containing the whole Nordic region.
- Introduce start and stop costs for thermal units.
- Look deeper into the settings in SOVN.ctrl and how they influence the results.
- Investigate differences in pumping pattern.

As mentioned, the major drawback of the SOVN model is the substantial simulation time and the huge computational load. From a research point of view, emphasis should be placed on developing algorithms to reduce the simulation time without compromising on the quality. This is a major task that requires complex mathematical modeling and programming. Nevertheless, there are likely opportunities for further development on warm-starting, modifications of the scenario fan, etc.

The individual water values in SOVN call for a more complex functionality for the graphical representation of the results and data. For instance, the possibility to retrieve water values for the individual reservoirs is something that has been missing

during this analysis. This is strictly speaking not an issue related to the SOVN model itself, but such an improvement of the ancillary programs will help to further improve the usability of the model.

References

[1] Norges Vassdrags-og Energidirektorat. Vindkraft - gitt konsesjon. http://www.nve.no/no/Konsesjoner/Konsesjonssaker/Vindkraft/. Accessed: 2015-10-05.

[2] International Energy Agency. Key World Energy Statistics. Technical report, IEA, 2014.

[3] D. Weisser. A guide to life-cycle greenhouse gas (GHG) emissions from electric supply technologies. *Elsevier*, 2006.

[4] H. Farahmand, T. Aigner, G. Doorman, M. Korpås, and D. Huertas-Hernando. Balancing Market Integration in the Northern European Continent: A 2030 Case Study. *IEEE Transaction on Sustainable Energy*, 3(4):918–930, 2012.

[5] G. Doorman. Energy system planning and operation, 2013. Compendium used in undergraduate course TET4135 - Energy planning.

[6] E. Ostrom, R. Gardner, and J. Walker. *Rules, games and common-pool resources.* University of Michigan Press, 1994.

[7] I. Wangensteen. *Power system economics - the Nordic Electricity Market.* Tapir Academic Press, 2007.

[8] European Comission. Comission staff working paper - Analysis of options beyond 20% GHG emission reductions: Member State results, 2012.

[9] The Economist. European utilities - How to lose half a trillion euros. *The Economist Printed Edition*, 2013.

[10] Statnett SF. Reservemarkeder. http://www.statnett.no/Drift-og-marked/Markedsinformasjon/. Accessed: 2016.01.23.

[11] P. Tielens and D. van Hertem. Grid Inertia and Frequency Control in Power Systems with High Penetration of Renewables. *Proceedings of the 3rd IEEE Benelux Young Reserachers Symposium in Electrical Power Engineering*, 2012.

[12] J. Aarstad. Simulations of the impact of interconnectors on prices and water values in the Nordic power market. Project thesis, NTNU, 2015.

[13] A. Helseth, B. Mo, and G. Warland. Long-term scheduling of hydro-thermal power systems using scenario fans. *Energy Systems*, (1):377–391, 2010.

[14] M. Pereira, N. Campodónico, and R. Kelman. Long-term Hydro Scheduling based on Stochastic Models. *Proceedings of EPSOM'98, Zürich, September 23-25*, 1998.

[15] D. Kirschen and G. Strbac. *Fundamentals of Power System Economics*. John Wiley & Sons, Ltd., 2004.

[16] O. Fosso and G. Doorman. Produksjonsplanlegging i vannkraftbaserte systemer - del 1, 2014.

[17] Statnett SF. Håndbok for Samlast, 2009.

[18] G Doorman, O. Fosso, A. Haugstad, and B. Mo. Produksjonsplanlegging i vannkraftbaserte systemer - del 2.

[19] G. Doorman. Course ELK15 - Hydro Power Scheduling, 2015.

[20] S. Stage and Y. Larsson. Incremental Cost of Water Power. *Transactions of the American Institute of Electrical Engineers*, 80(3):361–364, 1961.

[21] F. Hillier and G. Lieberman. *Introduction to Operations Research*. McGraw-Hill, 2010.

[22] SINTEF Energy Research. *Brukerveiledning Samkjøringsmodellen*.

[23] M. Pereira and L. Pinto. Stochastic Optimization of a Multireservoir Hydroelectric System: A Decomposition Approach. *Water Resources Research*, 21(6):779–792, 1985.

[24] E. Bøhnsdalen, A. Kringstad, and L. Christiansen. Kabler til Tyskland og Storbritannia - analyse av samf.øk. nytte ved spothandel. Technical report, Statnett SF, 2013.

[25] A. Henden. Storskala pumpekraft. Master's thesis, NTNU, 2014.

[26] M. Pereira. Optimal stochastic operations scheduling of large hydroelectric systems. *Electrical Power & Energy Systems*, 11(3):161–169, 1989.

[27] M. Pereira and L. Pinto. Multi-stage stochastic optimization to energy planning. *Mathematical Programming, vol. 52, pp. 359-375*, 52:359–375, 1991.

[28] T. Røtting and A. Gjeldsvik. Stochastic dual dynamic programming for seasonal scheduling in the Norwegian power system. *Transactions on Power Systems*, 7:273–279, 1992.

[29] L. Martinez and S. Soares. Primal and Dual Stochastic Dynamic Programming in Long Term Hydrothermal Scheduling. *IEEE Power Systems Conference & Exposition 2004*, 3:1283–1288, 2004.

[30] C. Cervellera, V. Chen, and A. Wen. Optimization of a large-scale water reservoir network by stochastic dynamic programming with efficient state space discretization. *European Journal of Operational Research*, 171(3):1139–1151, 2005.

[31] B. Dias *et al.* Stochastic Dynamic Programming Applied to Hydrothermal Power Systems Operation Planning Based on the Convex Hull Algorithm. *Mathematical Problems in Engineering, Article ID 390940, 20 pages*, 2010.

[32] S. Yakowitz. Dynamic Programming Applications in Water Resources. *Water Resources Research, vol. 18, no. 4, pp. 673-696*, 18(4):673–693, 1982.

[33] A Helseth *et al.* Stochastic optimization model with individual water values and power flow constraints. Technical report, SINTEF Energy AS, 2014.

[34] D. Morton. An enhanced decomposition algorithm for multistage stochastic hydroelectric scheduling. *Annals of Operations Research*, 64(1):211–235, 1996.

[35] J. Birge and F. Loveaux. *Introduction to Stochastic Programming.* Springer Verlag, NY, 1997.

[36] O. Egeland *et al.* The extended power pool model. Operation planning of a multi-river and multi-reservoir hydro-dominated power production system. A hierarchial approach. *CIGRE*, 32(14), 1982.

[37] G. Warland. Sovn user manual. Technical report, SINTEF Energy AS.

[38] L. Escudero *et al.* The value of stochastic solution in multistage problems. *TOP*, 15(1):48–64, 2007.

[39] H. Hamnaberg and Vattenfall Power Consultants. Pumpekraft i Noreg - Kostnadar og utsikter til potensial. Technical report, NVE, 2011.

[40] R. Walpole *et al. Probability & Statistics for Engineers & Scientist.* Pearson Education, 2007.

[41] M Sidelnikova *et al.* Kostnader i energisektoren. Technical report, Norges Vassdrags- og Energidirektorat, 2015.

[42] J. Lundgren, M. Rönnqvist, and P. Värbrand. *Optimization.* Studentlitteratur, 2010.

Appendix A
Mathematical background

A.1 Statistical concepts

Given a set of data $x_1, x_2, \ldots x_N$, the arithmetic mean $\bar{x}$ is defined as follows:

$$\bar{x} = \frac{1}{N} \sum_{i=1}^{n} x_i \tag{A.1}$$

The standard deviation represents the amount of dispersion or variation within a data set. In economical terms this is equivalent to *volatility*. The standard deviation is defined as follows:

$$\sigma = \sqrt{\frac{1}{N-1} \sum_{i=1}^{N} (x_i - \bar{x})^2} \tag{A.2}$$

and is not to be confused with *variance* which equals σ^2.

Correlation is a statistical term that defines the level of dependence between two sets of data. The sample correlation coefficient ρ_{xy} between two sets of data X and Y - where both sets contain N elements - is given as:

$$\rho_{xy} = \frac{\sum_{i=1}^{N}(x_i - \bar{x})(y_i - \bar{y})}{\sqrt{\sum_{i=1}^{N}(x_i - \bar{x})^2 \sum_{i=1}^{N}(y_i - \bar{y})^2}} \tag{A.3}$$

A.2 Benders decomposition

The optimization problem presented in subsection 5.3.2 is too extensive to solve directly using LP. Instead, the SFS algorithm utilizing Benders decomposition is used, as shown in subsection 5.3.3. This appendix aims to demonstrate the principles of Benders decomposition, and is largely based on the work by Pereira and Pinto in [23]. This appendix aims to work as a guidance to understand the logic of the SFS algorithm, but a more general notation is adopted in order to easily show the key aspects of the decomposition.

A.2.1 Derivation of Benders decomposition

Let equation (5.5) be written as:

$$\begin{aligned} &\min\ c^T x + d^T y \\ &\text{s.t. } Ax \geq b \\ &\qquad Fy \geq g - Ex \end{aligned} \tag{A.4}$$

Variables x denote the first stage variables, and the associated costs are given as $c^T x$. A is the constraint matrix for the first stage problem, and the following line refers to the set of transitional constraints. $d^T y$ refers to the set of second stage problems, and the point of Benders decomposition is to approximate this function in an iterative process. The master problem can be written as

$$\begin{aligned} &\min\ c^T x + \theta \\ &\text{s.t. } Ax \geq b \end{aligned} \tag{A.5}$$

Where θ is an approximation of the second stage cost, which in turn can be formulated as:

$$\begin{aligned} &\theta = \min\ d^T y \\ &\text{s.t. } Wy \geq h(\omega_n) - Tx \end{aligned} \tag{A.6}$$

ω_n is a discrete realization of scenario $n \in \mathcal{N}_K$.

A.2.2 Obtaining valid cuts

As seen, the second stage problem is a function of the first stage variables, which is a manifestation of the dynamic nature of the optimization problem. From duality theory, it is known that problem (A.6) can be written as

$$\begin{aligned} &\max\ \pi^T(h(\omega_n) - Tx) \\ &\text{s.t. } \pi^T W \leq d \end{aligned} \tag{A.7}$$

where π^T is a row vector of dual variables. In economic theory this is equivalent to marginal costs, or water values in this case. The feasible region $\pi^T W \leq q$ is a convex hull characterized by a set of vertices. Let Π denote the set of $K = |\mathcal{N}_R|$ such vertices, such that $\Pi = \{\pi_1, \pi_2, ..., \pi_K\}$. The optimal solution of any LP problem is always obtained in a vertex of the feasible region, thus problem (A.7) can be written as:

$$\begin{aligned} &\max\ \pi_n^T(h(\omega_n) - Tx) \\ &\qquad \pi_n \in \Pi \end{aligned} \tag{A.8}$$

Performing the dual transformation on problem (A.8) yields:

$$\begin{aligned} &\min \theta \\ &\text{s.t. } \theta \geq \pi_1(h(\omega_1) - Tx) \\ &\qquad \theta \geq \pi_2(h(\omega_1) - Tx) \\ &\qquad \dots \\ &\qquad \theta \geq \pi_K(h(\omega_1) - Tx) \end{aligned} \tag{A.9}$$

From the constraints in problem (A.9) it can be seen that θ is greater than or equal to every $\pi_n(h(\omega_n) - Tx)$, which can be seen as the lower bound of θ. Given the minimization criterium it can be thus be concluded that $\theta = \max_n\{\pi_n(h(\omega_n) - Tx)|n = 1, \dots, K\}$. From this it can be concluded that the set of constraints in (A.9) corresponds to the approximation of θ. Every constraint is therefore a valid cut for θ, and can be iteratively added to the set of constraints in order to approximate the true second-stage costs of the two-stage problem. So, after solving the initial first-stage problem, a valid cut on the form

$$\theta \geq \Big[\sum_{n\in\mathcal{N}_K} p_n\pi^l_{an}\Big]h_n - \Big[\sum_{n\in\mathcal{N}_K} p_n\pi^l_{rn}\Big]u^l_{t,m} \tag{A.10}$$

is added to the original problem which is then recalculated. If the difference between the upper and lower bounds is not below a predetermined threshold, new cuts are generated based on the first-stage variables obtained in iteration number two. Now, there will be two valid cuts added to the initial problem. So the multi-stage nature of the origianl problem is now, through decomposition, merely a function of the first-stage variables. Even with a great number of iterations, this is computationally much easier for any LP solver to handle.

A.3 Water values as dual variables

In SOVN, the water values of the individual reservoirs are obtained from the dual formulations of the subproblem, as shown in subsection 5.3.3. The water values are actually the shadow prices of the reservoir balances of the subproblems. The individual reservoir balances were given in equation (5.2), which is repeated below:

$$\begin{aligned} x_{r,t} + v^S_{r,t} - q_{r,t} + \sum_{\rho\in\mathcal{R}r)} q_{\rho,t} \\ -s_{r,t} + \sum_{\rho\in\mathcal{R}(r)} s_{\rho,t} - b_{r,t} + \sum_{\rho\in\mathcal{R}(r)} b_{\rho,t} = x_{r,t+1} \end{aligned} \tag{A.11}$$

Note that subscript i denoting subarea i is omitted for convenience. From introductory operational research it is known that the *shadow price* of a constraint is given as the

marginal change of the objective function resulting from a marginal change in the right hand side coefficient[42]. This can be formulated generally as

$$y_k = \frac{\partial Z^*}{\partial b_k}, \quad \forall k \tag{A.12}$$

where y_k is the shadow price of constraint k, Z^* is the solution to problem Z and b_k is the right hand side coefficient of constraint k. From equation (A.11) it can be seen that the right hand side of the constraint is equal to next week's reservoir balance, i.e. $x_{r,t+1}$. So the shadow price for a given reservoir balance r for an arbitrary scenario is given as

$$\pi_r = \frac{\partial Z^*}{\partial x_{r,t+1}} \tag{A.13}$$

This is entirely in accordance with the definition of water values derived in equation (4.9).

Appendix B
Matlab codes

The chapter gives a thorough explanations to some of the codes used in the thesis, as well as providing the codes themselves. The EMPS and SOVN models generate vast amounts of data, and there is often a long process from the raw data material to the resulting plot, table, etc. The data is obtained through the modular program Kurvetegn, that writes the desired data to .csv files that are imported to Matlab. The imported data is frequently combined to structs or arrays, which are then saved as .mat files. These are files that stores selected variables from the workspace.

B.1 Miscellaneous functions

In this section a number of functions will be presented. These are mostly non-generic functions tailor-made to solve specific problems. The functions are mostly used to sort data and perform minor operations with broader utilization.

B.1.1 Function `priceSeg.m`

This function is used to solve problems related to the partition of price segments. Throughout this thesis, the price segments are treated accumulatively, which means that data such as prices, production, transmission, etc. are given in five weekly segments. In a vector containing e.g. prices, weekly prices will be given as $< Price - segment1 >, < Price - segment2 >, \ldots, < Price - segment5 >$. This is repeated for each week consecutively. When dealing with duration curves, etc. it is important to note that the weekly segments are not uniformly distributed[1].

`priceSeg.m` takes one vector of data and one vector containing distribution of weekly hours per segment, and returns a (5×1) cell array. Each cell contains a vector with the accurate number of hours for each price segment, for all inflow scenarios.

[1] The hourly distribution throughout the week is given in appendix C

```
>> segV = [25 35 25 49 34];
>> R = priceSeg(krvBEMPS(:,1),segV)

R =

    [ 9100x1 double]
    [12740x1 double]
    [ 9100x1 double]
    [17836x1 double]
    [12376x1 double]
```

Figure B.1: Screenshot from Matlab command window - `priceSeg.m`

```
function realSeg = priceSeg(priceVec,segV)

if mod(length(priceVec),numel(segV))~=0
    error('Invalid number of price segments');
end


segMat = zeros(length(priceVec)/numel(segV),numel(segV));
realSeg = cell(numel(segV),1);

for i = 1:numel(segV)
   realSeg{i} = zeros(((numel(priceVec))/numel(segV))*segV(i),1);
end

k = 0;
for i = 1:numel(priceVec)/numel(segV)
    for j = 1:numel(segV)
        segMat(i,j) = priceVec(k*numel(segV)+j);
    end
    k = k+1;
end

for i = 1:numel(segV)
    t = 0;
    for j = 1:length(segMat)
        realSeg{i}(t+1:t+segV(i)) = segMat(j,i).*ones(length(segV(i)),1);
        t = t + segV(i);
    end
end

end
```

B.1.2 Function `gwh2MW.m`

This function takes a vector of production in GWh, in addition to a vector of price segments, and converts the production vector into a corresponding vector of mean production in MWh/h, or MW. For each price segment, the function merely divides the total production throughout the time segment by the total number of hours in the given segment.

```
function MWv = gwh2MW(GWHv,segV)

MWv = zeros(length(GWHv),1);

k = 0;
for i = 1:5:length(GWHv)
    for j = 1:5
        MWv(k+j) = (1000/segV(j))*GWHv(k+j);
    end
    k=k+5;
end

end
```

B.2 Scripts

B.2.1 Generate `.flx` files

The code below shows the Matlab script used to generate `.txt` files, which are later converted to `.flx` files. These files are run in the modular program Kurvetegn in order to easily retrieve all detailed production data.

```
areas =

     finn: [1x1 struct]
    troms: [1x1 struct]
    svart: [1x1 struct]
     helg: [1x1 struct]

>> areas.finn

ans =

       mod: [23x1 double]
       res: [23x1 double]
    regInf: [23x1 double]
       pow: [23x1 double]
    regDeg: [23x1 double]
```

Figure B.2: Nested structure of power station data

The script loads the nested structure `areas`, as shown in figure B.1 above. Area `finn` is merely given as an example, but the structure is equal for each of the subareas. The vectors within `finn` contain power station data, and are written to files by the EMPS model and imported to Matlab. They contain module numbers for power stations in the detailed hydropower files; reservoir sizes in GWh; expected regular inflow in GWh; production capacity in MW; and degree of regulation.

```
%% generateFlxFile.m

%% LOADING STRUCTURED HYDROPOWER areasIONS

load AreaProduction.mat

%% SETTING FILENAMES

names = fieldnames(areas);
prodFiles = cell(numel(names),1);

for i = 1:numel(names)
    prodFiles(i) = strcat('prod',names(i),'.txt');
end

%% GENERATING INDIVIDUAL FILES FOR EACH SUBAREA

for i = 1:numel(names)

    % Obtaining vector of hydropower modules for subarea i.
    indTable = getfield(areas,char(names(i)));
    modVector = indTable.mod;

    % Generating and writing to file
    file = fopen(char(prodFiles(i)),'w');
    fprintf(file,['SI\n\n\nALLE\n',num2str(i),'\nALLE\n']);

    for j = 1:length(modVector)
        fprintf(file,'prod\n');
    end

    fprintf(file,'\n');

    for j = 1:length(modVector)
       fprintf(file,[num2str(modVector(j)),'\n']);
       fprintf(file,'GWH\n');
    end

end
```

B.3 Create scatter plots

This scrips loads a two (4×1) cell arrays containing the full production of all individual plants for EMPS and SOVN respectively, in addition to the struct containing information about each individual hydropower module. The script computes the change in FLH, as given in equation (7.1) for all individual plants and stores them in cell arrays. The calculated change in % is plotted against the respective degrees of regulation for each case.

```
%% plotProd.m

clc,clear,close all                 % Clearing command window
load ProdInd                        % Loading arrays of detailed production
load areaStruct.mat                 % Loading struct of modular data

%% INITIALIZING

names = fieldnames(areas);          % Obtaining name of subareas

numScen = length(prodEMPS);          % Obtaining number of scenarios

utilCell = cell(1,numScen);         % Array structure of changes in util.


%% CALCULATING CHANGES IN FULL LOAD HOURS

for scen = 1:numScen                                        % SCENARIO LEVEL

   numAreas = length(prodEMPS{scen});
   utilCell{scen} = cell(numAreas,1);

    for area = 1:numAreas                                   % SUBAREA LEVEL

       numPlants = size(prodEMPS{scen}{area},2);
       utilCell{scen}{area} = zeros(numPlants,2);

       for plant = 1:numPlants                              % PLANT LEVEL
          areaData = getfield(areas,char(names(area)));

          if sum(prodEMPS{scen}{area}(:,plant)) ~= 0

                   utilCell{scen}{area}(plant,1) = ...
              100*((((sum(prodSOVN{scen}{area}(:,plant))/7)-...
                   (sum(prodEMPS{scen}{area}(:,plant))/7)))/...
                                 (areaData(plant,4)/1000))/...
                    ((sum(prodEMPS{scen}{area}(:,plant))/7)/...
                                 (areaData(plant,4)/1000));

          else
               utilCell{scen}{area}(plant,1) = NaN;
```

```
            end

            utilCell{scen}{area}(plant,2) = areaData(plant,5);

        end

    end

    totalMat = cell2mat(utilCell{scen});

    figure(scen)
    hold
    scatter(totalMat(:,2),totalMat(:,1),'filled')
    plot(0:4,zeros(5,1),':k','LineWidth',1)
   axis([0 4 -100 100])
    grid on
    xlabel('Degree of regulation')
    ylabel('Change in FLH [%]')

end
```

Appendix C
Partition of price segments

Given below is the full partition of price segments used throughout this thesis. The week is partitioned into days, which then again is partitioned into hours with given price segments. Table C.1 shows the different types of price segments, as well as the total number of hours per week for each segment. Table C.2 shows the total distribution of weekly segments.

1	Peak	25 h
2	Day	35 h
3	Morning/evening	25 h
4	Night	49 h
5	Weekend	34 h

Table C.1: Definitions of price segments

	0-1	1-2	2-3	3-4	4-5	5-6	6-7	7-8	8-9	9-10	10-11	11-12	12-13	13-14	14-15	15-16	16-17	17-18	18-19	19-20	20-21	21-22	22-23	23-24
Mon	4	4	4	4	4	4	3	3	1	1	1	1	1	2	2	2	2	2	2	2	3	3	3	4
Tue	4	4	4	4	4	4	3	3	1	1	1	1	1	2	2	2	2	2	2	2	3	3	3	4
Wed	4	4	4	4	4	4	3	3	1	1	1	1	1	2	2	2	2	2	2	2	3	3	3	4
Thur	4	4	4	4	4	4	3	3	1	1	1	1	1	2	2	2	2	2	2	2	3	3	3	4
Fri	4	4	4	4	4	4	3	3	1	1	1	1	1	2	2	2	2	2	2	2	3	3	3	4
Sat	4	4	4	4	4	4	5	5	5	5	5	5	5	5	5	5	5	5	5	5	5	5	5	4
Sun	4	4	4	4	4	4	5	5	5	5	5	5	5	5	5	5	5	5	5	5	5	5	5	4

Table C.2: Partition of weekly price segments

Appendix D
Results and data

This chapter aims to review the same observations as was shown in the main part of the thesis, but this part is only intended as an additional support. Some of the figures and graphs in this chapter could advantageously be included in the main part, but was referred to the appendix simply in order to minimize the result chapter of the thesis. Others are considered to provide useful additional insight to the results, but are not considered essential for the discussions. The chapter also covers input data, which is not to be considered as results, *per se*.

The chapter mostly consists of graphs and plots. Unless first introduced in the appendix, these figures will not be discussed in this chapter, as they are only meant to substantiate the discussion in the main part of the thesis. It should nonetheless be understood from the heading and captions what the graphs represents.

D.1 Inflow data

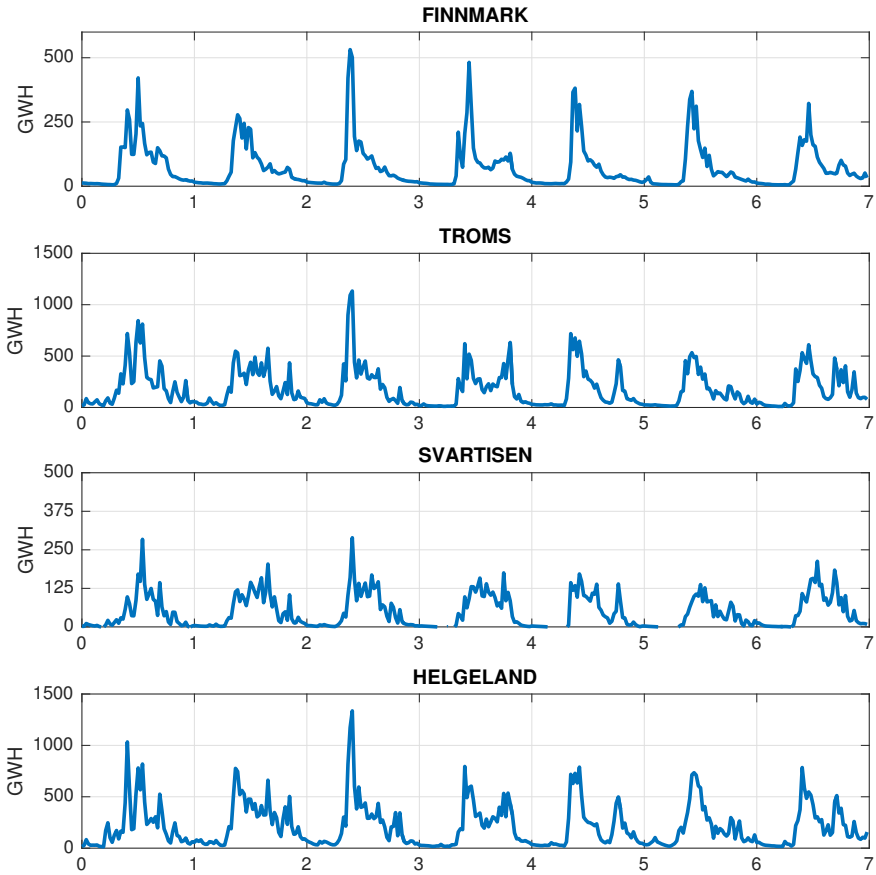

Figure D.1: Aggregate inflow for all inflow scenarios

The aggregate inflow for all subareas are given in figure D.1 above. The aggregate inflow consists of regulated and unregulated inflow, in addition to spillage. The table below shows the total annual inflow for each subarea:

	FINNMARK	TROMS	SVARTISEN	HELGELAND	Tot
1982	4,302	11,186	2,316	11,079	28,882
1983	3,789	10,374	2,762	13,303	30,228
1984	3,973	10,317	2,772	12,225	29,289
1985	3,898	8,612	2,543	10,414	25,466
1986	3,272	8,793	2,216	10,015	24,296
1987	3,381	7,440	1,177	10,171	22,770
1988	3,307	9,162	2,811	10,147	25,428

Table D.1: Total annual inflow per subarea [TWh/y]

As seen the inflow years represent a broad range of inflow scenarios. Inflow scenario 1983 is characterized by large amounts of precipitation resulting in more than 30 TWh total inflow. Inflow scenario 1987, on the other hand, has merely 22.7 TWh annual inflow and represents a typical dry year.

D.2 Prices

D.2.1 Duration curves

This subsection provided the price duration curves for all subareas and all scenarios and models.

D.2.1.1 EMPS

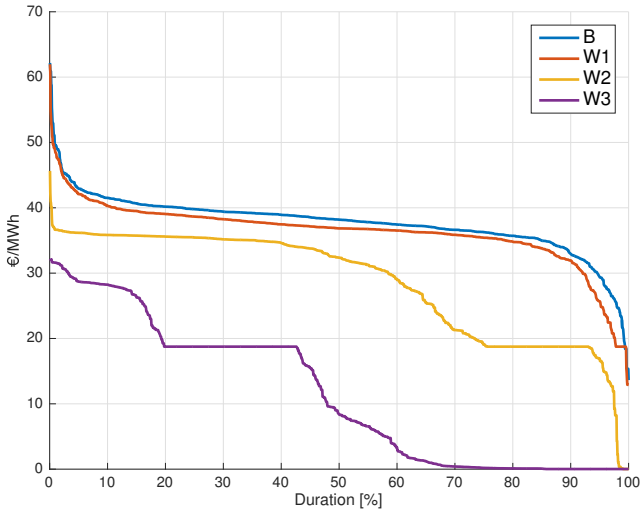

Figure D.2: Price duration curves for FINNMARK - EMPS

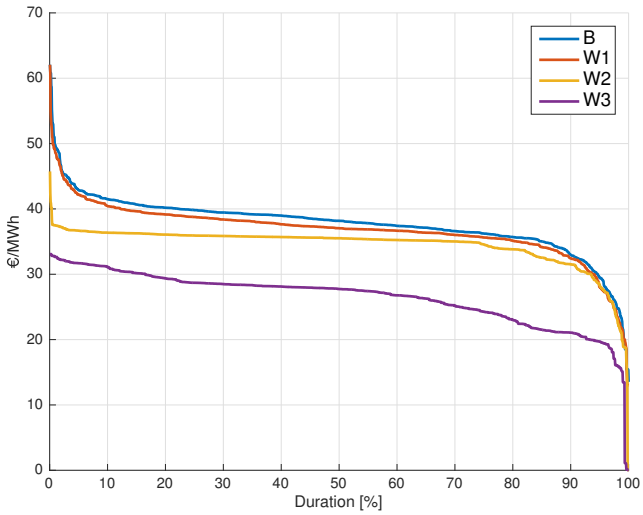

Figure D.3: Price duration curves for TROMS - EMPS

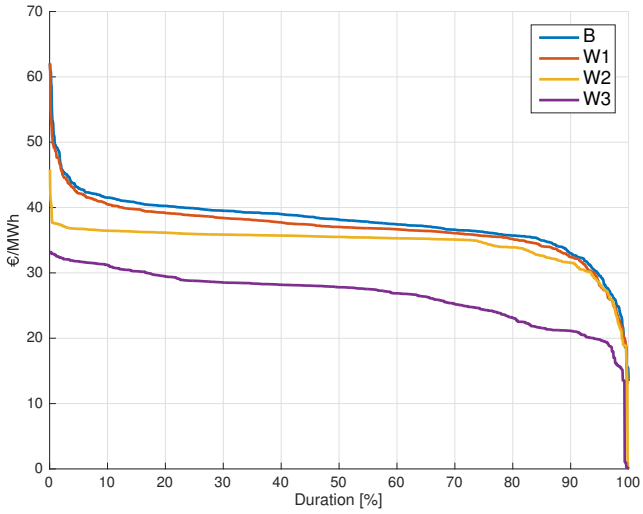

Figure D.4: Price duration curves for SVARTISEN - EMPS

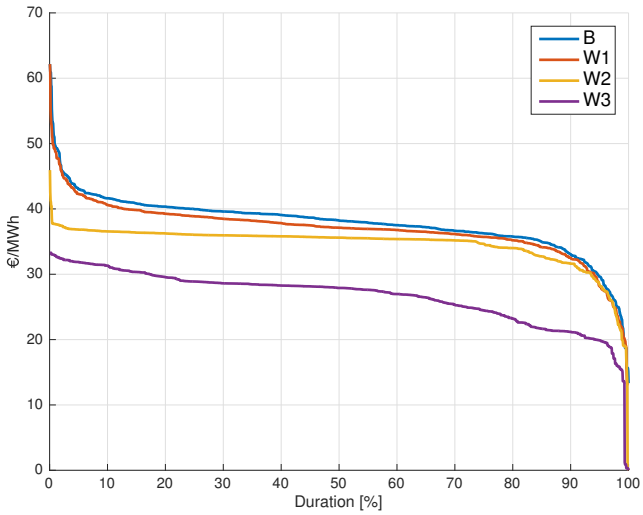

Figure D.5: Price duration curves for HELGELAND - EMPS

D.2.1.2 SOVN

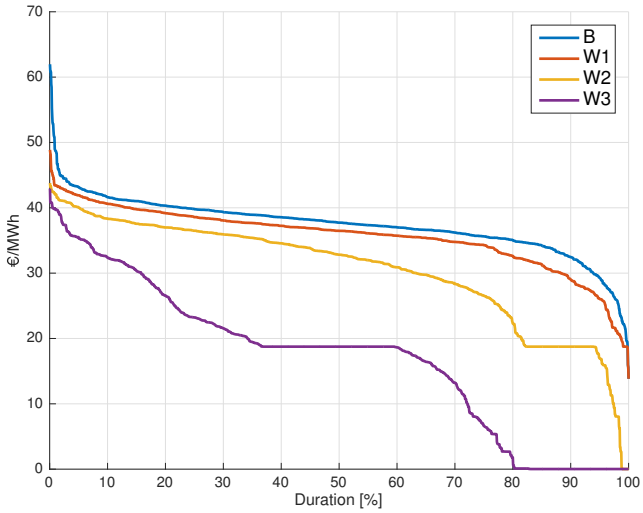

Figure D.6: Price duration curves for FINNMARK - SOVN

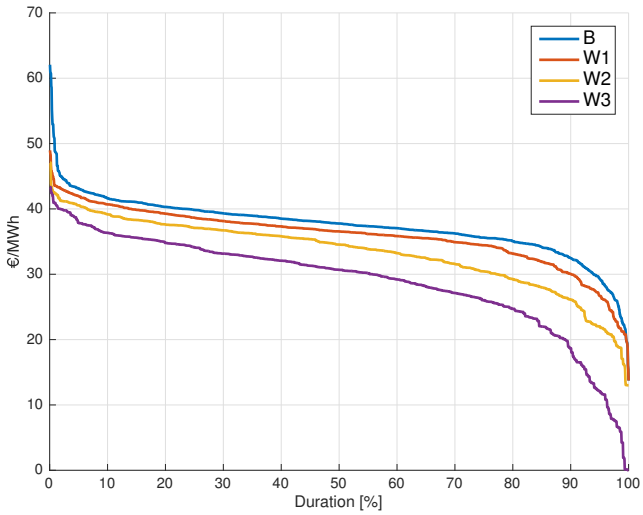

Figure D.7: Price duration curves for TROMS - SOVN

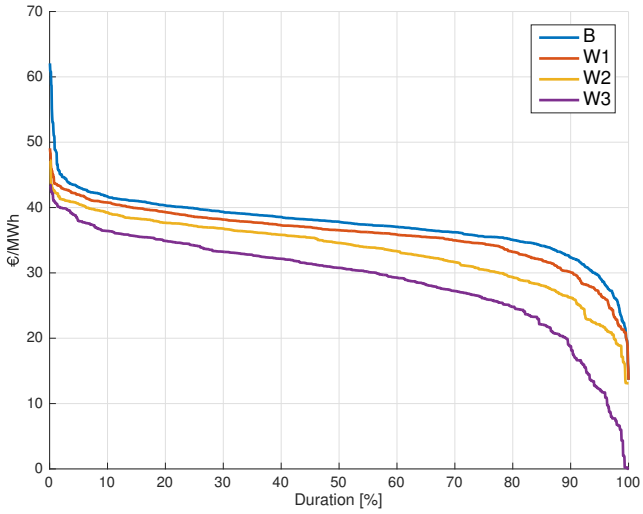

Figure D.8: Price duration curves for SVARTISEN - SOVN

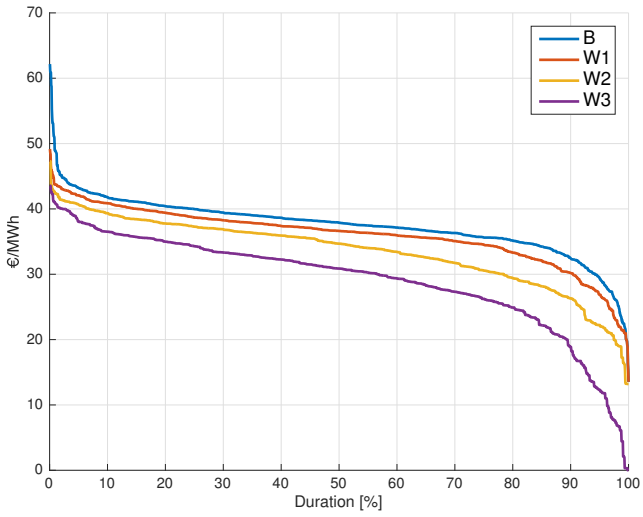

Figure D.9: Price duration curves for HELGELAND - SOVN

D.3 Pumping

D.3.1 Original price price files

All figures in this section refer to simulations in SOVN. Figure D.10 shows the price difference for FINNMARK and TROMS with and without pumps. Denoting the price *without* pumps in load segment n as $p_{n,0}$ and similarly price *with* pump in load segment n as $p_{n,p}$, the figure below can be interpreted as $p_{n,0} - p_{n,p}$ for all load segments.

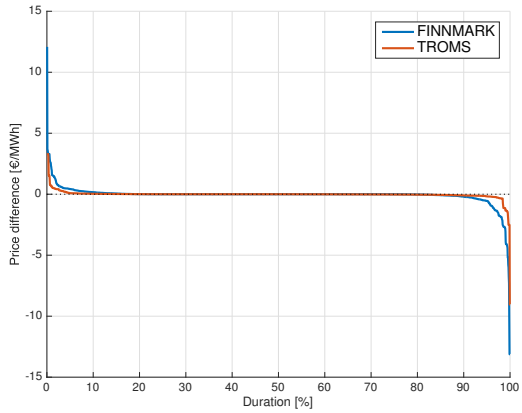

Figure D.10: Price difference with v without pumps - W3

Figure D.11 shows the energy consumed by pumps in unsorted order.

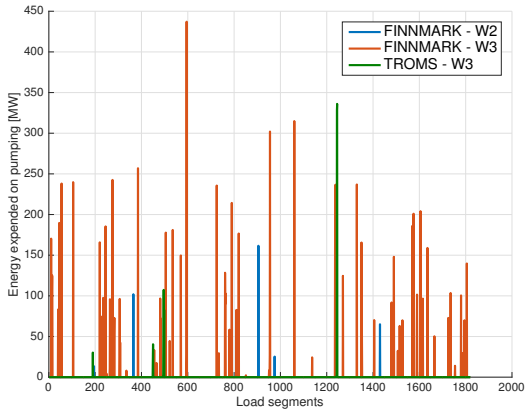

Figure D.11: Energy consumed by pumps, unsorted

D.3.2 German price files

Figure D.12 shows the difference for FINNMARK and TROMS with and without pumps for the subcases with German price files. The graphs are given with the same definition of price difference as stated above. Thus a single simulation without pumps, but with the German price files was needed. This simulation was run with the same settings of the SOVN.ctrl file as the remaining scenarios.

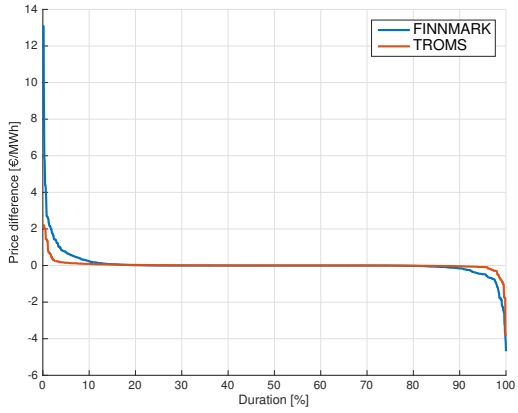

Figure D.12: Price differene with v without pumps with German price files - W3